Follicle Selection Dynamics in the Mammalian Ovary

María Alexandra Chávez-Ross

Thesis submitted for the degree of
Doctor of Philosophy

Supervisor: Dr. J. Stark
Centre for Nonlinear Dynamics and its Applications
University College London
March 1999

To my mother and all her legacy...

Abstract

The main objective of this thesis is to develop and analyse mathematical models of the regulation of the ovulation cycle in mammals. Specifically, we are interested in understanding the mechanisms that control the number of follicles ovulated in each cycle. In humans, a failure of such control mechanisms can lead to Polycystic Ovary Syndrome (PCOS), which accounts for a substantial fraction of all cases of anovulatory infertility found in women of reproductive age. Although treatment is available, it is highly desirable to improve it. Thus, a better understanding of the selection process of the ovulatory follicle is still required.

The thesis begins with a biological description of the terminal phase of the ovarian cycle. This provides the necessary background for the understanding and formulation of the mathematical models presented in later chapters. Next, a review of existing models found in the literature is given and their relevance to the regulation process is analysed. Of these, the one due to Lacker (also referred as the symmetric model) is the best understood in terms of the control of ovulation and PCO. It is given by a system of non-linear differential equations and assumes the same growth rate for each follicle. This assumption is biologically implausible and leads the model to exhibit unrealistic behaviour in some cases. A non-symmetric generalisation is therefore developed and Lacker's theoretical analysis of the symmetric model is extended to this case. The non-symmetric model exhibits behaviour which more closely reflects that observed in PCO. The thesis then goes on to present a theoretical and numerical analysis of another version of the symmetric model which has been proposed by Mariana *et al.* This incorporates a variable representing the ageing of the follicle in the same framework as that of Lacker's original model.

Finally, all of the above models use a somewhat arbitrary function to describe a follicle's sensitivity to hormonal stimulation. In order to provide a more biologically motivated basis for our analysis we therefore develop a model in terms of the gonadotropic receptors of follicular cells. It is believed that the degree of sensitivity of a follicle to pituitary hormones is one of the factors determining its selection. This model is studied using numerical techniques, since its mathematical structure is too complicated to allow a theoretical analysis.

Tentative conclusions underlying the mechanisms that select the ovulatory follicle are given in terms of the different models described in this thesis. Some of these are rather speculative due to the greatly simplified nature of the models in comparison to the real biological system. Nevertheless, since the behaviour of the models is qualitatively consistent with the results obtained from experimental data, they provide useful insights into the mechanisms that control the ovulation number in mammals.

Acknowledgements

I would like to begin by thanking my supervisor Dr. Jaroslav Stark for all his help and encouragement during my Ph.D. Thank you for providing me with continuous ideas and feedback towards the development of my research, and guiding me in this so important episode of my career. I would also like to thank Prof. Michael Thompson for his subsidiary supervision.

I am also extremely thankful to Prof. Steve Franks, Dr. Fréderic Clément, Dr. Helen Mason and Dr. Kate Hardy for all their invaluable biological contributions and supervision to this work.

I would also like to thank Prof. Peter Saunders and Dr. Mark Chaplain for their observations, comments and suggestions towards the improvement of this work.

This research would have been impossible to conduct without the financial support of the Dirección General de Asuntos del Personal Académico (DGAPA), Universidad Nacional Autónoma de México (UNAM) for the award of a scholarship giving me the opportunity to pursue my Ph.D. studies abroad. I am also thankful to the "Programa de Financiamiento Compartido 1994/95" of The British Council for the financial support of paying my first year tuition fees.

I would especially like to thank Dr. Pedro Miramontes for his continuous academic and moral support throughout my undergraduate and postgraduate studies.

My special gratitude goes to my father and brothers, for all their unconditional love and support from the other side of the Atlantic. Thank you Teresa for all your love, care and understanding.

I would also like to thank F. Alan for his spiritual guidance and friendship during my stay in London. Thanks to all and each one of my friends who made this experience so unique and unforgettable.

My last and most important gratitude is for Ricardo. Words are not enough to express all what you mean in my life and in particular in the development of my Ph.D. Without you it just would not have been the same. My love and admiration are yours always.

I bless you Lord for all the love you have given to me during this experience and throughout all the people mentioned above.

Alexandra Chávez-Ross

Contents

List of Figures

Chapter 1

INTRODUCTION

The production and fertilisation of mammalian eggs is now understood to be regulated by different elements of the reproductive system. The complete stock of oocytes in the ovary is formed during early fetal development. Only very few of these eggs will be selected for ovulation during the mammal's reproductive age. In the particular case of primates the number of eggs that are ovulated is fixed, being usually one every month. For the case of humans, out of the 250 000 eggs present at menarche in the ovary, less than 500 will be ovulated (approximately 0.2%) [Faddy and Gosden, 1995]. The remaining oocytes will end up regressing and disappearing from the ovary through an atretic process. In most mammalian species, a female dies before the complete reservoir of oocytes is exhausted, though for humans egg exhaustion normally happens at menopause.

In each ovarian cycle a group of follicles undergoes terminal development. This last phase of ovarian dynamics corresponds to the estrous cycle and is also referred to as the menstrual cycle in the particular case of primates. Although much is known about how follicles ovulate and the ways this procedure is controlled, it remains unclear when and under which circumstances ovulating follicles are selected from that group. Furthermore, it is also uncertain how the number of ovulating follicles is regulated.

It has been shown in humans that ovulating follicles develop from both ovaries in a random manner. Moreover, when one of the ovaries is removed, the remaining one takes over and is able to ovulate every month. This fact strengthens the idea that the control mechanism partly operates outside the ovaries. It is now well known that this control process involves the endocrine system including the hypothalamus, the pituitary glands and the ovary itself [Hodgen, 1982; Hillier, 1994; Spears *et al.*,

1996]. Therefore, follicular growth takes place as a response to a signalling network incorporating these organs and the follicles themselves. All of these factors, which interact either in an endocrine, paracrine or autocrine way result in a cascade of interrelated events, which are able to select and ovulate healthy mature oocytes at the optimal time for fertilisation.

However, such a mechanism of selection and ovulation can go wrong with the result that no follicle is able to release an egg. In the case of humans, the selection process can fail and instead of having one follicle ovulating every month, a considerable number of follicles are selected and reach pre-ovulatory maturity. Subsequently, they never ovulate but rather stay in the ovary for some time. This feature is referred to as a Polycystic Ovary (PCO), which together with its adjacent consequences accounts for the Polycystic Ovary Syndrome (PCOS).

Although this syndrome was first defined in 1935, very little is known about its underlying causes [Chang, 1996]. Since there are many factors which are thought to contribute to its occurrence, it has not even been possible to give a precise definition of the syndrome [Dewailly, 1997]. However, it occurs in approximately 20% of women of reproductive age, and in its most severe form is the most common cause of anovulatory infertility [Franks *et al.*, 1996]. An understanding of this failure is important medically; while many women suffering from anovulatory PCOS can be successfully made to ovulate by treatment with appropriate hormones, this can easily result in multiple ovulation, leading to multiple pregnancies with all their attendant adverse side effects. Whilst modern treatment protocols have to some extent overcome this problem, a better understanding of mechanisms leading to PCOS is still highly desirable.

Therefore, it is the main objective of this thesis to study the basic features that regulate the selection dynamics during the estrous/menstrual cycle from the mathematical viewpoint. It would be very ambitious to try to determine precisely all the actual factors that are involved in the follicle selection process, or to ascertain the causes of PCOS. Instead, it is our aim to develop models that qualitatively agree with experimental data, which may provide useful insights to the control mechanism of the selection process.

After describing the basic biology required to understand the cycle and follicular development, we review some of the existing mathematical models in the literature. These models try to describe, in a descriptive or functional way, the most important

features of the control system within the cycle. The descriptive models focus on an understanding of folliclegenesis in terms of follicular population and in terms of follicular cells. On the other hand, functional models range from an attempt to only reproduce the cyclic behaviour of estrogens to models of the whole system of interacting hormones, follicular growth and steroid production at each stage of the cycle.

All of these models relate biological to mathematical knowledge to obtain qualitative information about the different elements of the regulation process. In this thesis they were primarily analysed from the perspective of the control of the follicle selection.

In the early eighties Lacker was the first to publish a mathematical model which reflects the dynamics of many growing follicles during the follicular phase of the cycle. Many assumptions are made about the complex pituitary-ovary system and about follicular development in order to obtain a manageable system of differential equations. In chapter 4 we reproduce the analysis of this system in order to properly understand the way it is able to reflect the basic features of the cycle. Such features involve the emergence of pre-ovulatory and ovulatory follicles, control of the selection number, and atresia of the remaining non-selected follicles.

Furthermore, Lacker's model is the first to simulate anovulation either by manipulation of the relevant parameters or by changes in the initial conditions of the system. His model is able to select many pre-ovulatory follicles that never ovulate, but rather remain stuck with a fixed size. Although this may suggest features of PCOS in humans, Lacker's model is not accurate in reflecting this syndrome. This is mainly because the number of ovulatory follicles his model produces is always larger than the number of pre-ovulatory follicles selected in PCO. In reality this is not the case for there are women who ovulate one follicle in one cycle and in the next may present PCO with many pre-ovulatory mature follicles that never ovulate. Thus in reality, the number of ovulatory follicles is usually less than the number of PCO follicles, and not the other way around.

This particular issue and some others lead us to the generalisation of such a model, which is described in chapter 5. The symmetry assumed by Lacker in which all of the follicles grow in exactly the same manner is broken, and each follicle is made to have different parameter values. This is more biologically realistic since these parameters are assumed to account for the follicle sensitivity to hormone stim-

ulation. Allowing such parameters to vary from follicle to follicle is consistent with experimental observations [Hartshorne *et al.*, 1994].

The generalised non-symmetric model that we develop and analyse leads to a number of new conclusions about follicle selection dynamics. In particular, this non-symmetric model reflects PCO more accurately than the symmetric one. In the following chapter we study another interesting modification of the symmetric model published a few years later by Mariana *et al.* A thorough theoretical and numerical analysis is developed leading to a number of new conclusions. This model proposes a new maturity variable that involves a decaying factor also considered as the ageing of the follicle. When such a decaying factor is large enough with respect to the initial size of the follicle, the selection dynamics is disturbed and the follicle will always be atretic. Moreover, when such an ageing parameter is larger for one follicle than for the remaining ones, the number of selected follicles is not predictable and the type of cycle may be also altered.

Unfortunately, all of these models have a somewhat arbitrary function for the follicle growth rate. In fact, very little is known about the way follicles react to hormone stimulation, which regulates their growth and steroid secretion during the terminal phases of the ovarian cycle. It is believed that this follicular sensitivity is the main factor determining the selection of pre-ovulatory follicles [Gougeon, 1984]. It appears that follicles compete for the hormone resources in terms of their capacity to react to them. However, it is difficult to measure such sensitivity experimentally.

Although many biological studies on the follicular micro-environment have been considered (*e.g.* [Austin and Short, 1982; Richards, 1975; Gougeon, 1986; Fortune, 1994; Mason and Franks, 1997; Misrahi *et al.*, 1996; Rainey *et al.*, 1996]), the signalling network taking place inside the follicle during folliclegenesis is extremely complex. Follicles react to gonadotropins throughout protein-like receptors attached to their cell membranes. Once the binding reaction happens, a signalling transduction pathway develops inside such cells that ends up in cell proliferation and steroidogenesis. However, other kind of steroids, growth factors and cytokines have been detected in the follicle, which modulate the pathway [Adashi and Hsueh, 1982; Alouf *et al.*, 1997; Armstrong *et al.*, 1996; Bao *et al.*, 1995; Erickson *et al.*, 1979]. In particular, some individuals presenting PCOS suffer from obesity suggesting that insulin growth factors acquired from the blood stream arrest follicular development at some stage of the cycle [Rosenfield, 1997; McGee *et al.*, 1996].

Due to this complexity we need to focus only on the important factors to have any base of developing a biologically based growth function for follicles. We therefore choose to only consider the concentration of bound receptors of follicle cells. This allows the basic framework first proposed by Lacker to be maintained, and hence we can use most of the results provided by the three main models described in previous chapters.

It is also important to mention that the way follicles atrophy has been carefully studied for the development of this last model. Some biological studies have suggested that not only growth, steroidogenesis and selection of follicles is hormonally controlled, but also follicle atresia. It appears that the lack of gonadotropins not only stops follicular growth and steroid production, but at the same time triggers atresia [Brailly *et al.*, 1981; Garrett and Guthrie, 1996; Hillier and Tetsuka, 1997; Jablonka-Shariff *et al.*, 1996]. Atretic demise is believed to begin with the start of apoptotic cell death of follicular cells. Such apoptotic cells appear in both healthy and atretic follicles, although in the latter in a much larger proportion since it is believed that apoptosis has overcome cell proliferation and differentiation [Jolly *et al.*, 1997b; Jolly *et al.*, 1997a; Tsonis *et al.*, 1984]. Therefore, in the last model we investigate how such effects may be explicitly incorporated into the equations.

The final part of this thesis discusses and compares the results obtained from all of the above. The relevance of the models to the actual biology of the control of ovulation in mammals is considered as well as possible hypotheses that may suggest new mechanisms that determine and affect the selection process. Finally, some suggestions are made for future research in terms of mathematical modelling.

Chapter 2

THE BIOLOGY

2.1 Introduction

The selection of the ovulatory follicle within a mammalian ovary is a complex endocrine process of great medical importance. From an initial subset of recruited follicles developing towards terminal maturation, the number selected for ovulation is relatively small and remains fairly constant from cycle to cycle. Furthermore, the vast majority of follicles that do not ovulate degenerate through a process known as atresia. This suggests that a remarkably robust control scheme is involved. Moreover, it is thought that these selection and atretic procedures are associated with the parts of endocrine system consisting of the hypothalamus and pituitary glands as well as the ovary itself. The main purpose of this chapter is to describe the biological features of the ovulation cycle in primates. We do this at the level of detail required in later chapters to develop mathematical models of the regulation process.

2.2 Folliclegenesis and hormone stimulation

From the stock of oocytes formed during fetal development in the mammal, many thousands of primordial follicles are formed and remain scattered through the cortex of the ovary. It is not yet clear how individual oocytes are recruited to join the pool of growing follicles. However, once they initiate their maturation process they induce changes in the surrounding stroma cells which then differentiate into the granulosa and theca cells that form the follicle itself. The follicle is at this stage a unit built of two main types of cells that protect and support the oocyte in its development towards its eventual ovulation and fertilisation [Eppig, 1991].

In the case of humans, follicular cells continue to differentiate and proliferate for

approximately 120 days. During the early growing stage of folliclegenesis, granulosa cells aggregate around the oocyte and the follicle increases its diameter from 0.04 mm to 0.1 mm approximately. On the other hand, theca cells proliferate just outside a thick basement membrane containing the granulosa cells. When the follicle diameter is between 0.1 and 0.2 mm, the follicle is considered to be in the pre-antral stage of the cycle. When it is around 0.2 mm large, gaps of follicular fluid start appearing between the granulosa cells; this is defined as the antral phase. It is strongly believed that up to the end of the antral phase, the follicle is able to grow without essentially any hormonal stimulation. This is also known as basal follicular growth and usually lasts for about 65 days in humans. When the follicle is about 2 mm in size, it is then referred to as *Graafian* follicle. It is at this stage that the oocyte is immersed within a fluid cavity known as the antrum, and that the granulosa cells reach their proliferation peak. Granulosa cells are distributed in three to four layers surrounding the antrum and the vascularised network of theca cells is well established outside the basement membrane [Gougeon, 1996b; Gougeon, 1996a], see figure 2.1. Although

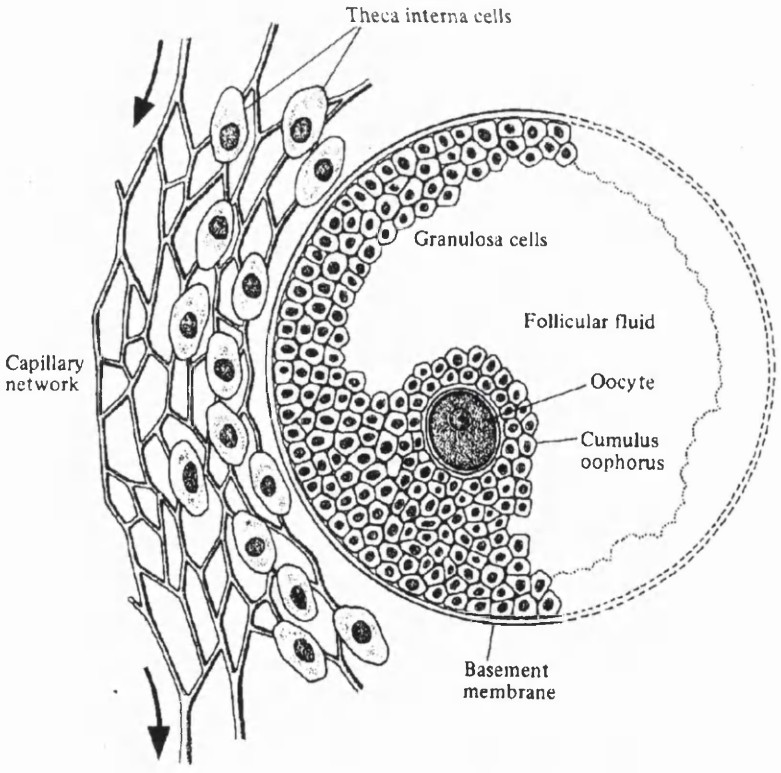

Figure 2.1: Graafian follicle structure. A capillary network of theca cells surrounds the basement membrane which, in turn, surrounds the three to four layers of granulosa cells. The oocyte is immerse within the antrum (follicular fluid) and is attached to the granulosa of the follicle through out the cumulus oophorus [Austin and Short, 1984].

antrum formation also increases follicular size, follicle diameter is well correlated with the number of granulosa cells, especially during the follicular phase of the cycle. It is believed that during the terminal part of follicular development, vascularisation of the theca cells increases, whilst granulosa cells progressively lose their proliferative ability and acquire a high steroidogenic activity.

It is at this stage that the follicle is believed to begin its endocrine development; that is the moment when it becomes sensitive and responsive to hormone stimulation. This endocrine function of the ovary ensures the regular production of healthy oocytes at a time when it is best for them to be ovulated and fertilised. The hypothalamus and pituitary glands are in charge of releasing specific hormones that help the Graafian follicles continue their maturation towards the pre-ovulatory stage. The follicle maturation process is now also affected by its estrogen production in response to gonadotropin stimulation, meaning that this steroidogenesis also contributes to the follicle's own development. These Graafian follicles are then ready to be recruited to the last part of follicular development, which is the ovulation cycle. Once selected, the human early pre-ovulatory follicle is around 5 mm in diameter and is able to ovulate under gonadotropin stimulation. From this stage onwards, the follicle increases its size mainly due to the growth of its antrum. In the case of a non-selected follicle, its atretic regression starts by the onset of apoptosis within its granulosa. Furthermore, this gonadotropic regulation proceeds to the formation of the *corpus luteum* once the oocyte has been extruded from the ovary at a size of 10 to 20 mm in diameter [Gougeon, 1996b; Gougeon, 1996a].

The primary endocrine system involved in follicular growth and maturation from the Graafian state up to the pre-ovulatory state is a negative feedback mechanism involving the hypothalamus, pituitary glands and the ovary. The hypothalamus releases Gonadotropin Releasing Hormone, GnRH. This acts on the pituitary gland which in response releases Follicle Stimulating Hormone, FSH, and Lutenizing Hormone, LH. FSH acts on the granulosa cells of the follicle to transform androgens into oestradiol. These androgens are transformed from progestins within the follicle theca cells with the help of LH (see figure 2.2). When certain oestradiol levels are reached in the blood stream, the pituitary responds by almost completely stopping the release of FSH. It is at this moment when the follicles that have not reached pre-ovulatory maturity start atrophying and ultimately dying [Hsueh *et al.*, 1994]. After the extrusion of the oocyte (ovulation) the remaining theca and granulosa cells

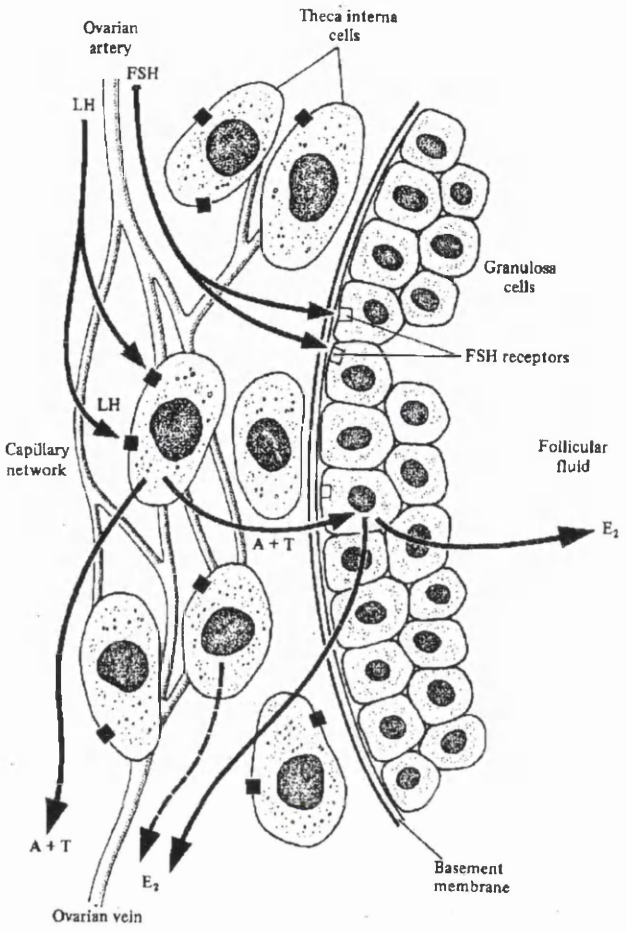

Figure 2.2: Steroidogenesis within the Graafian follicle. The theca interna cells produce androgens such as androstenedione and testosterone with the help of bound LH signal stimulation. These androgens get through the follicle basement membrane and reach granulosa cells. Once inside the granulosa cells, these steroids are inter-converted into oestradiol. Such a process is stimulated by the signalling process produced once FSH binds the granulosa cells receptors [Austin and Short, 1984].

within the ovary form the *corpus luteum.* The number of *corporea lutea* found in the ovaries is directly related to the number of eggs delivered and varies with the species [Austin and Short, 1984].

A more detailed characterisation of the cycle, also referred as the menstrual cycle for primates and as the estrous cycle for other mammals is explained in terms of the following four phases [Baird, 1983]:

a) Early follicular phase: both ovaries contain multiple immature follicles, so that secretion of oestradiol is minimal. Since the negative feedback effect from the previous cycle has finished, secretion of FSH and LH is raised. This heightened level of FSH stimulates the development of medium sized follicles and subsequently their

production of oestradiol.

b) Late follicular phase: selection of the pre-ovulatory follicle has taken place which monopolises the production of oestradiol within the ovary. Such follicle oestradiol production exerts a negative feedback control upon the pituitary production of FSH and a positive feedback control upon the pituitary production of LH that triggers the mid-cycle LH surge[Austin and Short, 1984]. The first of these has the consequence of atretic regression of the non-selected follicles, and the second one is also thought to increase the aromatisation of androgens into oestradiol within the granulosa cells of the pre-ovulatory follicle. Such cells are now able to react to LH stimulation thanks to their acquisition of LH receptors at this stage of their differentiation [Monniaux *et al.*, 1997]. Moreover, the positive feedback effect upon LH pituitary secretion triggers the mid cycle LH surge, which a short while later induces ovulation of the pre-ovulatory follicle.

c) Early luteal phase: after the surge of the ovulation-inducting gonadotropin (LH), oestradiol and progesterone produced by the *corporea lutea* induce a negative feedback in the pituitary in order to terminate LH secretion. *Corporea lutea* also produce inhibin which in synergy with oestradiol continues to suppress pituitary FSH release; the surviving medium sized follicles do not keep growing but regress.

d) Late luteal phase: if pregnancy is not initiated *corporea lutea* regress. Therefore, the negative feedback of luteal steroids (oestradiol and progesterone) and inhibin stops. Finally, adequate levels of gonadotropins are restored to permit the growth of the new medium sized follicles. The cycle starts once again (see figure 2.3).

The ovulation cycle duration and the number of follicles ovulated varies amongst species. For the particular case of humans, the menstrual cycle ideally lasts 28 days. The follicular phase starts at the beginning of the menstrual period up to the LH surge that induces ovulation of the selected follicle – since for this case it is usually only one – after approximately 14 days. We are mainly interested in analysing and reproducing this first half of the cycle which is where selection takes place.

2.3 Polycystic Ovary Syndrome

There are many different causes of infertility in mammals originating at different levels of the reproduction cycle. In the case of humans these include genetic mutations,

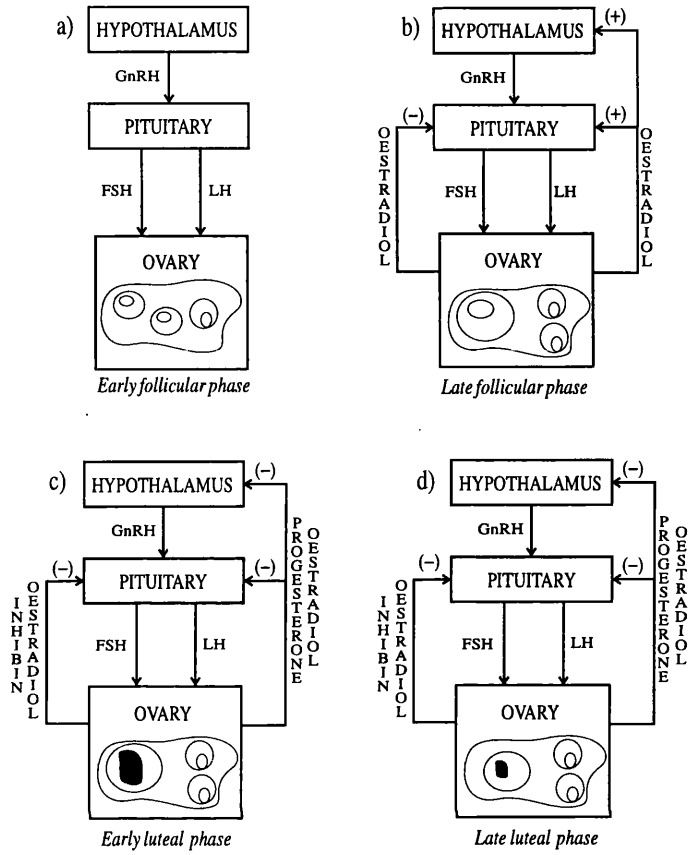

Figure 2.3: The four main phases of the endocrine feedback mechanism of the human menstrual cycle. a) Early follicular phase: both ovaries contain multiple immature follicles with small steroidogenic activity. Both gonadotropic hormones stimulate follicular growth and oestradiol production. b) Late follicular phase: the negative feedback of oestradiol upon the pituitary FSH production has started and selection of the ovulatory follicle has occurred. c) Early luteal phase: after the LH surge and ovulation, the corpus luteum produces progesterone to stop the LH pituitary secretion. d) Late luteal phase: if pregnancy is not initiated the corpus luteum regresses so its feedback effects upon the pituitary gonadotropic production ceases; the cycle is ready to start once again [Baird, 1983].

nutritional deficiencies, emotional disturbances, systemic diseases and disturbance of the ovary and pituitary gland [Taymor, 1996]. In particular, failure may occur in the endocrine feedback mechanism leading to anovulation. The form of anovulation caused by the condition known as Polycystic Ovary Syndrome (PCOS) accounts for some three-quarters of anovulatory infertility. However, PCOS may not affect the reproductive cycle in such a drastic way, but be present in ovulatory cycles. Indeed this is a quite common condition, which affects, in different degrees of severity, up to twenty percent of women of reproductive age [Polson *et al.*, 1988]. It is possible for women to only have a polycystic ovary (PCO) without other apparent clinical or biochemical symptoms which characterise the syndrome. Although it has been very

difficult to give a proper clinical definition for PCOS throughout the years, Mason suggests the following "...the presence of polycystic ovaries in conjunction with at least one other manifestation of the syndrome such as anovulation or evidence of androgen excess" ([Mason, 1994], p.48).

One of the main characteristics of PCOS is that the ovary contains a substantial number of large follicles which reach 5-10 mm in diameter but fail to ovulate. A reasonable interpretation is that this is caused by a failure of the selection mechanism; instead of one follicle coming to dominate and the remainder degenerating through atresia, a large group become arrested at some intermediate stage.

The underlying cause for the failure of the hormonal feedback mechanism leading to PCOS is basically unknown. The main reason for this is the lack of a precise understanding of the selection process of the pre-ovulatory follicle. This is due to the number of interacting elements leading to a complex signalling network during the cycle. Therefore, it is important to identify whether the problem is at a global level, local level or both. By global level we mean the signalling between the pituitary and ovary through circulating hormones and steroids. In contrast, by a local level we mean the signals exchanged amongst the different follicular cells and different follicles inside the ovary.

Nevertheless, a number of explanations of PCOS have been proposed based on the many different studies that have taken place since the syndrome was first described in 1935. One of the most popular is that once selection has occurred, circulating FSH levels are not high enough to permit the selected follicles to keep on growing towards ovulation. This is why treatment with appropriate hormones can make some PCOS women ovulate. On the other hand, it has also been observed that there are cases of ovulatory or anovulatory PCO (ovPCO and anovPCO respectively) with normal serum FSH concentrations [Mason *et al.*, 1994]. Furthermore, FSH follicular levels can even be high enough to promote oestradiol production by granulosa cells and yet, the follicle does not ovulate. One plausible explanation for this is that as a result of abnormal thickening, FSH is not able to permeate the basement membrane of the follicle.

Another potential explanation for PCOS is the inability of granulosa cells to respond to gonadotropins due to an abnormal expression of some unidentified inhibitory factor within the follicle, which is also needed to enable cell differentiation and proliferation. The lack of estrogen creation due to a failure of granulosa cells

to respond to FSH also causes a rise in androgen follicular levels. This in turn, may affect either the hypothalamus or pituitary hormonal production or lead to the thickening of the follicular basement membrane.

Chapter 3

MATHEMATICAL MODELS OF OVARIAN DYNAMICS: A REVIEW

3.1 Introduction

Many mathematical models of the ovarian cycle in mammals have been developed since the 1940s. The basic purpose of all of them has been to understand the different types of regulatory procedures that are involved in the dynamics of the ovaries. Therefore, most of these mathematical and theoretical models have been concerned with evolution of the follicular population, folliclegenesis and hormonal interactions during the endocrine behaviour of the cycle.

After classifying the models into two main approaches according to the way they reflect the ovarian cycle, it is the aim of this chapter to give a brief chronological description of the models found in the literature. We shall particularly highlight to what extent each model deals with the processes that regulate the number of follicles that ovulate per cycle.

3.2 Morphology vs. physiology

The present review classifies the mathematical models of the ovarian cycle into morphological and physiological categories. The main emphasis in the study of the regulation of the ovarian cycle has been physiological rather than morphological. In other words the main focus has been on the different types of hormones circulating through the cycle and the functional features of follicular development, rather than a description of the shape and general appearance of interacting follicles. However, it

is difficult to completely disconnect these two points of view when describing folliclegenesis. Moreover, it is strongly believed that the process of follicular development can be divided into two main stages according to both criteria, namely those of basal and endocrine growth. As can be seen in section (2.2), for each of these stages the morphology and physiology of the follicle are very different.

A comparative analysis of many published mathematical models has been presented in [Clément, 1997]. Nevertheless, it is important for the development of this thesis to analyse such models in terms of the selection procedure of the ovulatory follicles. In fact, some of these models have served as the basis of the models analysed, improved and developed in subsequent chapters.

3.3 Descriptive models

Most of the descriptive models are an attempt to explain the mechanism used in folliclegenesis to control the number of ovulating follicles in each estrous cycle in terms of the follicular population. First of all follicular development is discretised into a number of stages (compartments). Then, the transition rates of follicles evolving from one stage to the next, and the atresia rates from each stage are estimated from data on follicular populations measured first from mice ovaries and then from human ovaries.

The first attempt to model follicular dynamics in terms of the granulosa tissue of the follicle is also described below. The authors divide the granulosa cell population of a single follicle in three different kinds according to their physiologic status as, proliferating, differentiating and apoptotic cells. Then a compartmental model which describes the transition dynamics of proliferating to differentiating cells, and differentiating to apoptotic cells is described for pre-ovulatory and atretic follicles.

3.3.1 Compartmental models

Since 1976, Faddy *et al.* have been developing and refining an analytical model for the change of follicular number in the ovary throughout the life of a mammal. Initially they worked with mice [Faddy *et al.*, 1976; Faddy, 1976; Faddy and Jones, 1988], but subsequently have applied their model to the human ovary [Faddy and Gosden, 1995]. They were particularly motivated by trying to explain how ovulation number could possibly remain constant despite the fact that the initial number of growing

follicles decreased with the age of the mammal.

They investigated the relationship between follicles of different sizes in order to understand the control procedure that keeps ovulation number constant. They classified the follicular growth into five different compartments and applied this to measured follicular populations in mice [Faddy *et al.*, 1976]. Classification begins with Group I containing follicles with an incomplete or complete layer of flattened or cuboidal granulosa cells; these follicles are also referred to as small follicles. Follicles in Groups II and III are referred to as medium follicles, and they have one layer of columnar cells and two layers of granulosa cells respectively. Groups IV and V^+ comprise large follicles, Group IV follicles have three layers of granulosa cells, whereas Group V^+ follicles have four or more granulosa cell layers. Besides, Group V^+ contains follicles with and without an antrum. This latter group was divided into Group V and Group VI in previous studies, but was subsequently amalgamated into only one since follicles within both groups were responsive to gonadotropins. This amalgamation avoided an unmanageable number of variables in the equations.

Once this classification was established, data of the follicular populations in each group was used to calculate the age dependent migration rates for follicles moving from one group to the other. In the same manner the time dependent death rates for each follicular compartment were also computed since atresia was observed to occur in all of them. They proposed a stochastic compartmental model for the group mean sizes at any time t.

Let $\lambda_i(t)$ for $i = 1, \cdots, 5$ be the mean sizes of Group I, II, III, IV and V^+ respectively. Also, let $\nu_i(t)$ and $\mu_i(t)$ for all $i = 1, \cdots, 5$ be the corresponding transition and death rates for each group. The corresponding time dependent migration and death rates were assumed to have a simple probabilistic interpretation. For instance, given a follicle in say Group I, then for $\nu_1(t)$ and $\mu_1(t)$ at age t, such a follicle would become a member of Group II at age $t + \delta(t)$ with probability $\mu_1(t)\delta(t)$. Since folliclegenesis is a continuous development, $\delta(t)$ was considered to be an infinitesimal age increment. Furthermore, the authors also assumed that at age 0, all follicles are in Group I and nowhere else, and for any time $t > 0$ they considered a multinomial probability distribution of the follicular population in all groups.

However, although the initial follicular population size N can be known in terms of the model, it is unknown for the ovary. Therefore, if such an initial follicle population is being originated in Group I following a Poisson probability distribution, the

above mentioned multinomial distribution reduces to independent Poisson counts of the group sizes at any time t. Such Poisson distributions are characterised by the mean sizes of the follicular population for each group, which are given by

$$\lambda_1 = \lambda \exp\left(-\int_0^t [\nu_1(x) + \mu_1(x)]dx\right) \tag{3.1}$$

and

$$\lambda_i(t) = \int_0^t \nu_{i-1}(x) \exp\left(-\int_x^t [\nu_i(y) + \mu_i(y)]dy\right) \lambda_{i-1}(x)dx \tag{3.2}$$

for $i = 2, \cdots, 5$, where λ is the initial mean size of Group I. Note that $\nu_5(t) = 0$ since no emigration takes place from Group V^+ (apart from atresia).

Nonetheless, this turns out to be an extremely difficult task when considering atresia and transition rates as variables. Thus, they regarded them as constants and only changed their value after 30 days, which accounts for the approximate age for puberty in mice.

Although they obtained interesting results about the change of follicular migration and death rates between pre-pubertal and post-pubertal mice, they could not give a functional explanation for the conservation of the ovulation number. For instance, a significant reduction of the Group I atresia rate from ovaries older that 30 days was registered. This means that the decrease in the follicular population in Group I of pre-pubertal mice is mainly due to substantial follicular degeneration, rather than follicles emigrating to Group II. However, this kind of argument turns out to be insufficient to explain why the ovulation number remains constant despite the fact that there are fewer follicles available after 30 days of age. This may be because their classification was merely based on morphological terms and no hormonal interaction was considered.

Nevertheless, in later work Faddy and Jones highlighted atresia as an important mechanism involved in follicular development [Faddy and Jones, 1988]. A multi-compartmental model was again established, but in a deterministic way. For the general case of m different compartments the number of follicles $y_i(t)$ in compartment i at time t is assumed to satisfy a linear system of differential equations,

$$\frac{dy}{dt} = Ay \tag{3.3}$$

where $y(t) = (y_1(t), \ldots, y_m(t))$, and the $m \times m$ matrix A contains the transfer rates of follicles from compartment i to j and the death rates for each compartment.

Considering similar assumptions, this is the equivalent version for the mean size formulae of the stochastic model given in (3.1) and (3.2). This can be observed since for the corresponding $\nu_i(t)$ and $\mu_i(t)$ for $i = 1, \cdots, m$, the number of follicles per unit of time leaving Group i and entering Group $i+1$ at age t is $\nu_i(t)n(t)$, where $n(t)$ is the size of Group i at age t. Similarly, the number of follicles per unit of time dying in Group i at time t is $\mu_i(t)n(t)$. This deterministic interpretation corresponds to a simpler way of describing the follicular emigration dynamics than that given by the stochastic version. In both cases, it is clearly seen how different compartments are interdependent. Solutions (3.4) and (3.5) form the basis for fitting parametric curves to temporal data for the m different compartments of the model. This can be achieved by computing the elements of matrix $A(t)$ in a similar way to that in the stochastic model.

A solution of equation (3.3) given an initial condition $y(0)$ is given by,

$$y_1(t) = y_1(0) \exp\left[\int_0^t a_{11}(u)du\right] \tag{3.4}$$

and,

$$y_i(t) = \int_0^t a_{i-1}(u) \exp\left[\int_u^t a_{ii}(v)dv\right] y_{i-1}(u)du \tag{3.5}$$

for $i = 2, \cdots, m$.

They also applied this model to data obtained for five different follicle sizes from a mice population. In this case, some temporal variations of the transition rates were considered which were biologically justified by the observed changes in the granulosa cell mitotic index with respect to mice age. However, the discussion in this paper concentrated on the interplay of parametric and non-parametric approaches to fitting curves to data, rather than on trying to give an explanation of the regulatory processes in folliclegenesis.

In the last published study of the multi-compartmental model, Faddy and Gosden applied these ideas to the human [Faddy and Gosden, 1995]. Follicle sizes were divided into three different compartments and the mathematical model was used to estimate the growth (or transition) and death rates in human ovaries in women between the ages of 19 and 50. This model indicated such rates were age dependent with a strong transition at 38 years of age.

Despite the particular problems of obtaining experimental data from human ovaries, reflected in the possibility of only getting three different groups from adult

women, there was a good fit of the model to the data. One of the motivations of this study was the fact that during the approximately 36 years of reproductive life of women, less than 500 follicles are able to ovulate from a population of 250 000 follicles present at menarche. However, instead of explaining such a waste in terms of the selection process, they justified it in terms of the continuous loss of follicles that eventually leads to complete follicular depletion of the ovaries before death. They were more interested in understanding how the ovaries age with time by losing their follicular population, than by how the selection process works in each cycle. This follicular depletion accounts for the menopause, which is a unique characteristic of humans.

They found that the daily egress rate of follicles leaving stage III, which corresponds to those follicles ready for selection, steeply decreased from women around 24-25 years old to women older than 38 years of age. Moreover, significant follicular loss was found within stage I of folliclegenesis for ovaries older than 38 years due to a great increase in the death rate. These results are consistent with those experimentally obtained by Gougeon *et al.* [Gougeon *et al.*, 1994]. Faddy and Gosden argued the possibility of follicles belonging to stage I of old ovaries atrophying more than follicles of young women, due to structural damage acquired during their prolonged wait in their primordial stage. Whether or not this is the case, they did not clarify the effects of the diminished number of stage III follicles on the control of the ovulation number.

Although the follicular population of each compartment is described in terms of the preceding one, this representation, either stochastic or deterministic, does not give a functional explanation for the changes observed in such transition and atresia rates during the reproductive age of the mammal. Moreover, such compartmental models are not able to offer any plausible explanation for the constant number of ovulating follicles every cycle. For instance, in the particular case of the human, changes in transition rates from the last compartment of follicular development in women older than 38 years old gave a plausible cause for menopause, rather than a justification for a single ovulating follicle. This strongly suggests that estimating the number of follicles within each stage of folliclegenesis is insufficient to understand the control of ovulation number, but rather factors external to the ovary itself must intervene.

In conclusion we see that since the multi-compartmental model is more a de-

scriptive than a functional model, it fails to explain the regulatory procedures of the ovulation number in each cycle during the reproductive life of a mammal. This may strengthen the idea that such a control process relies more on physiological factors, rather than on any kind of auto regulation mechanism involving the number of follicles at different stages of follicular development.

3.3.2 A descriptive model in terms of granulosa cells

As more comes to be known about the follicle micro-environment, the first attempt to build a mathematical model of folliclegenesis based on the perspective of the granulosa cell dynamics was recently published by [Clément *et al.*, 1997]. They derived a model in terms of the number of proliferating, differentiating and apoptotic granulosa cells from the time of peak of granulosa proliferation until ovulation. A deterministic system of three linear differential equations for the change rate of the number of each granulosa cell type was derived:

$$\begin{aligned} \frac{dN_p(t)}{dt} &= (\mu - \delta(t))N_p(t) \\ \frac{dN_d(t)}{dt} &= \delta(t)N_p(t) - \alpha(t)N_d(t) \\ \frac{dN_a(t)}{dt} &= \alpha(t)N_d(t) - \int_0^s \omega(\tau)\alpha(t-\tau)N_d(t-\tau)d\tau \end{aligned} \tag{3.6}$$

The age dependent parameters $\delta(t)$ and $\alpha(t)$ were experimentally estimated for ewe follicles. They correspond respectively to the rate of cell cycle exit of the proliferating cells and the rate of differentiating cells entering apoptosis. The cell division rate, μ, was assumed to be constant, and the rate of phagocytosis for apoptotic cells, $\omega(s)$, was considered for cells that had entered apoptosis s hours previously.

The model was analysed for two different kinds of follicles, ovulatory and atretic. For the former, α and hence ω were considered to be zero. The solution for the total number of granulosa cells was well fitted by experimental data and was observed to reach a temporary equilibrium point. This was the result of proliferating cells tending to zero and the differentiating cells reaching a constant number just before the LH surge. Furthermore, they argued that the number of differentiated granulosa cells is directly related to their oestradiol secretion capacity at this stage of follicular development.

For the case of atretic follicles the authors used the same δ as for the ovulatory follicles and the occurrence of apoptosis was added. Cell entry into apoptosis was considered to start after the follicle has reached a fixed age t_A. Before t_A there are no apoptotic cells within the follicle granulosa, and after t_A the apoptotic process quadratically accelerates with time. Different solutions were computed for different follicular ages for the onset of apoptosis (t_A). These solutions were obtained by fixing the value of t_A before and after the follicle has exhausted its proliferating granulosa cells. Then, the different atretic curves obtained were analysed and discussed.

Neither the estimation of δ nor α were in terms of the FSH concentration. Hence, the physiological dependence of follicular growth on gonadotropins was not explicitly introduced into the model. However, what was explained in terms of the model was the causes of different ovulatory rates between monovulatory and polyovulatory ewes. It has been observed that the selected follicles of a multi-ovulatory ewe are smaller than those observed in monovulatory ewes. The difference in size is in both diameter and total granulosa cells number. The justification was based on the difference in the cell cycle duration and FSH sensitivity of the granulosa between the two types of ewes. They finally concluded that since the selection process governing the ovulation rate arises from the interplay of proliferating, differentiating and apoptotic granulosa cells, it would be useful to develop a model which couples the changes in the granulosa cell population in different interacting follicles. Although they were able to depict ovulating and atretic follicles in terms of their granulosa cells, they did not describe this difference in terms of the feedback mechanism which selects one from the other.

3.4 Functional models

The first model interested in studying any kind of control process within ovarian dynamics was the one developed by Lamport in 1940. His attempt was a strictly functional description to show the periodicity of the human menstrual cycle in terms of gonadotropin and estrogen serum levels. However, his approach was somehow incomplete, so his model was not able to fit the existing experimental data reflecting a 28-periodic cycle.

In the following few years Thompson *et al.* as well as Schwartz and Waltz showed that the dynamics of a dominant follicle had to be explicitly coupled to the endocrine system in order to produce oscillations of the circulating blood levels of oestradiol.

The former used FSH concentration interacting with estrogens and the follicle, whilst the latter described their model in terms of LH concentration levels. Instantaneous changes in both models were introduced. Thompson and collaborators fixed an ovulatory size, and Schwartz and Waltz introduced the LH surge dynamics as a decision function. In such a way, the system was able to produce periodic behaviour, not only in the levels of estrogens and gonadotropins but also in the size of the dominant follicle.

A relatively dramatical change in the interest in modelling the control of ovarian dynamics occurred during the seventies. The motivation became more medical since by that time, some treatments for anovulatory women, principally amenorrheic women, were already in use. However, as Vande-Wiele and other collaborators commented, the majority of these treatments were only able to produce spontaneous ovulation in the cycles during which treatment was administrated. Once such treatment stopped, the cycle went back to its anovulatory behaviour. Hence, more information about the actual control mechanisms that the ovarian cycle uses to maintain ovulation was needed. Therefore, four models are described below which study in more depth the various functional and even morphological features that regulate the cycle.

As a consequence, by the end of the seventies little attention was given to describing the selection procedure that keeps the ovulation number constant in terms of functional models. Instead, interest was focused on trying to describe the regulation procedures that makes one follicle actually ovulate in the human menstrual cycle. However, at the beginning of the eighties the first mathematical models considering more than one follicle within the cycle emerged. As a result, some insight into how the selection of the number of ovulating follicles occurs could be offered in terms of mathematical models.

Scaramuzzi and other collaborators gave a theoretical model to explain this characteristic in ewes. The off-spring of these particular mammals is usually fixed at three, however there are cases of monovulatory ewes. This situation can be inconvenient for agricultural purposes. In contrast, the case of more than one follicle being selected is potentially very dangerous for humans. In particular, Lacker and some other workers tackled the particular case of PCOS in women, which has already been described in section 2.3.

Although the models developed during the eighties and nineties had particularly

focused on the ovulation rate, Selgrade and Schlosser [Selgrade and Schlosser, 1999] went back to reproduce the periodicity within the menstrual cycle. They have very recently produced a mathematical model which theoretical analysis was able to prove the existence of a periodic solution of the ovulation cycle. They related the functional dynamics of gonadotropins and steroids with different stages of the cycle. Thus, by describing folliclegenesis as a succession of several ovarian states the mathematical demonstration was achieved.

3.4.1 A functional compartmental model

A particular study of the selection procedure and the determination of the ovulation number (also referred to as the ovulation rate) in the ewe was studied by [Scaramuzzi *et al.*, 1993]. The reproductive endocrinology of the sheep has been the subject of extensive experimental investigation in the last 25 years. A considerable amount of information about the particular feedback relationship between LH pulsatile secretion and FSH secretion by the pituitary has been gathered for the 17-day sheep estrous cycle during this period.

Although Scaramuzzi *et al.* classify follicular development into different stages, a functional description rather than a morphological one is given since follicles within the same physiological stage may be anatomically very different. The authors divided folliclegenesis into five different physiological stages. The first is the stage of primordial follicles followed by the stage of committed follicles (pre-antral follicles with several granulosa cells layers). Gonadotropin-responsive follicles belong to the third stage, followed by gonadotropin-dependent follicles in the fourth, and ovulatory follicles in the fifth stage.

The mechanism that controls the ovulation rate is suggested to be mainly due to the somehow restricted viability of class four follicles. This restriction has many possible reasons. It could be due to the increasing requirement for FSH, it could also be due to the inhibitory feedback activity of the ovulatory follicle and/or due to the limited number of follicles available from the previous class. The authors also suggested that the pituitary sensitivity to oestradiol and inhibin secreted from the ovulatory follicles also affects the availability of class four follicles.

They also proposed that the viability of gonadotropin dependent follicles is indirectly regulated by the hypothalamus-pituitary system by influencing the FSH production rate. Thus, a rapid fall of FSH plasma levels may be associated with

a shorter period of class 4 follicle viability and would favour the development of a single ovulatory follicle. On the other hand, for the case of multiple ovulatory sheep, they suggested two plausible mechanisms. One of them describes the situation where viability of class 4 follicles is increased by extending the length of exposure to FSH or by increasing the follicle sensitivity to FSH stimulation. The other mechanism explains multiple ovulation by an increase of class 3 follicles, possibly achieved by an increase of class 1 follicles.

Despite these results produced by their model, the authors concluded that little is known about the actual effects of FSH on folliclegenesis. In particular despite the central importance of FSH in determining the ovulation rate, there is a poor association between blood FSH concentration and the latter.

3.4.2 Periodicity of the ovarian cycle

The first mathematical model to deal with the cyclical behaviour of the dynamics involving the pituitary (also known as hypophysis) and the ovary is that of [Lamport, 1940]. At that time, the endocrine feedback mechanism between the pituitary and ovary was not biologically completely understood. Therefore, Lamport seems to be the first to try to give a mathematical approach to the field and show that such a mechanism was the cause of the monthly periodicity of the human menstrual cycle.

He developed a mathematical explanation for the previously stated "push/pull" theory of Corner, which in turn was based in former studies by himself and other workers during the thirties. This theory was the first attempt to understand the endocrine feedback loop involved in the cycle. It considers the pituitary gland as the driving force of the clock like see-saw mechanism between hormones produced by the pituitary and the ovary. The theory states in old terminology: "The hypophysis starts the production of oestrin... The rise in oestrin then checks the production of pituitary hormone, which begins to fall as estrous occurs. The oestrin is used up or excreted, or both, and as it falls to a low ebb in the diestrous interval, the hypophysis begins again to produce its hormone." ([Lamport, 1940], p.673).

From four main assumptions, Lamport produced a second order differential equation for what he supposed to be the damped harmonic motion of the circulating estrogen hormone, E. Let r be the secretion rate of the estrogen amount used by the pituitary, and let k be the secretion rate of estrogen produced by the ovary. On the other hand, let q be the production rate of the amount of blood FSH used by

the ovary and let, J and c respectively represent the secretion and clearance rates of effective blood FSH produced by the pituitary. Thus, the equation obtained is

$$\frac{d^2E}{dt^2} + (q+r)\frac{dE}{dt} + (qr+ck)E = kJ. \tag{3.7}$$

The constant parameters in this equation may also be interpreted as mechanical terms of elasticity $(qr + ck)$ and friction $(q + r)$ of the oestradiol dynamics. In theory, simple and damped harmonic motions are possible solutions of this equation. However, non-damped oscillations cannot be obtained for the particular case of the human menstrual cycle since the parameters q and r are non-zero. Otherwise, that would mean that there is no interaction at all between the pituitary gland and the ovary. Hence, Lamport tried to show that the damping $q + r$ was light in order to fit a solution of equation (3.7) to the 28 day period curve that is observed experimentally. However, he failed to prove the existence of cyclic estrogen behaviour for parameter values that were thought to be realistic. Nevertheless, his work served as an important motivation for later mathematical studies published around the seventies.

After a brief discussion and analysis of previous work on modifications to Lamport's model during the fifties, Thompson *et al.* improved the pituitary-ovary system to produce estrogenic monthly oscillations [Thompson *et al.*, 1969]. Their improvement was mainly due to implementation of the growth rate of one dominant ovarian follicle. They also incorporated the luteal phase of the cycle and derived a system of three coupled linear differential equations for the FSH and estrogen blood amounts, and the size of the dominant follicle

$$\begin{aligned}
\frac{dX}{dt} &= k_1(E_1 - \frac{E}{V_E}) + k_2 - k_3\frac{X}{V_X} && (a)\\
\frac{dS}{dt} &= k_4\frac{X}{V_X} \text{ and } S = 0 \text{ when } S \geq S_{max} && (b)\\
\frac{dE}{dt} &= k_6S + k_7 - k_8\frac{E}{V_E}. && (c)
\end{aligned} \tag{3.8}$$

For this case, X and E correspond to the quantity of FSH and oestradiol respectively. V_X and V_E represent the serum volumes which homogeneously contain FSH and oestradiol respectively, and S stands for the size of the dominant follicle. The FSH dynamics is directly proportional to an initial standard concentration of oestradiol, E_1. As the total oestradiol amount increases, in equation (3.8.a) we observe

the negative feedback effect of oestradiol concentration on FSH plasma levels. The constant value k_2 accounts for a minimal FSH production rate existing even though $E_1 = E/V_E$. Furthermore, the dominant follicle growth rate is proportional to FSH concentration, whilst the oestradiol secretion rate is proportional to such a follicle size (see equations (3.8.b) and (3.8.c)). Also, the oestradiol contribution of the remaining non-dominant follicles is considered by the constant production rate k_7 in (3.8.a).

The authors argued that since a complete mathematical analysis of system (3.8) was too complicated, they just studied its behaviour for some particular cases. Therefore, given the corresponding values for the dimensional parameters obtained from physiological data, they were able to show periodic behaviour of the three variables during computer simulations of their equations for the equivalent of 90 days. This model was able to produce oscillatory behaviour for oestradiol by making FSH affect its dynamics in an indirect way. The ovulatory size of the dominant follicle was fixed to a finite value, S_{max}, so that when the follicle reached ovulation it was instantaneously excluded from the system, and a new follicle would start growing again. In such a way, the cycle starts again, and they were able to produce three cycles in 90 days.

A year later, Schwartz and Waltz developed a theoretical model of the rat estrous cycle focusing on blood levels of estrogen and LH, and the timing of ovulation [Schwartz and Waltz, 1970]. The four to five day rat estrous cycle was described biologically and in terms of the theoretical system. *Decision functions* were used to represent the signalling behaviour of the LH surge. In general terms, *decision functions* often used in control systems theory [Mesarovic, 1968] are signalling functions, which are triggered whenever certain conditions are satisfied, *i.e.* if a certain condition is accomplished the system follows a given path, otherwise it follows a different one. A system of three non-linear differential equations was established for LH and estrogen blood concentrations, LH and Es respectively, as well as for the

follicle radius dynamics , Fr, as

$$\begin{aligned} \frac{dLH}{dt} &= -\beta LH - A_2 Es + A_0 + Su \\ \frac{dEs}{dt} &= -\alpha_2 Es + A_3 LH \\ \frac{dFr}{dt} &= \gamma LH(Fr_{min} + Fr). \end{aligned} \tag{3.9}$$

Here, β is the LH loss rate, A_2 represents the negative feedback rate of oestradiol on LH production, A_0 is the tonic constant LH secretion rate, and Su is non-zero when the surge system is activated. Parameter α_2 accounts for the oestradiol loss rate, and A_3 is the gain rate of oestradiol as a result of LH stimulus. Finally, γ is the constant growth rate of the follicle radius.

Since the experimental procedures so far used were not able to distinguish the controlling effects of FSH and LH in the rat estrous cycle, they regarded them as one single hormone. Although dynamics of the dominant follicle was also considered, this time it was not directly affecting the estrogen production rate as in the Thompson *et al.* model. However, the cyclic motion of the system was also artificially introduced by events occurring at discrete points in time after continuous changes of estrogens have reached certain threshold values. As in the previous model, after this threshold was reached, estrogen levels were set at a low rate and the cycle began again.

In this manner, Schwartz and Waltz's model suggested that the process of ovulation itself is crucial for generating the periodicity since the drop of estrogen secretion accompanying ovulation allows the next cycle to commence. This is because of the removal of the negative feedback effects of estrogens on the pituitary gland. However, the usage of decision functions for modelling the LH surge dynamics complicated the system to the extent that it was no longer possible to give any theoretical analysis of its behaviour. The periodic behaviour could thus only be shown by simulation for particular parameter values.

It is important to highlight that the principal topic of interest in ovarian dynamics at the beginning of the forties was that of finding the causes of periodicity of the estrogen dynamics. Lamport intended to show the periodic behaviour of oestradiol was the result of a "light" endocrine feedback mechanism between the pituitary gland and the ovary. He was unsuccessful in doing this since the parameters reflecting such interactions were larger than the maximum his equation required to allow harmonic

solutions.

However, just very recently, Selgrade and Schlosser gave a mathematical demonstration of the periodicity of the human menstrual cycle [Schlosser and Selgrade, 1997]. They were able to analytically prove the existence of a unique solution of the model they derived, which is globally asymptotic with a period of 30 days. Although their model tackles the issue of external effects that could disrupt the cycle, they do not study such a failure at the level of the selection of the ovulatory follicle.

The authors started by developing two different models, one for gonadotropin synthesis and release, and the other for the ovarian production of oestradiol (E_2), progesterone (P_4) and inhibin (Ih). These models are given by coupled systems of non-autonomous linear differential equations. Although the dynamics of pituitary storage of LH and FSH, and the dynamics of gonadotropin plasma levels were treated as different in the models of [Shack *et al.*, 1971; Bogumil *et al.*, 1972a], Selgrade and Schlosser's innovation was to describe gonadotropin synthesis and secretion dynamics separately. In fact, ovarian steroids have different effects on each of these dynamics, *e.g.* for the particular case of LH pituitary synthesis and secretion, oestradiol has positive and negative effects respectively. Moreover, ovarian hormone control of gonadotropin production was introduced by input functions that describe how ovarian hormones change with time. Such functions fitted experimental data reasonably well, and included a delay between steroid changes in the ovary and steroid dynamics at the pituitary level.

For the model of ovarian hormone dynamics, gonadotropin effects were given through input functions explicitly depending on time. The form of these functions was obtained from data provided by [McLachlan *et al.*, 1990], and is given by,

$$\begin{aligned} FSH(t) &= 250 - \frac{250(t-15)^4}{1+(t-15)^4} + 175\exp\left(-\frac{(t-5)^2}{120}\right) + 150\exp\left(-\frac{(t-35)^2}{160}\right) \\ LH(t) &= 380 - \frac{352(t-15)^4}{1+(t-15)^4}. \end{aligned}$$

Despite the fact they did not explicitly introduce a variable describing any kind of follicle measure, the authors described the dynamics of the ovarian hormone *capacity* for the follicular and luteal phases of the cycle. Hence, the ovarian dynamics for each

stage of the cycle is given by

$$\begin{aligned}
\frac{d}{dt}MsF &= bFSH(t) + [c_1 FSH(t) - c_2(LH(t))^a]MsF \\
\frac{d}{dt}GrF &= c_2(LH(t))^a MsF + [c_3(LH(t))^a - c_4 LH(t)]GrF \\
\frac{d}{dt}PrF &= c_4 LH(t)GrF - c_5(LH(t))^a PrF \\
\frac{d}{dt}Sc_1 &= c_5(LH(t))^a PrF - d_1 Sc_1 \\
\frac{d}{dt}Sc_2 &= d_1 Sc_1 - d_2 Sc_2 \\
\frac{d}{dt}Lut_1 &= d_2 Sc_2 - k_1 Lut_1 \\
\frac{d}{dt}Lut_2 &= k_1 Lut_1 - k_2 Lut_2 \\
\frac{d}{dt}Lut_3 &= k_2 Lut_2 - k_3 Lut_3 \\
\frac{d}{dt}Lut_4 &= k_2 Lut_2 - k_3 Lut_3
\end{aligned} \tag{3.10}$$

where MsF represents the hormone capacity variable during the menstrual stage, *i.e.* early follicular stage, GrF is the variable for the follicle growth stage, that is before selection takes place, PrF describes the pre-ovulatory follicular stage, Sc_1 and Sc_2 describe the transition from the follicular to the luteal phase when the follicle has ovulated leaving an *ovulatory scar*, and each of the Lut_i for $i = 1, \cdots, 4$ represent four different stages of the luteal phase. Such luteal stages are chosen to put capacity peaks at times which correspond to experimental data. In this way they avoided the need to incorporate delay effects in the differential equations which would complicate subsequent analysis of the model.

The authors assume that E_2, P_4 and Ih serum levels were constant since their clearance rates are fast enough. Thus, they considered them proportional to the hormone capacity of the appropriate stage of the cycle as follows,

$$\begin{aligned}
E_2(t) &= e_0 + e_1 GrF(t) + e_2 PrF(t) + e_3 Lut_4(t) \\
P_4(t) &= p_1 Lut_3(t) + p_2 Lut_4(t) \\
Ih(t) &= h_0 + h_1 PrF(t) + h_2 Lut_2(t) + h_3 Lut_3(t) + h_4 Lut_4(t)
\end{aligned}$$

Although system (3.10) could be solved analytically, its solutions did not give any

insight into the qualitative behaviour of ovarian dynamics. Furthermore, they were not useful for parameter estimation. Thus, parameters were estimated numerically. The authors also gave a mathematical proof to show that the system has a unique globally asymptotic solution with a period of 30 days. This period was the same as that used for the input gonadotropin functions in system (3.10). This means that women having the same gonadotropin profile will have the same ovarian hormone behaviour.

Once these two models were established the idea is to merge them together to obtain a non-linear system of differential equations describing the five hormones involved in the whole cycle. The main motivation for the development of this model was to predict the effects of hormonally active environmental substances on the menstrual cycle. Such environmental effects may disrupt the cycle at several levels, however the authors did not mention any kind of failure at the level of selection of the ovulatory follicle. Hence, their model does not describe the control of the ovulatory number. However, for the transition between the follicular growth stage and the pre-ovulatory stage shown in the second and third equations of system (3.10), they proposed a process entirely depending on the full effects of LH. Even though they did not give any kind of justification for this assumption, we suppose that they considered this transition step to be solely dependent on LH because sufficient FSH is no longer available by that time of the cycle.

3.4.3 Folliclegenesis and hormonal interactions

During the seventies, the mathematical models developed were not interested in "proving" the periodic behaviour of estrogens anymore. Rather, they tried to reflect, as accurately as possible, the different control mechanisms that relate the various endocrine hormones and follicular development within the cycle. Like the preceding models, their complexity increased to a great extent, and their analytical study was minimal.

Specifically, four mathematical models for the particular case of the human menstrual cycle were developed in these years [Vande-Wiele *et al.*, 1970; Shack *et al.*, 1971; Bogumil *et al.*, 1972a; Bogumil *et al.*, 1972b; Feng *et al.*, 1977]. Most of them were refinements of earlier models, and concentrated on describing the regulation mechanisms within the cycle in a more robust way. All of them were deterministic models incorporating both follicular development of one or more follicles and

hormonal interactions.

For Vande-Wiele *et al.* one of the most important reasons that justified the formulation of their model was the numerous cases of anovulatory women. Although many clinical treatments had been able to produce spontaneous ovulation in women with anovulatory cycles, in most of these it was observed that after treatment the cycle became anovulatory once again. Therefore there was a real need to understand the way in which the most important features involved in the cycle interact resulting in the spontaneous ovulation of one follicle.

To start their analysis, they were interested in studying the particular relationship between FSH and estrogens [Vande-Wiele *et al.*, 1970]. The FSH and LH blood concentrations with respect to oestradiol concentration were fitted from experimental data as

$$\begin{aligned} FSH &= a_1 e^{-\alpha_1 EST} + a_2 e^{-\alpha_2 EST} + a_3 \\ LH &= \frac{1}{2}\left(a_1 e^{-\alpha_1 EST} + a_2 e^{-\alpha_2 EST} + a_3\right) + SURGE\ LH \end{aligned} \tag{3.11}$$

([Shack *et al.*, 1971], p.838). Notice that the FSH and LH concentrations identically decrease with respect to the oestradiol concentration before the LH surge takes place. In the experimental data obtained for the changes of both LH and FSH with respect to oestradiol levels in regular menstrual cycles, they considered LH to vary just like FSH before the surge takes place. However, the variation in LH concentration throughout the cycle is about 1/2 of that of FSH. This negative effect of oestradiol upon LH tonic secretion is questionable since now a days it is believed that the frequency of pituitary pulsatil LH secretion increases during the follicular phase of the cycle due to the positive effects of oestradiol [Austin and Short, 1984].

Since the ovarian response to gonadotropins is even harder to analyse, the authors introduced the *measure* of a follicle to represent changes of follicular sensitivity to LH and FSH during its maturation process. They postulated growth rate equations for two kinds of follicles, the pre-ovulatory large follicles and the remaining smaller ones. No atresia was incorporated for the small non-selected follicles. To model the effects of gonadotropins on ovarian hormone levels they also considered the complex ovarian local behaviour of androgens. Functions of oestradiol and androgen serum concentration with respect to FSH and follicle measures were given as,

$$\begin{aligned} EST &= EST_T + Fs_1 FSH \\ AND &= AND_A + Fs_2 FSH, \end{aligned} \tag{3.12}$$

([Shack *et al.*, 1971], p.838), where EST_T represents tonic levels of estrogens obtained from the contribution of androgens from the adrenal gland, And_A represent the androgens secreted by the adrenal gland, and Fs_i, for $i = 1, 2$, stands for the functions with respect to the two follicle *measures* considered. These are given as

$$Fs_i = a^i(MF_i - 1.0)^2 + 25(MF_i - 0.008)^2.$$

Furthermore, the growth rate equation for the two kinds of follicles is given by,

$$\frac{dMF_i}{dt} = [a_3(FSH)(LH) + a_4(EST) - a_5^i(AND)](MF_i)^2 - a_6(MF_i)^3 \qquad (3.13)$$

for $i = 1, 2$ ([Vande-Wiele *et al.*, 1970], p.73). If we interpret the follicle measure by its radius, we observe that follicular radius rate is proportional to the effects of both gonadotropins and oestradiol concentration distributed on the surface of the follicle. At the same time, androgen concentration on the follicle area has a negative effect, and to avoid the dominant follicle from reaching explosive values, its growth rate is restricted by its own volume.

Although the regulation mechanisms during pre-ovulatory and post-ovulatory stages were analysed, the authors only developed a mathematical model valid up to ovulation. Specifically, for this complicated model a *threshold* dynamics was introduced for the LH surge with an example of the resulting behaviour due to two different threshold values. Although this model was able to qualitatively explain the regulatory mechanism during the first part of the menstrual cycle in humans, it was unable to produce quantitative information about the functional relationships amongst the different variables. The right combination of the time of the LH surge and of the follicle acquiring maturity were shown to be the key for successful ovulation. While numerical simulations of this model were able to explain the functional relationships amongst the variables considered (gonadotropins, follicular hormones and follicle size) in a qualitative way, quantitative information could not be derived.

Moreover, despite the fact that the authors mentioned *amenorreha* as a failure in spontaneous ovulation present in the human menstrual cycle, their model does not exhibit such abnormal behaviour.

The primary variables used in the model of Shack *et al.* are similar to those of Vande-Wiele *et al.*, but different assumptions were made for the derivation of their model [Shack *et al.*, 1971]. The whole ovarian cycle is modelled and interactions between gonadotropins, estrogens, progesterone, one follicle and one corpus luteum are

described in a system of five first order differential equations. Gonadotropin plasma levels and pituitary storage are considered separately. Additionally, estrogen and progesterone produced by the adrenal gland are also taken into account. Ovulation time, LH surge and transition of the ovulatory follicle into a corpus luteum are introduced by *decision functions.* Furthermore, the follicle is also assumed to produce estrogens and the contribution to the follicular estrogen production of selected and regressing follicles are represented separately. The resulting equations for the model are

$$\begin{aligned}
\frac{dFSH}{dt} &= FSH_T - cl_1 FSH - EST_1 - Prod_1(PROG) + \frac{dSFSH}{dt} \\
\frac{dLH}{dt} &= LH_T - cl_2 LH - EST_2 - Prod_2(PROG) + \frac{dSLH}{dt} \\
\frac{dFLS}{dt} &= \begin{cases} 0 & \text{if } FSH < FSHC \\ F(1 - \exp(-f * FSH * LH)) & \text{if } FSH \geq FSHC \end{cases} \\
\frac{dPROG}{dt} &= PROG_T - cl_3 PROG + CPL \\
\frac{dEST}{dt} &= EST_T - cl_4 EST - FLEST + E(CPL).
\end{aligned} \tag{3.14}$$

Variables LH, FSH, $PROG$ and EST represent plasma levels of the corresponding hormones. Pituitary tonic secretion of gonadotropins is represented by FSH_T and LH_T respectively. Parameters cl_i for $i = 1, \cdots, 4$ describe clearance rates of FSH, LH, progesterone and oestradiol respectively. $Prod_j(PROG)$, for $j = 1, 2$ are functions describing the negative feedback effect of progesterone on FSH and LH production respectively, and $dSFSH/dt$, $dSLH/dt$ are surge FSH and surge LH contribution to the FSH and LH dynamics respectively. Follicular growth is given by the FLS equation, where the threshold value $FSHC$ is the FSH serum level at which follicles start growing. CPL represents the corpus luteum contribution to progesterone production, while $E(CPL)$ corresponds to the corpus luteum oestradiol production. The adrenal contribution of steroids is depicted by $PROG_T$ and EST_T, and $FLEST$ is the follicular oestradiol production.

The authors particularly argued that since the mechanisms that determine when ovulation occurs as well as when the follicle starts changing into a corpus luteum are basically unknown, the model should consider three important features. First of all, ovulation will not occur without an LH surge as the follicle approaches its full

maturity. Therefore, if the LH surge does not happen, the growing follicle regresses without transforming into a corpus luteum. Finally, the follicle begins its progesterone production before ovulation, a function which had been mainly observed from the corpus luteum. Although the authors did not compare the results of their simulations with experimental data, parameter values used for the model were obtained from data found in the literature. And as we have said before, results obtained for parameter values experimentally observed gave rise to functional relationships between hormonal levels and these three signalling procedures.

The model developed by Bogumil *et al.* is probably the most complete of all since it involves morphological and physiological representations of most of the different components of the whole menstrual cycle [Bogumil *et al.*, 1972a]. They are modelled using 34 equations involving nonlinear terms and time dependent coefficients. In particular, FSH dynamics, tonic LH and LH surge dynamics are depicted by three different equations. Storage and plasma LH levels are again considered separately and besides, there are two different LH pituitary compartments with different change rate dynamics.

As far as folliclegenesis is concerned, the physiology and anatomy of two different kinds of follicles is considered. The authors particularly described the number of follicles at a given time as an equilibrium number of recently growing follicles and atretic follicles. Such a balance was thought to be induced by FSH accumulated in the preceding days. The dynamics of antrum formation in the follicle is also taken into account as a function of gonadotropin and oestradiol levels. For a description of the luteal phase, four different kinds of follicular cells are used as the selected follicle develops to form the corpus luteum after the LH surge and ovulation. Such a follicular transformation is reflected in the corresponding differential equations for the four kinds of cells.

Finally, the physiological role of follicles during the menstrual cycle is also incorporated. A steroid secretory potential is introduced for large and small follicles. The follicular conversion of androgens into oestradiol is also considered, and the controlling mechanisms for androgen and oestradiol secretion are similarly represented. Androgens and progesterone secretion during the luteal phase is influenced by the morphological dynamics of follicular cells as well as by LH plasma levels during that particular period of the cycle.

The analysis of the numerical results produced by this model was published in

a subsequent paper [Bogumil *et al.*, 1972b]. The agreement of their model to experiment is shown to be good. However, they made the following comment: "... it is not difficult to write equations which have solutions that fit an arbitrary curve. The value of simulation lies not in programming a computer to plot a curve but rather in the ability to analyse the mechanisms and conditions which yield the resultant response." ([Bogumil *et al.*, 1972b], p.48). Therefore, they also investigated some stochastic variations of their model which led them to other interesting results regarding the control mechanism itself. They showed that short duration random effects may influence the model to an extent that the length of the pre-ovulatory period may change as well as the LH surge characteristics. More importantly, these effects may alter the selection process causing transient anovulatory episodes, which are independent of any kind of pathology.

Therefore, a new control mechanism within the cycle that had not been previously considered was also proposed. This suggested that instead of the control mechanisms depending on hormonal levels or on the rate of change of such hormonal levels at a given time in the cycle (as had been conventionally assumed until then), the authors proposed such control mechanisms were the result of a low amplitude and short duration incremental changes in the hormone levels occurring many times a day. Moreover, artificial external random alterations implemented in their model revealed interesting behaviour in terms of the selection process.

Five years later, Feng *et al.* discussed the work of Bogumil *et al.* and derived a modified improved model based on specific problems occurring in Bogumil's model [Feng *et al.*, 1977]. They established a family of simultaneous differential, algebraic and logical equations for the definition of the model, and produced some numerical solutions. They were concerned with modelling physiological features more than morphological ones. Also, they thoroughly studied the feedback mechanism between pituitary LH production and ovarian oestradiol secretion. Hence, their major improvement was the introduction of a "hypothalamic-pituitary clock" that regulated the pulsatile secretion of LH in response to oestradiol stimulation. Therefore, the superimposed random fluctuations suggested by Bogumil and collaborators was substituted by inherent pulsatile LH secretion. They also introduced delayed responses of the LH and FSH induced ovarian production of oestradiol.

From these four models developed during the seventies we could say that Vande-Wiele *et al.* and Bogumil *el at.* were the only ones which described any kind of

failure in the spontaneous ovulation process. In the former this was due to bad synchronisation between appropriate follicular development and LH surge timing. In the latter this arose as a result of external random fluctuations affecting the system. Such variations could be interpreted as any kind of external physiological effect (including any kind of pathology) or behaviour that could interfere with the metabolism. However, neither of these gives any insight into the regulation of the number of ovulating follicles.

Furthermore, it is observed that the implementation of artificial decision functions for the simulation of events like the LH surge, ovulation and follicular transition into the corpus luteum is a way to overcome the lack of knowledge of the actual physiological and morphological development of these events. This fact only permitted the derivation of computational more than mathematical models since the analytic analysis was impossible. However, these models were a strong motivation for further mathematical modelling of ovarian dynamics. Moreover, they served as way of clarifying some of the basis in which the relevant hormones interact and the role of folliclegenesis in the control of spontaneous ovulation.

3.4.4 Control of the ovulation number

Despite the high level of biological information incorporated into such mathematical models during the seventies, they were largely unable to give any insight into the control of the ovulation number. This is mainly because the primary motivation behind these models was the accurate description of the dynamics of hormone levels, rather than that of follicle selection.

This problem was first addressed by Lacker and various collaborators. He developed a much simpler model than the extremely complicated systems published in the seventies. Despite the fact that its equations were not biologically justified and the great extent of the simplification of the endocrine system, they were able to offer insight into the selection procedure. Results of this model were shown to be consistent with experimental observations [Meuli *et al.*, 1987]. The selection process was regarded as a kind of competition amongst many interacting follicles. This model has been an important motivation for new research of the ovulation cycle. Thus at the beginning of the nineties, Mariana *et al.* discussed and modified this model and Thalabard *et al.* developed the stochastic version of the selection of the ovulatory follicle.

During the eighties Lacker and various collaborators published a number of papers focusing on this problem [Lacker, 1981; Lacker *et al.*, 1987; Lacker and Akin, 1988; Lacker and Percus, 1991]. In Lacker's first paper of 1981, he developed a deterministic model that for the first time reflected the dynamics of many interacting follicles. This is given by a system of non-linear differential equations assuming the same growth rate for each follicle. Such a growth rate implicitly involved the effects of FSH and LH, which were considered as a single hormone. Further papers were about the analysis and improvements of the model.

However, the symmetry assumed for his model has the consequence of the largest follicles being always the ones selected to ovulate. This hierarchy is not necessarily kept for all mammals. Furthermore, Lacker's model is able to produce non-ovulatory mature follicles that despite being selected they remain with a stable pre-ovulatory maturity and never ovulate. Although this feature can be interpreted as PCOS, it does not reflect the behaviour observed in reality. Therefore, in chapter 5 detailed description of Lacker's model is given to the case of non-identical growth functions as well as a generalisation of the stability analysis (also look at [Chávez-Ross *et al.*, 1997]). Moreover, due to its relevance to the aims of this thesis, the particular modification subsequently published by [Mariana *et al.*, 1994] is also analysed and discussed in chapter 6.

In 1989, Thalabard *et al.* produced a model described by a set of stochastic differential equations, which also simulated the interaction of many follicles during the follicular phase of the cycle. Emergence of the ovulatory follicle from a population of follicles with identical initial maturities was also seen in this model. Unlike Lacker's model, the ovulatory follicle that emerges is not necessarily the one that starts growing fastest. Differences between follicles which obey the same deterministic growth law were introduced via random fluctuations once the cycle had been initiated. This randomness may be a reflection of the unknown way in which follicles react to gonadotropin stimulation or could be a stochastic feature inherent in the biological system as has been proposed by Baird in [Ledger and Baird, 1995]. Furthermore, the feedback control of the cycle was established by making the growth rate of the follicles dependent on FSH concentrations. Although proportional to each other, follicle size and oestradiol production were described by different variables. Due to the stochastic nature of the model, a numerical simulation was the only possible way of analysing the system. This model gave a good stochastic approach to the selection

process at a global macroscopic level.

3.5 Discussion

The review of the mathematical models of the ovarian cycle developed in the present chapter has classified them into two basic categories. The first one includes descriptive models, which are based on morphological criteria, and the second one describe functional models mainly based on physiological representations of the cycle.

Descriptive models are basically compartmental models which either classify follicular population or granulosa cells of a single follicle into different stages of development. In the former, stochastic and deterministic approaches are given, which are used to determine the migration and death rates from each compartment. Interesting results about migration rates to the compartment of selectable follicles and death rates of follicles from the first compartment are obtained for mammals of different ages.

Particularly, for the case of humans, a considerable reduction of migration rate from the selectable stage is registered for women older than 38 years of age. Moreover, an increase of the atresia rate of stage one follicles is also observed for these women. However, all of these results regard atresia as an important factor regulating follicular population rather than a factor providing an insight into the control mechanism that keeps the ovulation rate constant.

For the model in terms of granulosa cells of the follicle, migration and death rates are experimentally measured from ewes' follicles. However, no apoptosis is considered at all when describing growth of follicles that reach pre-ovulatory size. Whereas in the case of atretic follicles, a discrete function for the apoptosis rate is considered. This model is the first mathematical description of follicular development in terms of granulosa cells, but no suggestions are made about the selection process itself. It appears, that once some apoptosis appears within the granulosa of the follicle, there is no chance of surviving and atresia is the fate of the follicle. Although it is clear that selection of pre-ovulatory follicles is the result of a dynamic equilibrium between proliferating, differentiating and apoptotic granulosa cells, this is not expressed in terms of any kind of endocrine feedback mechanism.

We may conclude that descriptive models are insufficient to understand the regulation of the selection of pre-ovulatory follicles, so functional models are considered.

Functional models relate physiological and morphological changes of the different components of the menstrual cycle. The central importance of the dominant follicle within the system in order to produce a periodic behaviour of estrogens is shown by Thomson *et al.* Schwartz and Waltz also introduce an explicit variable for follicular development to show that ovulation is crucial to produce periodicity of the cycle. However, the introduction of instantaneous or decision functions complicate the system to an extent that no theoretical analysis is provided. It is not until very recently when Selgrade and Schlosser are able to theoretically demonstrate the approximately 30-day period of the human menstrual cycle.

With the basic aim to improve anovulation treatments more complicated models are developed. They try to incorporate as many factors as possible that are thought to generate spontaneous ovulation every cycle. The results are extremely complicated models that at best can give qualitative insight into the problem. Only the models of Vande-Wiele *et al.* and Bogumil *et al.* describe a failure in spontaneous ovulation.

The functional compartmental model of Scaramuzzi *et al.* investigates the number of ovulating follicles in terms of the pituitary-ovary feedback system. They discretised folliclegenesis in physiological conditions, and explain the mechanism that regulates the ovulation rate in terms of the availability of follicles of the different classes, and their exposure to FSH concentrations. They analyse the particular cases of monovulatory and multi-ovulatory ewes. It is worth mentioning that Clément *et al.* also provide some suggestions for possible causes of follicle number variation in these types of ewes. They do this in terms of the granulosa cell proliferation rate and granulosa cell sensitivity to FSH stimulation.

However, the first model incorporating folliclegenesis and gonadotropin feedback mechanism in a system of $N \geq 1$ interacting follicles is provided by Lacker. Therefore, pre-ovulatory follicles are selected from atretic follicles in a functional way. This suggests how follicles' sensitivity to gonadotropins interfere in the feedback loop, and cannot only produce variations in the number of selected follicles, but can either produce anovulation or ovulation depending on the parameter or initial condition of the system.

Although all of the above models have contributed a great deal to the understanding of ovarian dynamics and most of all, provide fruitful ways of relating mathematical with biological knowledge, Lacker's model is the one that best addresses the control of the number of selected follicles problem. Therefore, we consider it to

be the starting point of our study, and the basic motivation for the models analysed and developed later on.

Chapter 4

LACKER'S SYMMETRIC MODEL

4.1 Introduction

From the number of models of the control of ovulation rate which have been described in the previous chapter (*e.g.* [Lacker, 1981; Akin and Lacker, 1984; Lacker *et al.*, 1987; Lacker and Akin, 1988; Lacker and Percus, 1991; Thalabard *et al.*, 1989; Scaramuzzi *et al.*, 1993; Mariana *et al.*, 1994]), those developed by Lacker and his group are by far the most studied and best understood, and will be the starting point of our analysis. Based on simple qualitative assumptions about the primary hormonal feedback loop involving the pituitary, Lacker's model is able to reflect most of the basic physiological features of the ovulation cycle in mammals, including the regulation of the ovulation number, the fact that almost all of the follicles that start a given cycle atrophy and die, and the fact that it is possible for follicles to arrest at an intermediate stage, neither ovulating nor degenerating through atresia.

However Lacker's model in its present form is incapable of successfully modelling the qualitative features of *polycystic ovaries* (PCO) in humans. As we shall see later in this chapter, if the model's parameters are set to values appropriate for humans (*i.e.* one follicle ovulating per cycle) it is impossible to obtain a situation where more than a single follicle can arrest. One can of course achieve the arrest of a larger number of follicles by drastic changes in the parameters. However, this pushes the model into regimes characterised by a large number of follicles ovulating in each cycle, and is hence unrealistic in the human case. Since PCO covers a whole spectrum of conditions, ranging from almost normal ovulation to the most severe cases of anovulation, we do not expect to have to make large changes to the model

to move from normal to PCO behaviour and vice versa. Indeed, since it is possible to find individuals who switch between approximately normal ovulatory cycles and anovulation apparently at random, it should be feasible to observe both types of behaviour for a single set of parameters, just by changing the initial conditions at the start of a cycle (*i.e.* the number and precise maturity of the follicles entering that cycle).

Lacker's model has also been criticised [Thalabard *et al.*, 1989; Mariana *et al.*, 1994] because it maintains a strict hierarchy amongst the follicles developing in a given cycle. Thus, follicles which start out largest remain the largest and hence are the ones that ovulate. This feature is unrealistic, and it has been biologically proposed that the selected follicles are amongst the largest ones they are not necessarily the largest [Gougeon and Lefèvre, 1983; Ledger and Baird, 1995]. Since the maturity of the follicle is determined by both size and oestradiol production, its selection seems to depend on the right combination of these two characteristics. Besides, the way follicles react to hormone stimulation has not yet been well determined, and it cannot be only thought to be proportional to its oestradiol secretion. Therefore, although it is possible to assume that the largest follicle produces the largest amount of oestradiol it is not necessarily the one being selected. Therefore, the largest follicles are not always the ones selected. Both Thalabard *et al.* [Thalabard *et al.*, 1989], and Mariana *et al.* [Mariana *et al.*, 1994] have proposed models which overcome this restriction, but neither of these appears to be amenable to the same level of rigorous analysis as it is possible with Lacker's model. We shall particularly discuss this for the Mariana model in chapter 6.

4.2 Lacker's symmetric model of the ovulation cycle

In this section we briefly describe the model developed and analysed by Lacker and his collaborators (*e.g.* [Lacker, 1981; Akin and Lacker, 1984; Lacker *et al.*, 1987; Lacker and Akin, 1988; Lacker and Percus, 1991]). The model seeks to describe the maturation of a group of N follicles, and their interaction via oestradiol and the gonadotropins with the pituitary using a system of N non-linear differential equations which are the same for each follicle.

4.2.1 Assumptions and formulation of the model

We start by describing the assumptions behind the model and the formulation of the model. Each maturing follicle produces oestradiol which is released into the blood circulation. The larger and more mature the follicle is the more oestradiol it produces. The oestradiol levels in the blood stream have a negative effect on the rate of release of gonadotropins (FSH and LH) by the pituitary, and these gonadotropins in turn stimulate the growth of the follicles and their production of oestradiol (FSH and LH do play somewhat different roles, but this is ignored in Lacker's model). Overall, therefore the feedback loop is a negative one: the larger and more mature the follicles are, the less FSH and LH is released by the pituitary, which serves to limit the further growth of the follicles. However, because more mature follicles are more sensitive to FSH and LH their growth is restricted less. This serves to amplify differences between follicles with the larger and more mature ones being selected to ovulate, and the others first arresting their growth, and then becoming atretic.

For the purposes of the models described here the effect of GnRH in the pituitary is assumed to be constant in time, and hence can be ignored in the selection process. Furthermore, the pulsatile behaviour of the LH secretion is also ignored. Note also that just prior to ovulation the sign of the feedback in the pituitary changes, leading to the so called LH surge. This again is not incorporated in Lacker's model, since by the time of the surge the ovulating follicles have already been selected.

In summary, the model is based on the following simplifying assumptions:

a) Follicle size, maturity and oestradiol secretion are all proportional.

b) The rate of release of FSH and LH is a function of the blood concentration of oestradiol.

c) The growth rate of a follicle is determined by the blood concentration of FSH and LH, and the follicle's own maturity.

d) All follicles respond identically to FSH and LH and obey the same growth law.

e) No distinction is made between the effects of FSH and LH, which are represented implicitly through their assumed control by a single hormone.

f) The effect of GnRH is ignored.

g) Hormonal clearance rates as well as pituitary response to circulating oestradiol are relatively fast compared to the selection process, and hence hormone levels and pituitary response are always assumed to be in equilibrium.

Each follicle is therefore modelled by a single variable x_i which reflects its size and hence its maturity and oestradiol production. Follicles interact among themselves *via* their contribution to the total blood concentration of oestradiol. In a way, they compete between each other in order to be the ones able to ovulate. The growth rate of the ith follicle is thus some function $g(x_i, X)$ of the follicle size x_i and the total circulating oestradiol concentration X, where

$$X = \sum_{i=1}^{N} x_i. \tag{4.1}$$

The function g incorporates both the response of the pituitary to oestradiol and the follicle response to the resulting levels of FSH and LH. Since follicles are assumed identical, we have the same function g for each one of them. The dynamics of the ith follicle is therefore given by

$$\frac{dx_i}{dt} = x_i g(x_i, X). \tag{4.2}$$

This was first deduced by Lacker in 1981, [Lacker, 1981]. Considering h_1 and h_2 as FSH and LH blood concentrations respectively, and σ_1 and σ_2 as their correspondent secretion rates, the dynamics of FSH and LH concentrations are given by,

$$\frac{V dh_i}{dt} = \sigma_i - \gamma_i h_i \quad \text{for} \quad i = 1, 2 \tag{4.3}$$

where V is the blood or serum volume and γ_1 and γ_2, the FSH and LH serum clearance rates respectively. On the other hand, the dynamics for the total amount of oestradiol is:

$$\frac{V dX}{dt} = \sum_{i=1}^{N} s_i - \gamma_3 X \tag{4.4}$$

where s_i is the oestradiol secretion rate of each follicle i and γ_3 the corresponding oestradiol serum clearance rate.

It has been observed that hormone serum dynamics is much faster than that of folliclegenesis [Cargille *et al.*, 1969]. Whilst hormones take just a few minutes to reach their corresponding target organs, the time required for a follicle to pass

through different steps of maturity is on the order of weeks. Thus, it is assumed that:

$$\frac{dh_1}{dt} = \frac{dh_2}{dt} = \frac{dX}{dt} = 0. \tag{4.5}$$

Therefore, from (4.4) and (4.1) we get,

$$\sum_{i=1}^{N} s_i = \gamma_3 \sum_{i=1}^{N} x_i \Rightarrow x_i = \frac{s_i}{\gamma_3}.$$

In contrast, the dynamics suggested for the oestradiol production of a follicle is a function of the follicle's own oestradiol secretion rate and of FSH and LH concentrations, such that:

$$\frac{ds_i}{dt} = \bar{f}(s_i, h_1, h_2). \tag{4.6}$$

Hence, from (4.3) and the equilibrium assumption (4.5) we get,

$$\frac{ds_i}{dt} = \gamma_3 \frac{dx_i}{dt} = \bar{f}(\gamma_3 x_i, \frac{\sigma_1}{\gamma_1}, \frac{\sigma_2}{\gamma_2}),$$

redefining,

$$f(x_i, X) = \frac{1}{\gamma_3} \bar{f}(\gamma_3 x_i, \frac{\sigma_1}{\gamma_1}, \frac{\sigma_2}{\gamma_2}).$$

Therefore, Lacker also considered each ratio σ_i/γ_i for $i = 1, 2$ as functions of X; thus, he obtained the system

$$\frac{dx_i}{dt} = f(x_i, X),$$

for all $i = 1, \cdots, N$, which he re-wrote as (4.2). Initial conditions of each follicle maturity value are chosen essentially arbitrarily.

Given that the selection process may be viewed as a competitive one it is not surprising that the above model has much in common with models of competition used in ecology or evolution (*e.g.* [Hofbauer and Sigmund, 1988]).

4.2.2 Analysis of the model and results

Since the above model is far too general to be analysed, Akin and Lacker make the assumption that the growth function g can be separated in the following way [Akin and Lacker, 1984]:

$$g(x_i, X) = \delta(X)[\rho(X) + \xi(p_i)] \tag{4.7}$$

where

$$p_i = \frac{x_i}{X}$$

is the relative maturity of the ith follicle, *i.e.* the oestradiol production of the ith follicle relative to the total oestradiol concentration. Note that without loss of generality we may assume $\xi(0) = 0$, as otherwise we may replace ξ by $\xi - \xi(0)$ and ρ by $\rho + \xi(0)$ without changing the dynamics. The function ρ is assumed to be monotone decreasing for $X > 0$ and $\rho(X) \to -D$ for some constant $D > 0$ as $X \to \infty$, and $\rho(X) \to \infty$ as $X \to 0$.

When g is of the form (4.7), the dynamics of p_i can be written as:

$$\frac{dp_i}{d\tau} = p_i[\xi(p_i) - \bar{\xi}(p)] \tag{4.8}$$

where, $p = (p_1, \ldots, p_N)$ and

$$\begin{aligned} \bar{\xi}(p) &= \sum_{i=1}^{N} p_i \xi(p_i) \\ \sum_{i=1}^{N} p_i &= 1. \end{aligned} \tag{4.9}$$

This new system is referred as the *interaction dynamics* where τ is the new rescaled time defined in terms of the *rescaled time function* $\delta(X)$ as,

$$\frac{d\tau}{dt} = \delta(X). \tag{4.10}$$

The derivation of these equations can be found in for instance [Akin and Lacker, 1984], and is also given in the more general case of non-identical follicles in the next chapter.

System (4.8) can be transformed into a gradient system on the unit $N-1$ sphere S, which implies that all initial conditions ultimately tend to some equilibrium point of the system. This means that there is neither oscillatory nor any other kind of complex behaviour within the dynamics (see Appendix (4.A)). The conditions for this equilibrium point in terms of the *interaction dynamics* are either:

$$\begin{aligned} p_i &= 0 \\ &\text{or} \\ \xi(p_i) &= \bar{\xi}(p). \end{aligned} \tag{4.11}$$

Thus at an equilibrium point all non-zero p_i must have the same value of ξ. The stability for the resulting equilibrium point is determined by the common value $\bar{\xi}(p)$ which we shall denote as λ, and by the interaction function $\xi(p_i)$. More precisely,

if the equilibrium point is non-degenerate then it is stable if and only if $\lambda > 0$ and $\xi'(p_i) < 0$ for all non-zero p_i or $\xi'(p_i) \geq 0$ for exactly one non-zero p_i and

$$\sum_{i=1}^{M} \frac{1}{\xi'(p_i)} > 0$$

[Akin and Lacker, 1984], see below.

An equilibrium point of the interaction dynamics can correspond to ovulatory and anovulatory cases depending on the value of λ, and the behaviour of the *intensity dynamics*

$$\frac{dX}{d\tau} = X[\rho(X) + \bar{\xi}(p)]$$

which governs the total concentration of circulating oestradiol. The ovulatory case is characterised by $\rho(X) + \bar{\xi}(p) > 0$, so that X grows without bound (in the biological system it of course cannot grow infinitely, and one assumes that when it reaches a sufficiently large value an LH surge is triggered, followed by ovulation). The anovulatory case occurs when the intensity dynamics has a fixed point, *i.e.* a value of $X > 0$ such that $\rho(X)+\bar{\xi}(p) = 0$; follicles can then grow to a given size but no further. Akin and Lacker also analyse the dynamics of the *time rescaling function* $\delta(X)$ for both situations, finding that under reasonable conditions on δ, in the ovulatory case there is a finite value of T in which X grows to infinity; this is interpreted as the time taken to ovulate [Akin and Lacker, 1984].

The fact that the growth function ξ is the same for all follicles, results in a symmetric situation for which the symmetric point that satisfies both equilibrium conditions of the *interaction dynamics* is:

$$p_i = \begin{cases} \frac{1}{M} & 1 \leq i \leq M \\ 0 & M < i \leq N \end{cases}$$

for some $0 < M \leq N$. The above stability analysis shows that this is stable if $\xi(1/M) > 0$ and $\xi'(1/M) < 0$.

The particular growth function proposed by Lacker is:

$$g(x_i, X) = K - D(X - M_1 x_i)(X - M_2 x_i) \tag{4.12}$$

where D, K, M_1 and M_2 are parameters. With out loss of generality $M_1 < M_2$ and

$$\frac{1}{M_1} + \frac{1}{M_2} < 1 \tag{4.13}$$

(by rescaling we may assume $K = 1$). In this case

$$\begin{aligned} \xi(p_i) &= Dp_i(M_1 + M_2 - M_1M_2p_i) \\ \rho(X) &= \frac{K}{X^2} - D \\ \delta(X) &= X^2. \end{aligned} \tag{4.14}$$

The symmetric equilibrium is then stable for all M such that:

$$\frac{1}{M_H} < \frac{1}{M} < \frac{2}{M_H}$$

where M_H is the harmonic mean of M_1 and M_2:

$$\frac{1}{M_H} = \frac{1}{2}\left(\frac{1}{M_1} + \frac{1}{M_2}\right).$$

Thanks to assumption (4.13) it can be shown geometrically that non-symmetric equilibria are never stable [Akin and Lacker, 1984; Lacker and Percus, 1991]. Given the parameter values M_1 and M_2 there can be as many different M-fold stable equilibrium points as there are different integer values of M within the interval $(M_H/2, M_H)$. From the *intensity dynamics* we see that these M follicles will eventually ovulate if $\xi(1/M) > D$ or they will get stuck if M is such that $\xi(1/M) < D$. If $D = 1$ and $M_1 < M_2$ it can easily be verified that $M_H/2 < M < M_1$ corresponds to anovulation, and $M_1 < M < M_H$ corresponds to ovulation.

We therefore see that if the interval $(M_H/2, M_1)$ contains an integer, the model will exhibit anovulatory states, and if both $(M_H/2, M_1)$ and (M_1, M_H) contain integers then we can get both ovulatory and anovulatory behaviour in the same model starting with different initial conditions (*i.e.* different initial maturities for the N follicles). This might appear to be the behaviour precisely corresponding to PCOS. However, the above analysis immediately shows that in such a situation the number that can arrest must always be less than the number that can ovulate. Thus if we set the parameters to values appropriate to the human, anovulation cannot occur, and very drastic changes to the parameters are required to achieve large numbers of follicles getting stuck. Thus to see normal human ovulation, we want $0 < M_1 < 1 < M_2 < 2$ (so that 1 is the only integer between M_1 and M_H), while to get say 10 follicles to get stuck we require $M_1 > 10$ and hence, $M_2 > 10$. As we argued in the introduction of this chapter this does not give a very realistic picture of PCOS.

Figures 4.2 and 4.1 show a numerical simulation of this model for the two cases of ovulation and anovulation. Both of these were carried out at the same parameter values $D = K = 1$ and $M_1 = 2.9$ and $M_2 = 3.9$, but with different initial conditions. The values of M_1 and M_2 are such that M lies within the interval $(M_H/2, M/H)$ for $M = 2$ and $M = 3$. For $M = 2$ we have that $\xi(1/M) < D$, therefore there are two follicles that get stuck (see figure 4.1). For $M = 3$ we have that $\xi(1/M) > D$ which means that three follicles may ovulate (see figure 4.2). Therefore, for these very particular examples we can see that by changing the initial conditions of the system we can either get three follicles to ovulate or two to arrest. However, no possible set of initial conditions at these parameter values will lead to more than two follicles arresting. Of course, this argument is only valid for the precise maturation

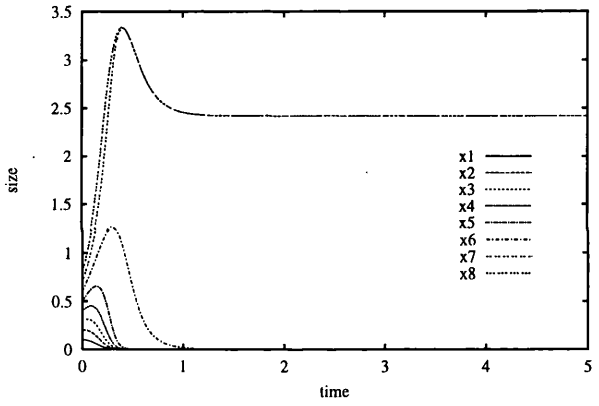

Figure 4.1: A numerical simulation of eight follicles interacting according to Lacker's original model given by equations 4.2 and 4.12. A *4th* order Runge-Kutta numerical method with a step size of 0.001 was programmed in C language to simulate the cycle. The parameter values used are $K = 5.0$, $D = 0.5$, $M_1 = 2.9$, $M_2 = 3.9$. Follicles x_7 and x_8 have relatively large initial sizes and the remainder $x_1, \ldots, x_6$ have smaller initial sizes. The two largest follicles tend to a constant maturity value as $t \to \infty$ and the rest atrophy by atresia.

function (4.12), and one might hope that other choices of ξ would lead to more realistic anovulatory behaviour. It turns out however that functions which can give the right spectrum of ovulatory and anovulatory cases are rather complex and appear rather contrived. Certainly none of the broad class of functions considered by Akin and Lacker in 1984 can lead to the desired behaviour [Akin and Lacker, 1984]. In particular, we see that if ξ is to allow a one follicle ovulatory state (and no other ovulatory states) and an anovulatory state involving more than one follicle then it must have at least two maxima in the unit interval, with the left maximum being lower than the right. For the particular example given in figure 4.3, we can see that

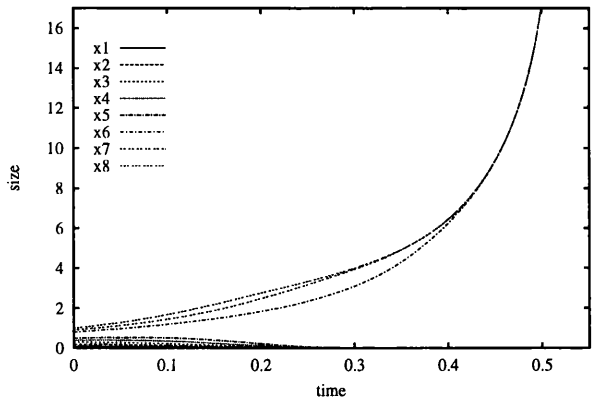

Figure 4.2: Simulation using the same method, step size and parameter values as in figure 4.1, but different initial conditions. Three follicles x_6, x_7 and x_8 have similar and relatively large initial sizes with the remaining five follicles $x_1, \ldots, x_5$ having small initial sizes. Follicles x_6, x_7 and x_8 ovulate in a finite time and the remainder die by atresia.

for $M = 4$, $M = 3$ and $M = 1$, $\xi(1/M) > 0$ and $\xi'(1/M) < 0$. However, $\xi(1/3) < D$ and $\xi(1/4) < D$, whereas $\xi(1) > D$ (where D is still assumed to be equal to one). Thus, just by changing the initial follicular distribution, this would be the case for exactly one follicle to ovulate or for three to four follicles to remain stuck in the ovary. We are not aware of any kind of biological argument which might even begin to justify such a form for the follicle response, and hence such a model of PCOS type behaviour would be tenuous at best.

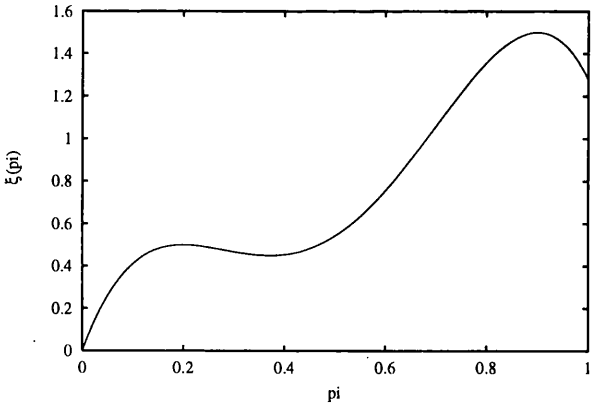

Figure 4.3: An example of a positive function $\xi(p_i)$ in the unit interval with two maxima. In particular for $M = 3$ and $M = 4$, $\xi'(1/M) < 0$ and given $D = 1$, $\xi(1/M) < D$. On the other hand, $\xi'(1/M) < 0$ and $\xi(1/M) > D$ for $M = 1$. This means such an interaction function allows three to four follicles arresting inside the ovary, and only one follicle ovulating. Either situation would depend on the initial maturity distribution of the interacting follicles.

4.3 Discussion

The current model ignores a number of important aspects of the real system, such as the modulation of the behaviour of the pituitary by the hypothalamus, the pulsatile nature of the release of the relevant hormones, the mechanisms controlling atresia, and the different roles played by FSH and LH. These are likely to be important, since the roles played by these two main gonadotropins, is quite different [Watson *et al.*, 1993; Mason *et al.*, 1994; Franks *et al.*, 1996].

We also notice that due to the fact that all the follicles respond in the same way to oestradiol concentrations, a strict hierarchy is preserved amongst the follicles. Thus, if the ith follicle is initially larger that the jth, then it will remain so through out the ovulation cycle. Hence in the context of this model the largest follicles will always either ovulate or get stuck and the smallest ones will atrophy.

As has already been pointed out by other authors [Thalabard *et al.*, 1989; Mariana *et al.*, 1994], such perfect ordering amongst the follicles does not always happen in real life. Particularly, Thalabard *et al.* argue that the data obtained from the ultrasound studies of normal or stimulated cycles in primates shows great variability in the growth curve profiles, and involves some curve crossing during the early stages of folliclegenesis [Thalabard *et al.*, 1989].

Even more explicit evidence is provided by Gougeon and Lefèvre [Gougeon and Lefèvre, 1983] who performed a careful study of the conditions required for a follicle to be selected in the human menstrual cycle. In their attempt to determine the stage of the cycle when the ovulatory follicle is selected, they found out that for the particular case of large healthy follicles smaller than 13 mm, a size criterion was insufficient. They also found that during the early follicular phase, there are no morphological differences amongst the largest healthy follicles which would guarantee the features of a pre-ovulatory follicle. Therefore, they proposed two basic conditions needed to be satisfied to determine whether a large healthy follicle is selected: 1) its diameter should be significantly larger than other large healthy follicles, and 2) the granulosa cell mitotic index of smaller healthy follicles should not exceed that of the largest one. Therefore, this may imply that if a healthy growing follicle is amongst the largest, and its granulosa cell mitotic index is the largest of all, then it will be the selected follicle.

Moreover, quite recently Baird *et al.* argued that there is no biological evidence

that could confirm the criteria by which a follicle is selected, hence they assume it to be a random choice [Ledger and Baird, 1995]. Nevertheless, this also strengthens the idea that it is not the largest follicles that are automatically selected. However, since Lacker makes many strong assumptions about the system, and in particular he considers follicular size and steroidogenesis as proportional, the fact that the selected follicles are the largest may be consistent with this assumption. Nevertheless, biologically speaking, the precise criteria of selection is not well defined, so we cannot be satisfied by Lacker's approach.

4.A Appendix

Definition 4.A.1 *Let U be an open subset of $\mathbb{R}^n$ and $V \in C^2(U)$. A system of the form*

$$\dot{\mathbf{x}} = -\nabla V(\mathbf{x})$$

where,

$$\nabla V = \left(\frac{\partial V}{\partial x_1}, \cdots, \frac{\partial V}{\partial x_n}\right)$$

is called a gradient system *on U.*

The function $V(\mathbf{x})$ is referred to as the potential of the system

$$\dot{\mathbf{x}} = f(\mathbf{x}) \tag{4.A.1}$$

if

$$V(\mathbf{x}) = -\int_{x_0}^{x} f(s)ds,$$

for a smooth integrable vector field $f : U \to \mathbb{R}^n$ on an open subset $U \in \mathbb{R}^n$ [Perko, 1991].

Definition 4.A.2 *If $f \in C^1(U)$, $V \in C^1(U)$ and φ_t is the flow of the differential equation (4.A.1), then for $\mathbf{x} \in U$ the derivative of the function $V(\mathbf{x})$ along the solution $\varphi_t(\mathbf{x})$ is*

$$\dot{V}(\mathbf{x}) = \frac{d}{dt}V(\varphi_t(\mathbf{x})) = \langle \nabla V(\mathbf{x}), f(\mathbf{x}) \rangle .$$

Furthermore, since V is such that

$$\dot{V} = \langle \nabla V(\mathbf{x}), \dot{\mathbf{x}} \rangle = -\langle \nabla V(\mathbf{x}), \nabla V(\mathbf{x}) \rangle = -norm(V(\mathbf{x}))^2 < 0,$$

it is a strict *Lyapunov function* [Glendinning, 1994].

Definition 4.1.3 *Let $V : U \to \mathbb{R}$ be a continuously differentiable function. Let $g : U \to \mathbb{R}$ be a differentiable function such that $S = \{x | g(x) = 0\} \subseteq U$. Then for $\mathbf{x} \in S$, $V(\mathbf{x})$ is a strict minimum restricted to S if $V(\mathbf{x}) < V(x)$ for all $x \in S$.*

Theorem 4.1.4 *[Lang, 1987] Let g be a continuously differentiable function on an open set U. Let $S = \{x | g(x) = 0\} \subseteq U$ such that $\nabla g(x) \neq 0$. Let V be a continuously differentiable function on U and assume $\mathbf{x} \in S$ is an extremum for V, subject to the constrain g. Then there exists a number β such that*

$$\nabla V(\mathbf{x}) = \beta \nabla g(\mathbf{x}).$$

Let $L(x) = V(x) - \beta g(x)$, such that $\nabla L(\mathbf{x}) = 0$. Thus we have the following theorems:

Second order necessary condition:

Theorem 4.1.5 *[Avez, 1986; Fletcher, 1981] Let $L : U \to \mathbb{R}$ be twice differentiable at $\mathbf{x} \in S$. If L has a local minimum at $\mathbf{x}$, then $D^2L(\mathbf{x})(v,v) > 0$ for all $v \in T_{\mathbf{x}}S$.*

Second order sufficient condition:

Theorem 4.1.6 *[Avez, 1986; Fletcher, 1981] Let $L : U \to \mathbb{R}$ be twice differentiable at $\mathbf{x} \in U$. If $\mathbf{x}$ is a non-degenerate critical point of L, and if $D^2L(\mathbf{x})(v,v) > 0$ for all $v \in T_{\mathbf{x}}S$, then L has a strict minimum at $\mathbf{x}$.*

Chapter 5

A NON-SYMMETRIC GENERALISATION

5.1 Introduction

We believe that the root cause of the problems found in Lacker's model is the symmetry inherent in the system: every follicle is presumed to have identical characteristics and to respond to hormonal signals in exactly the same way. This is unrealistic: it is almost impossible to find two biological systems which behave in absolutely identical fashions. Our aim in this chapter is therefore to remove this assumption of symmetry from Lacker's model. It transpires that we can do this in a way which still permits Lacker's mathematical analysis to hold essentially unchanged. The behaviour of the resulting model is, however, much more general, and in particular it is possible to obtain a more realistic model of the behaviour of follicles in PCO in this way. We would like to mention that the analysis of this chapter has already been published in [Chávez-Ross *et al.*, 1997].

5.2 A generalisation of the symmetric model

Basically, the symmetry assumption is broken by making each follicle grow in a different way. In particular we shall assume that the *interaction function* ξ is different for each follicle, but the *intensity* and *time* functions ρ and δ remain the same for all follicles. This allows the follicles to be sufficiently different to give us the behaviour we desire, but maintains sufficient common structure to separate the dynamics in the same way as in the symmetric model (if we were to allow each follicle its own ρ and δ then we can see no hope of analysing the resulting model). The effect is to

replace (4.7) by the following system:

$$g_i(x_i, X) = \delta(X)[\rho(X) + \xi_i(p_i)] \tag{5.1}$$

Then, if as before

$$p_i = \frac{x_i}{X}$$

we have,

$$\begin{aligned}
\frac{dp_i}{dt} &= \frac{d}{dt}(\frac{x_i}{X}) \\
&= \frac{1}{X}\frac{dx_i}{dt} - \frac{x_i}{X^2}\sum_{j=1}^{N}\frac{dx_j}{dt} \\
&= \frac{1}{X}(x_i\delta(X)[\rho(X) + \xi_i(p_i)]) - \frac{x_i}{X^2}\sum_{j=1}^{N} x_j\delta(X)[\rho(X) + \xi_j(p_j)] \\
&= \delta(X)\frac{x_i}{X}\xi_i(p_i) - \delta(X)\frac{x_i}{X}\sum_{j=1}^{N}\frac{x_j}{X}\xi_j(p_j) \\
&= \delta(X)p_i[\xi_i(p_i) - \bar{\xi}(p)]
\end{aligned}$$

where now $\bar{\xi}$ is defined by

$$\bar{\xi}(p) = \sum_{j=1}^{N} p_j\xi_j(p_j).$$

Rescaling time by

$$\frac{d\tau}{dt} = \delta(X)$$

as before, we obtain the *interaction dynamics*

$$\frac{dp_i}{d\tau} = p_i[\xi_i(p_i) - \bar{\xi}(p)]. \tag{5.2}$$

This is identical to the symmetric case (4.8), apart from the fact that ξ_i replaces ξ. Similarly the *intensity dynamics* is given by

$$\begin{aligned}
\frac{dX}{dt} &= \sum_{j=1}^{N}\frac{dx_j}{dt} \\
&= \sum_{j=1}^{N} x_j\delta(X)[\rho(X) + \xi_j(p_j)] \\
&= \delta(X)X[\rho(X) + \bar{\xi}(p)]
\end{aligned}$$

and hence,

$$\frac{dX}{d\tau} = X[\rho(X) + \bar{\xi}(p)]$$

as before.

5.3 Stability analysis

The equilibrium condition for this *interaction dynamics* is similar as in the symmetric case, *i.e.*

$$p_i = 0$$

or

$$\xi_i(p_i) = \bar{\xi}(p).$$

Thus just as before, all the non-zero coordinates have to take a common value. By permuting the follicles if necessary we can always assume that the non-zero coordinates are the first M, and hence will denote an M-fold equilibrium as $p_e = (p_1, \ldots, p_M, 0, \ldots, 0)$. Following Lacker's analysis, we obtain a gradient system on the unit sphere by making a variable transformation:

$$y_i = \sqrt{p_i}$$

which implies that

$$\sum_{i=1}^{N} y_i^2 = 1$$

and hence, $y = (y_1, \ldots, y_N)$ lies on the unit $N-1$ dimensional sphere S. Now consider the following potential function:

$$V(X) = -\frac{1}{2}\sum_{i=1}^{N} \int_0^{y_i} s\xi_i(s^2)ds.$$

Then the dynamics of (5.2) is given by the gradient dynamics on S

$$\frac{dy}{dt} = -\nabla_S V$$

where $\nabla_S V$ is the gradient restricted to S,*i.e.*

$$\nabla_S V = \nabla V - \langle \nabla V, y \rangle y.$$

Here ∇V is the usual gradient of V

$$\nabla V = (\frac{\partial V}{\partial y_1}, \cdots, \frac{\partial V}{\partial y_N})$$

and $\langle , \rangle$ is the usual inner product

$$\langle u, v \rangle = \sum_{i=1}^{N} u_i v_i. \tag{5.3}$$

Hence the ith component of the ∇V is such that:

$$[\nabla V]_i = -\frac{1}{2} y_i \xi_i(y_i^2).$$

Therefore,

$$\langle \nabla V, y \rangle = -\frac{1}{2} \sum_{i=1}^{N} y_i^2 \xi_i(y_i^2)$$

thus,

$$[\nabla V - \langle \nabla V, y \rangle y]_i = -\frac{1}{2} y_i [\xi_i(y_i^2) - \sum_{j=1}^{N} y_j^2 \xi(y_j^2)]$$

i.e. the ith component of the projection of ∇V onto the tangent plane of S at y. An equilibrium point of (5.2) will be a critical point of the potential function V, *i.e.* a point such that $\nabla_S V = 0$. Let $y_e = (a_1, \ldots, a_M, 0, \ldots, 0)$ be such critical point, then extending Akin and Lacker's stability theorem we get the following result:

Theorem 5.3.1 *An M-fold non-degenerate equilibrium y_e of the gradient system*

$$\frac{dy}{dt} = -\nabla_S V$$

for $y \in S$ is stable if and only if the common value $\lambda > \xi_i(0)$ for all $i = M+1, \ldots, N$ and either $\xi_i'(a_i^2) < 0$ for all nonzero co-ordinates $a_1, \ldots, a_M$ or $\xi_i'(a_i^2) > 0$ for exactly one non-zero co-ordinate and

$$\sum_{i=1}^{M} \frac{1}{\xi_i'(a_i^2)} > 0.$$

We prove this in a similar way to Lacker and Akin's original demonstration of the analogous result for the symmetric case [Lacker and Akin, 1988]. Note than in Lacker's symmetric version the condition on λ is simply $\lambda > 0$ which is difficult to interpret biologically. On the other hand, our formulation $\lambda > \xi_i(0)$ makes this condition much clearer: recall that $\lambda = \bar{\xi}(p)$, and hence at the equilibrium the relative growth rate, $dp_i/d\tau$, of the ith follicle is just $[\xi_i(p_i) - \bar{\xi}(p)] = [\xi_i(p_i) - \lambda]$. For follicle $i = M+1, \ldots, N$, we have $p_i = 0$, and hence the growth rate is exactly $\xi_i(0) - \lambda$. Thus, the condition $\lambda > \xi_i(0)$ for $i = M+1, \ldots, N$ is simply saying that at a stable equilibrium those follicles for which $p_i = 0$ have a negative growth rate, in other words such p_i cannot grow. Such a condition is of course intuitively obvious.

We begin the proof of the above result by defining the function $\sigma : \mathbb{R}^N \to \mathbb{R}$ by

$$\sigma(y) = \sum_{i=1}^{N} y_i^2 - 1$$

thus, $S = \sigma^{-1}(0)$. Then if y is a critical point of V restricted to S, there exists a *Lagrange multiplier* β such that

$$\nabla L(y) = 0$$

where,

$$L(y) = V(y) + \beta\sigma(y).$$

Now, by above $[\nabla V(y)]_i = -y_i\xi_i(y_i^2)/2$ and $[\nabla\sigma(y)]_i = 2y_i$ and hence, the condition for a critical point of L is that $y_i[\xi_i(y_i^2) - 4\beta] = 0$ for all i. Thus, $\xi_i(y_i^2) = 4\beta$ for all i such that $y_i \neq 0$, and hence we see that

$$\beta = \frac{1}{4}\bar{\xi}(p).$$

Furthermore recall that

$$\frac{dp_i}{d\tau} = p_i[\xi_i(p_i) - \bar{\xi}(p)]$$

and $y_i^2 = p_i$. Thus, $dp_i/d\tau = 0$ if and only if $y_i^2[\xi_i(y_i^2) - 4\beta] = 0$, in other words if and only if $[\nabla L(y)]_i = 0$. Thus, y is a critical point of V restricted to S if and only if it is an equilibrium point of the follicle interaction dynamics.

Furthermore, if such an equilibrium point is non-degenerate, then it is stable if and only if it is a local minimum of V on S. Now, a non-degenerate critical point y of a constrained function V on S is a local minimum if and only if $Q(v) = D^2L(v,v) > 0$ for all non-zero $v \in T_yS$, where T_yS is the tangent space of S at y [Fletcher, 1981]. So to prove the above stability theorem it remains to show that $Q(v) > 0$ if and only if $\lambda > \xi_i(0)$ for all $i = M+1,\ldots,N$ and either $\xi_i'(a_i^2) < 0$ for all $i = 1,\ldots,M$ or $\xi_i'(a_i^2) > 0$ for exactly one $i = 1,\ldots,M$ and

$$\sum_{i=1}^{M} \frac{1}{\xi_i'(a_i^2)} > 0.$$

In component form we have

$$\begin{aligned} Q(v) &= \sum_{i=1}^{N}\sum_{j=1}^{N} \frac{\partial^2 L}{\partial y_i \partial y_j} v_i v_j \\ &= -\sum_{i=1}^{M} v_i^2 a_i^2 \xi_i'(a_i^2) + \frac{1}{2}\sum_{i=M+1}^{N} v_i^2[\lambda - \xi_i(0)] \end{aligned}$$

(recall that $a_i = 0$ for $i = M+1,\ldots,N$ and $\xi_i(a_i^2) = \lambda$ for $i = 1,\ldots,M$). Note that

$$\sum_{i=1}^{N} v_i^2 \neq 0$$

and since v lies in the tangent space of S at y, it must be orthogonal to y, and hence

$$\langle y, v\rangle = \sum_{i=1}^{N} a_i v_i = \sum_{i=1}^{M} a_i v_i = 0.$$

First consider $v \in T_y S$ such that $v_i = 0$ for all $i = 1, \ldots, M$ and $v_i = 1$ for all $i = M+1, \ldots, N$. Then,

$$Q(v) = \frac{1}{2} \sum_{i=M+1}^{N} [\lambda - \xi_i(0)].$$

Hence, if $Q(v) > 0$ for all $v \in T_y S$ we must have $\lambda > \xi_i(0)$ for all $i = M+1, \ldots, N$.

Conversely, suppose that $\lambda > \xi_i(0)$ for all $i = M+1, \ldots, N$. We then immediately see that if $\xi_i'(a_i^2) < 0$ for $i = 1, \ldots, M$ then $Q(v) > 0$ for all $v \in T_y S$. On the other hand, suppose that $\xi_i'(a_i^2) \geq 0$ for more than one non-zero co-ordinate. Without loss of generality we may assume $\xi_1'(a_1^2) \geq 0$ and $\xi_2'(a_2^2) \geq 0$. Then consider $v = (a_2, -a_1, 0, \ldots, 0)$; this is nonzero and satisfies $\langle y, v\rangle = 0$. Then,

$$Q(v) = -(a_1 a_2)^2 (\xi_1'(a_1^2) + \xi_2(a_2^2)).$$

Hence if $\xi_1'(a_1^2) = \xi_2'(a_2^2) = 0$, then $Q(v) = 0$ and so y is a degenerate critical point, and if one or both of $\xi_1'(a_1^2)$, $\xi_2'(a_2^2)$ are positive, then $Q(v) < 0$ and y is not a minimum. Thus, if y is a non-degenerate minimum at most one of $\xi_i'(a_i^2)$ for $i = 1, \ldots, M$ can be non-negative or all of them have to be negative.

It remains to consider the case of exactly one $\xi_i'(a_i^2) > 0$ (still assuming that $\lambda > \xi_i(0)$ for all $i = M+1, \ldots, N$). Without loss of generality we may assume $\xi_1'(a_1^2) > 0$. Let

$$U = \{v \in T_y S : v_1 = 0\}$$

$$W = \{v \in T_y S : v_1 = -\frac{1}{a_1}\}.$$

Then $T_y S = U \cup \{cw : w \in W,\ c \in \mathbb{R}\}$. Since $Q(cw) = c^2 Q(w)$ the stability of y is determined by the sign of Q on U and W. First observe that if $v \in U$ then,

$$Q(v) = -\sum_{i=2}^{M} v_i^2 a_i^2 \xi_i'(a_i^2) + \frac{1}{2} \sum_{i=M+1}^{N} v_i^2 [\lambda - \xi_i(0)].$$

Thus, since $\xi_i'(a_i^2) < 0$ for all $i = 2, \ldots, M$ then $Q(v) > 0$ for all $v \in U$ such that $v \neq 0$. On the other hand if $v \in W$, then

$$Q(v) = -\xi_1'(a_1^2) - \sum_{i=2}^{M} v_i^2 a_i^2 \xi_i'(a_i^2) + \frac{1}{2} \sum_{i=M+1}^{N} v_i^2 [\lambda - \xi_i(0)].$$

Let

$$\bar{Q}(v) = -\xi_1'(a_1^2) - \sum_{i=2}^{M} v_i^2 a_i^2 \xi_i'(a_i^2).$$

We want to show that $\bar{Q}(v) > 0$ for all $v \in W$. On W, we can regard $\bar{Q}$ as a function of $v_2, \ldots, v_M$ and hence, we want to determine the minimum of $\bar{Q}(v)$ subject to the constraint $\langle y, v \rangle = 0$, or in other words $G(v) = 0$ where

$$G(v) = \sum_{i=2}^{M} a_i v_i - 1.$$

As in Lacker and Akin [Lacker and Akin, 1988], we do this using a standard Lagrange multiplier approach though the precise argument we use is somewhat different to that used there. Let $H(v, \gamma) = \bar{Q}(v) + \gamma G(v)$. Then completing the square we have

$$H(v,\gamma) = -\xi_1'(a_1^2) - \sum_{i=2}^{M} a_i^2 \xi_i'(a_i^2) \left(v_i - \frac{v}{2a_i \xi_i'(a_i^2)} \right)^2 + \sum_{i=2}^{M} \frac{x\gamma^2}{4\xi_i'(a_i^2) - \gamma}.$$

Since $\xi_i'(a_i^2) < 0$ for $i = 2, \ldots, M$, we see that for a fixed γ, the function H takes its minimum when

$$v_i = \frac{\gamma}{2a_i \xi_i'(a_i^2)}. \tag{5.4}$$

In order to satisfy $G(v) = 0$, we must have

$$\frac{\gamma}{2} \sum_{i=2}^{M} \frac{1}{\xi_i'(a_i^2)} = 1. \tag{5.5}$$

Together (5.4) and (5.5) determine the global minimum of $\bar{Q}(v)$ subject to the constraint $G(v) = 0$, in particular if v' also satisfies $G(v') = 0$ we have,

$$\bar{Q}(v) = \bar{Q}(v) + \gamma G(v) = H(v,\gamma) \leq H(v',\gamma) = \bar{Q}(v') + \gamma G(v') = \bar{Q}(v').$$

The value that $\bar{Q}$ takes at this minimum is

$$\begin{aligned} \bar{Q} &= -\xi_1'(a_1^2) - \sum_{i=2}^{M} \left(\frac{\gamma}{2a_i \xi_i'(a_i^2)}\right)^2 a_i^2 \xi_i'(a_i^2) \\ &= -\xi_1'(a_1^2) - \frac{1}{\sum_{i=2}^{M} \frac{1}{\xi_i'(a_i^2)}}. \end{aligned}$$

Thus, since

$$\sum_{i=1}^{M} \frac{1}{\xi_i'(a_i^2)} > 0 \tag{5.6}$$

we have that

$$\frac{1}{\xi_1'(a_1^2)} > -\sum_{i=2}^{M} \frac{1}{\xi_i'(a_i^2)},$$

which implies that

$$\frac{1}{\sum_{i=2}^{M} \frac{1}{\xi_i'(a_i^2)}} < -\xi_1'(a_1^2)$$

and hence, $\bar{Q}(v) > 0$ for all $v \in W$ as required. Finally to complete the proof of Theorem 5.3.1, we have to show that if (5.6) does not hold, then y is not stable. By above, if (5.6) is not satisfied, we have $\bar{Q}(v) \leq 0$ for some $v \in W$, with $v_i \neq 0$ for at least one $i = 2, \ldots, M$ and $v_i = 0$ for all $i = M+1, \ldots, N$. But if $v_i = 0$ for all $i = M+1, \ldots, N$ we have $Q(v) = \bar{Q}(v)$ and hence for this v we have $Q(v) \leq 0$, and since y is assumed non-degenerate this implies that it cannot be stable, which contradicts the hypothesis, therefore (5.6) holds as required.

We have analysed the stability conditions for the *interaction dynamics* so far. Now, suppose that we have a stable fixed point y on the unit sphere satisfying the conditions of the above theorem, what can we say about its stability for the full dynamics (4.2). To answer this, we have to study the stability of the *intensity dynamics*, recall that this is given by:

$$\frac{dX}{d\tau} = X[\rho(X) + \bar{\xi}(p)].$$

Also recall that ρ is monotone decreasing for $X > 0$ and $\rho(X) \to -D$ as $X \to \infty$, and $\rho(X) \to \infty$ as $X \to 0$. This in particular implies that $\rho(X) > -D$ for all $X > 0$. If p is an equilibrium point then $\bar{\xi}(p) = \lambda$, and if p is tending to such an equilibrium point then $\bar{\xi}(p) \to \lambda$ as $\tau \to \infty$. Then if $\lambda > D$ we have

$$\frac{dX}{d\tau} > (\lambda - D)X$$

with $(\lambda - D) > 0$ and hence $X \to \infty$ as $\tau \to \infty$. The total oestradiol concentration thus tends to infinity, and as already mentioned this corresponds to ovulation: one assumes that when X reaches a sufficiently large value this triggers an LH surge. Looking at the dynamics of the individual follicles, we have

$$\frac{dx_i}{d\tau} = x_i[\rho(X) + \xi_i(p_i)]$$

with $\xi_i(p_i) \to \lambda$ as $\tau \to \infty$ for $i = 1, \ldots, M$, and $\xi_i(p_i) \to 0$ as $\tau \to \infty$ for $i = M+1, \ldots, N$. Hence $x_i \to \infty$ for $i = 1, \ldots, M$, *i.e.* for those follicles which have non-zero

relative maturity at the equilibrium point, and $x_i \to 0$ for $i = M+1, \ldots, N$, *i.e.* for those follicles which have zero relative maturity. This case therefore corresponds to the first M follicles growing (and by implication ovulating) and the remainder ultimately dying by atresia.

On the other hand if $\lambda < D$ then there exists an X_e such that $\rho(X_e) = -\lambda$. Such an X_e is then a stable equilibrium point of the intensity dynamics (the stability follows from the fact that $\rho(X) > \rho(X_e)$ for $X < X_e$ and $\rho(X) < \rho(X_e)$ for $X > X_e$). This situation thus corresponds to the total oestradiol concentration, and hence the total size of the N follicles limiting to some finite value, and hence may be interpreted as an anovulatory case. As before, if a follicle relative maturity tends to zero then it will eventually die (*i.e.* follicles $M+1$ to N), but now if the follicle has a non-zero relative maturity a_i (follicles 1 to M) then its size tends to a finite size $X_e a_i$, corresponding to that follicle getting stuck and neither ovulating nor becoming atretic.

Finally it is left to analyse the dynamics of the *time rescaling function* $\delta(X)$, *i.e.* what happens to $\tau(t)$ when $t \to \infty$ where τ satisfies the dynamics

$$\frac{d\tau}{dt} = \delta(X).$$

Since $\delta(X)$ is assumed strictly positive, $\tau(t)$ is invertible. Then if $\lambda > D$ we have

$$\frac{d\tau}{dX} < \frac{1}{\lambda - D}\frac{1}{X}$$

and hence,

$$\begin{aligned}
\lim_{\tau\to\infty} t(\tau) &= \int_0^\infty \frac{d\tau}{\delta(X(\tau))} \\
&= \int_{X(0)}^{X(\infty)} \frac{1}{\delta(X)}\frac{d\tau}{dX}dX \\
&< \frac{1}{\lambda - D}\int_{X(0)}^{X(\infty)} \frac{1}{\delta(X)X}dX.
\end{aligned}$$

Thus if $\delta(X)$ grows faster than X^ϵ for some $\epsilon > 0$, the above integral is finite and $t(\tau)$ tends to a finite value T as $\tau \to \infty$, hence τ goes to ∞ in finite time, corresponding to ovulation in finite time.

On the other hand, if $\lambda < D$, we have $\delta(X) \to \delta(X_e) > 0$, and hence

$$\frac{dt}{d\tau} \sim \frac{1}{\delta(X_e)}.$$

Follicle	M_1	M_2
x_1	0.9	1.9
x_2	7.1	7.9
x_3	7.1	7.8
x_4	7.1	7.7
x_5	7.1	7.6
x_6	7.1	7.5
x_7	7.2	7.9
x_8	7.3	7.9

Table 5.1: Parameter values M_1 and M_2 for each of the follicles for the non-symmetric model

Thus $t(\tau) \to \infty$ as $\tau \to \infty$, corresponding to the anovulatory case, *i.e.* the follicle size converges to a finite limiting value and stays there for all time.

To summarise, the dynamics of the model as $\tau \to \infty$ can be classified into two different cases:

i) $\lambda > D$: ovulation

- **a)** $x_i \to 0$ if $p_i \to 0$
- **b)** $x_i \to \infty$ if $p_i \to a_i^2 \neq 0$
- **c)** $t \to T$

ii) $\lambda < D$: anovulation

- **a)** $x_i \to 0$ if $p_i \to 0$
- **b)** $x_i \to X_e a_i^2$ if $p_i \to a_i^2 \neq 0$
- **c)** $t \to \infty$

5.4 Numerical simulations and new results

We give an illustration of the dynamics of the non-symmetric model in figures 5.1, 5.2 and 5.3. In all these figures function g_i is Lacker's original function (4.12), but with different values of M_1 and M_2 for each i. The actual values used are given in Table (5.1). The parameters D and K were set to 1, as in figures 4.1 and 4.2.

Follicle x_1 thus has parameter values appropriate for normal human ovulation, while the other follicles $x_2, \ldots, x_8$ have parameters corresponding to the anovulatory

case. We see that in the non-symmetric case we can obtain a much greater variety of behaviours for the same parameter values just by changing the initial conditions of the system. Thus in 5.1 we consider a situation where the normal follicle x_1 has a relatively large initial size compared to the abnormal ones . In this case, $x_2, \ldots, x_8$ are too small to affect the development of x_1 which goes on to ovulate normally. Although on their own $x_2, \ldots, x_8$ would arrest at a finite size, the presence of x_1 suppresses their development and they die by atresia.

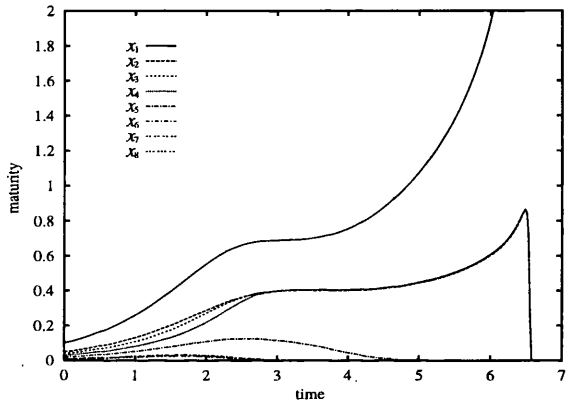

Figure 5.1: A numerical simulation for the non-symmetric model. The function g_i is given by 4.12 with $D = K = 1$ and different values of M_1 and M_2 for each i, according to Table 5.1. Follicle x_1 has parameter values appropriate for normal human ovulation, and a relatively large initial size. The other follicles $x_2 \ldots, x_8$ have parameters corresponding to the anovulatory case, and much smaller initial sizes. In this example their development is suppressed by x_1, and they die by atresia.

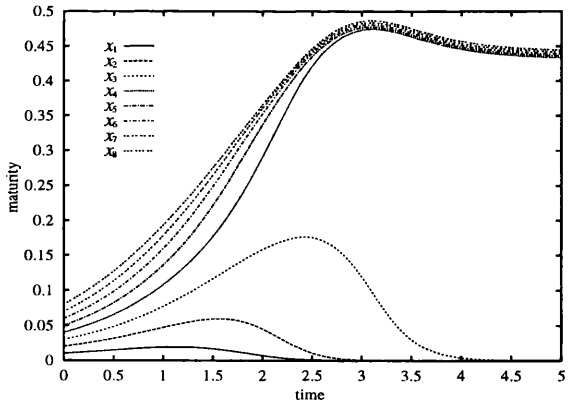

Figure 5.2: A simulation of the non-symmetric model with identical parameters to figure 5.1, but different initial conditions. The normal follicle x_1 now has the smallest initial size, with an increasing range of initial sizes for the remaining seven follicles. In this example five of the subgroup of seven abnormal follicles $x_4, \ldots, x_8$ arrest at a fixed size as $t \to \infty$, and the remainder die together with x_1.

By contrast, in 5.2, we take x_1 to have the smallest initial size with an increas-

ing range of initial sizes for the remaining seven follicles. The abnormal follicles $x_2, \ldots, x_8$ now dominate and prevent the ovulation of x_1. Instead the largest five abnormal follicles arrest at a finite size leading to anovulatory behaviour with the ovary containing a number of large follicles. This situation is thus consistent with the type of anovulation seen in PCOS. The comparison with 5.1 shows that we can move from a normal ovulatory case to an anovulatory one with a large number of arrested follicles just by changing the initial sizes of the follicles at the start of the cycle. This is something which cannot be achieved in Lacker's symmetrical model.

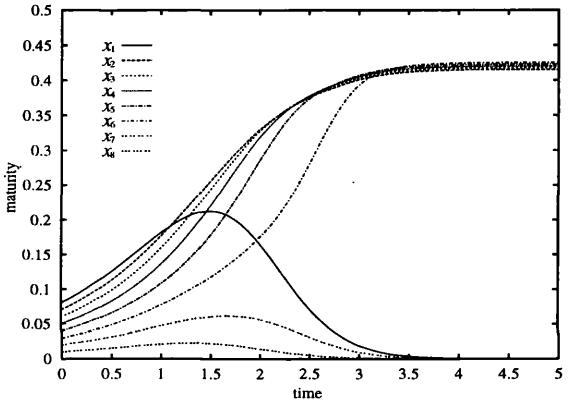

Figure 5.3: A simulation of the non-symmetric model with identical parameters to figures 5.1 and 5.2. The initial conditions are similar to figure 5.2 but with the order of sizes reversed: x_1 thus now has the largest initial size, identical to x_8 in figure 5.2, and x_8 the smallest. In this example, despite the fact the normal follicle x_1 is initially the largest, the presence of other abnormal follicles $x_2, \ldots, x_8$ prevents it from ovulating, and it dies by atresia together with the smallest abnormal follicles x_7 and x_8. The remaining abnormal follicles $x_2, \ldots, x_6$ arrest at a fixed size.

Finally in 5.3, we reverse the order of sizes compared to 5.2, so that x_1 has an initial size identical to x_8 in 5.2, and x_8 an identical initial size to x_1 in 5.2. We see that even though just as in 5.1, x_1 is initially the largest follicle, the overall behaviour is similar to that in 5.2, and x_1 dies by atresia, with the largest five abnormal follicles arresting as before. We thus have a situation where the presence of a group of abnormal follicles suppresses the ovulation of a normal follicle, despite the fact that the latter is initially the dominant follicle. This illustrates the fact that, unlike in Lacker's symmetrical model, the strict dominance of follicle sizes is broken, and the overall behaviour of the system does not just depend on the follicles with the largest initial size.

5.5 Discussion

In this chapter we have therefore generalised Lacker's model to the case of non-identical follicle growth functions. The resulting generalised model is able to successfully display PCOS type behaviour where a number of follicles arrest at a pre-ovulatory size, but fail to ovulate. Such behaviour can be seen at identical parameter values where for different initial conditions normal ovulation of a single follicle occurs.

Although highly simplified, our model does suggest a number of tentative conclusions about the nature of PCOS:

1. The primary cause of PCOS does not lie in a failure of the pituitary, or the ovary as a whole, but rather in the response of individual follicles to gonadotropins. This is in broad agreement with observations in clinical practice (*e.g.* [Yen, 1980; Franks *et al.*, 1996]).

2. Those follicles which arrest at pre-ovulatory stages but fail to either ovulate or atrophy have significantly different properties compared to normally ovulating follicles. The potential for the type of anovulation seen in PCOS thus appears to be already determined at the pre-antral stage of the follicle.

3. Although a number of different classes of abnormal response by a follicle can probably lead to the type of anovulation observed in PCOS, the most likely possibility within the context of our non-symmetric model appears to be a heightened sensitivity to gonadotropins. This is consistent with experimental evidence that follicles of PCOS patients are much more sensitive to FSH than those of normal women [Mason *et al.*, 1994].

4. The presence of follicles with abnormal gonadotropin response can (but need not) suppress the ovulation of normal follicles. The mechanism behind this is that the abnormal follicles, being more sensitive to gonadotropins produce a sufficiently high level of oestradiol to suppress the production of gonadotropins by the pituitary to a level so low that normal follicles cannot grow. In the presence of a mixed population of normal and abnormal follicles, therefore, the factor determining whether ovulation will, or will not occur, is the relative proportions of the two types of follicles, and their relative maturities at the start of the cycle.

Due to the simplified and rather abstract nature of both the symmetric and non-symmetric models discussed in this thesis, it is difficult, and perhaps even dangerous, to extrapolate from behaviour observed in such models to conclusions about the

real biological systems they represent. Nevertheless, the analysis and numerical simulations carried out in this chapter appear to offer some tentative insight into the mechanisms underlying PCO. Thus, within the context of this model the primary cause of PCO lies in the response of follicles to hormonal stimulation, rather than in the functioning of the pituitary or the ovary as a whole. This is consistent with clinical thinking about the nature of PCO (*e.g.* [Yen, 1980; Franks *et al.*, 1996]).

In particular, for an ovary to become polycystic in our model, it must contain a sub-population of follicles which have a significantly different response to gonadotropins from those follicles involved in normal ovulation. Given the simplicity of the model, it is difficult to be too specific about the types of abnormal gonadotropin response required to induce "PCO type" behaviour. One may tentatively conclude that such abnormal follicles should either achieve their maximal response to gonadotropins at earlier stages of their maturity (which is measured by their size in this model), or at a given size achieve their maximal response at lower levels of circulating gonadotropins. The model is too simplistic to distinguish between these two cases, and certainly other response patterns can lead to "PCO type" behaviour as well.

However, it should be pointed out that some kind of heightened sensitivity to gonadotropins which both of the above interpretations imply is in line with recent experimental observations that follicles of PCOS patients are much more sensitive to FSH than those of normal women [Mason *et al.*, 1994]. The model here may therefore help to explain the somewhat paradoxical nature of these observations.

A further interesting aspect of our model is that in certain circumstances the presence of follicles with abnormal gonadotropin response can suppress the ovulation of a normally functioning follicle. This appears to happen because such abnormal follicles, being more sensitive to gonadotropins, can produce a sufficiently high level of oestradiol to reduce the production of gonadotropins by the pituitary to a level so low that normal follicles cannot grow. In the presence of a mixed population of normal and abnormal follicles, therefore, the factor determining whether ovulation will, or will not occur, is the relative proportions of the two types of follicles, and their relative maturities at the start of the cycle. One can thus envisage that in marginal cases of PCO the determining factor of whether ovulation occurs in a given cycle or not is the number and maturity of abnormal follicles present at the start of the cycle.

Of course, since our model ignores many important aspects of the real system, such as the mechanisms controlling atresia, or the modulation of the behaviour of the pituitary by the hypothalamus, the above conclusions must be regarded as highly speculative. It would however be interesting to see whether any can be tested experimentally, or even duplicated in more complex and biologically realistic models.

Chapter 6

THE SYMMETRIC MODEL WITH AN AGE DECAYING FACTOR

6.1 Introduction

The modification of Lacker's symmetric model given by Mariana *et al.* a few years later [Mariana *et al.*, 1994] also avoids the strong hierarchy amongst the growing follicles, and the initial largest ones are not always the selected follicles. Just like the non-symmetric generalised version described and discussed in the previous chapter, this model is dynamically more interesting since the selected follicles are not determined in such an obvious manner; *i.e.* we do not know which follicles are going to be selected.

Mariana *et al.* basically agree that the interaction between the growing follicles happens in the way suggested by Lacker, but additionally suggest that these follicles also have the capacity of individually ageing. This is achieved by incorporating another variable that reflects an intrinsic deterioration of each follicle, independently of its response to any sort of hormone stimulation. Although the biological nature of this ageing process is not clearly specified, it is plausible and also leads to a more realistic model for the selection of the ovulatory follicle.

However, Mariana *et al.* have not published any kind of theoretical analysis for this model. Instead, they only presented a few numerical examples in order to show their model is still able to reflect the basic features of follicle selection, and its new advantages in terms of the regulation of ovulatory follicles. Since the study of the control of ovulation is the main interest of this thesis, we considered it important to

develop a more rigorous analysis of the behaviour of this ageing model.

6.2 Description of the model

For each follicle in a population of N follicles interacting in a given cycle, let y_i represent the follicle age. The former variable for the maturity of the ith follicle, x_i, is now renamed z_i. Therefore, the new modified maturity variable, x_i, is proportional to the former one and to the follicle age, *i.e.* $x_i = z_i y_i$. Moreover, the rate of change for the previous maturity variable and the ageing of the follicle are given by

$$\frac{dz_i}{dt} = x_i g(x_i, X)$$

and

$$\frac{dy_i}{dt} = -\mu y_i$$

respectively. Note that y_i is not the chronological age of the follicle since its magnitude is decreasing with time. Rather, it represents the age as a deteriorating capacity of the follicle to grow and ovulate. Here μ is the ageing parameter and the function $g(x_i, X)$ is the one originally proposed by Lacker, *i.e.*

$$g(x_i, X) = K - D(X - M_1 x_i)(X - M_2 x_i) \tag{6.1}$$

where,

$$X = \sum_{i=1}^{N} x_i. \tag{6.2}$$

Consequently, the modified dynamics for the follicle growth proposed by Mariana *et al.* is

$$\begin{aligned} \frac{dx_i}{dt} &= y_i x_i g(x_i, X) - \mu x_i \\ \frac{dy_i}{dt} &= -\mu y_i. \end{aligned} \tag{6.3}$$

6.3 The simplified system

The first step we choose for analysing the basic features of this model is to simplify the system by considering a number of follicles having the same initial maturity. Therefore, suppose that from N follicles starting the cycle M have the same initial maturity X/M, whereas the remaining $N - M$ follicles have zero initial maturity.

Moreover, suppose that all follicles have the same initial age y, this gives the simplified system

$$\begin{aligned} \frac{dX}{dt} &= y(KX + D\gamma X^3) - \mu X \quad (a) \\ \frac{dy}{dt} &= -\mu y \qquad\qquad\qquad\quad (b) \end{aligned} \tag{6.4}$$

where,

$$\gamma = -(1 - M_1/M)(1 - M_2/M) \tag{6.5}$$

involves parameters M_1 and M_2. Furthermore, $(X, y) = (0, 0)$ can be shown to be a local stable equilibrium point for any $\mu > 0$ by means of a linear stability analysis. It is worth highlighting that the ageing parameter, μ, is always positive and therefore, the dynamics of the ageing variable of the follicle, y, is always exponentially decreasing. For the particular case of $\mu = 0$ we see that system (6.4) reduces to

$$\frac{dX}{dt} = y(KX + D\gamma X^3) \tag{6.6}$$

where y remains constant for all t. If $y = 1$, equation (6.6) is Lacker's model.

By solving (6.4.b) and substituting into (6.4.a), we obtain the non-autonomous differential equation

$$\frac{dX}{dt} = y_0 e^{-\mu t}(KX + D\gamma X^3) - \mu X, \tag{6.7}$$

where $y_0 = y(0)$. The only equilibrium point possible is $X = 0$, which is locally stable.

We were able to analytically solve this equation using *Mathematica*, and compute the following solution

$$X(t) = \left[-\frac{D\gamma}{K} - \frac{D\gamma}{K^2 y_0}\mu e^{\mu t} - \frac{D\gamma}{2K^3 y_0^2}\mu^2 e^{2\mu t} + k e^{\left(\frac{2Ky_0}{\mu e^{\mu t}} + 2\mu t\right)} \right]^{-1/2} \tag{6.8}$$

where,

$$k = \left[X_0^{-2} + \frac{D\gamma}{K} + \frac{D\gamma}{K^2 y_0}\mu + \frac{D\gamma}{2K^3 y_0^2}\mu^2 \right] e^{\frac{-2Ky_0}{\mu}}$$

and $X_0 = X(0)$. Furthermore, initial conditions X_0 and y_0 are strictly positive.

Moreover, whenever $\gamma > 0$ there exists a separatrix of the dynamics given by

$$X_0^* = \left[\frac{1}{(\frac{1}{2}(e^{\frac{2Ky_0}{\mu}} - 1)\frac{\mu^2}{K^3 y_0^2} - \frac{\mu}{K^2 y_0} - \frac{1}{K})D\gamma} \right]^{1/2}. \tag{6.9}$$

The separatrix is the boundary that splits the phase space in two domains of attraction or basins of attraction [Baker and Gollub, 1990]. For this particular case, it is possible to regard the space of solutions of the non-autonomous differential equation, (6.7), as the phase space of the following autonomous system:

$$\begin{aligned} \frac{dX}{d\tau} &= y_0 e^{\mu t}(KX + D\gamma X^3) - \mu X \\ \frac{dt}{d\tau} &= 1. \end{aligned} \tag{6.10}$$

Hence, X_0^* given in (6.9) is a separatrix of the phase space of (6.10).

For a) $X_0 > X_0^*$, solution (6.8) grows to infinity at a finite time, whereas if b) $0 < X_0 < X_0^*$, $X(t)$ tends to zero as time tends to infinity. As we can see in figure 6.1, the separatrix behaves as neither of these. Instead, it can be regarded as growing to infinity in indefinite time, or like a solution where a maximum value is reached in an infinite time since it never decreases.

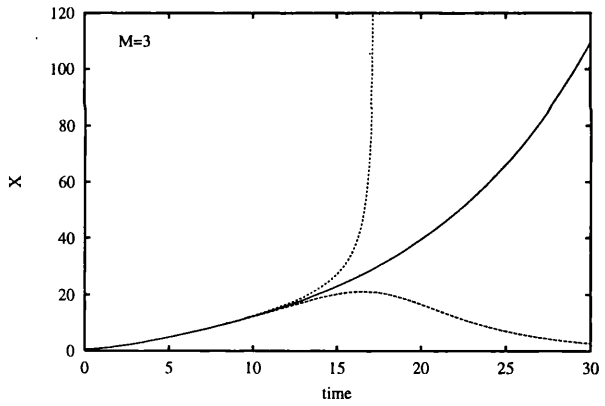

Figure 6.1: Phase space of system (6.10) for $y_0 = 1.0$, $\gamma = 0.01 > 0$, $\mu = 0.2$ and $X_0^* = 0.477106$. Given $\epsilon = 0.001$, for a) $X_{0_1} = X_0^* + \epsilon$, the solution grows to infinity at a finite time, while for b) $X_{0_2} = X_0^* - \epsilon$, the solution corresponds to an atretic follicle. The separatrix grows to infinity as $t \to \infty$.

Let us calculate the time derivative of solution (6.8), thus

$$X'(t) = -\frac{2k\exp(\mu t + \frac{2Ky_0}{\mu e^{\mu t}})(\mu e^{\mu t} - Ky_0) - \frac{D\gamma\mu^2 e^{\mu t}}{K^2 y_0} - \frac{D\gamma\mu^3 e^{2\mu t}}{K^3 y_0^2}}{\left[2k\exp(2\mu t + \frac{2Ky_0}{\mu e^{\mu t}}) - \frac{D\gamma\mu e^{\mu t}}{K^2 y_0} - \frac{D\gamma\mu^2 e^{2\mu t}}{2K^3 y_0^2}\right]^{\frac{3}{2}}}. \tag{6.11}$$

In particular we can express $X'(t) = F(t, X_0)$, where F is given in (6.11). To show how the value (6.9) was obtained, suppose that

$$F(t, X_0) = 0. \tag{6.12}$$

The values t and X_0 satisfying (6.12) give the initial condition and time for which solution (6.8) reaches its maximum value. Therefore, if we solve equation (6.12) as

$$X_0 = \left[\frac{2g(t)(Ky_0 - \mu e^{\mu t})}{\left(g(t)H(t) - \frac{\mu^2}{K^2 y_0} e^{\frac{2Ky_0}{\mu}} - \frac{\mu^3}{K^3 y_0^2} e^{(\frac{2Ky_0}{\mu} + \mu t)} \right) D\gamma} \right]^{\frac{1}{2}},$$

where

$$g(t) = e^{\frac{2Ky_0}{\mu e^{\mu t}}}$$

and

$$H(t) = -2y_0 - \frac{2\mu}{Ky_0} - \frac{\mu^2}{K^2 y_0^2} + \left(\frac{2\mu}{K} + \frac{2\mu^2}{K^2 y_0} + \frac{\mu^3}{K^3 y_0^2} \right) e^{\mu t}.$$

For the particular case of the separatrix, we find X_0 such that the solution reaches its maximum in an infinite time. In other words, we find the limit of the expression above when $t \to \infty$. In particular, $lim_{t\to\infty} g(t) = 1$. Hence, for t very large we have

$$X_0 \approx \left[\frac{-2\mu e^{\mu t}}{\left[\left(\frac{2\mu}{K} + \frac{2\mu^2}{K^2 y_0} + \frac{\mu^3}{K^3 y_0^2} \right) e^{\mu t} - \frac{\mu^3}{K^3 y_0^2} e^{\frac{2Ky_0}{\mu}} e^{\mu t} \right] D\gamma} \right]^{\frac{1}{2}} = X_0^*$$

It is possible to prove that X_0^* exists for any $\mu > 0$, *i.e.* given $\mu > 0$ there will always be an initial condition value above which all solutions escape to infinity.

To show this, it is sufficient to prove that if

$$f(\mu) = \left(e^{\frac{2Ky_0}{\mu}} - 1 \right) \frac{\mu^2}{(2K^3 y_0^2)} - \frac{\mu}{(K^2 y_0)} - \frac{1}{K}$$

then, $f(\mu) > 0$ for all $\mu > 0$, where $f(\mu)$ is the square of the denominator of the separatrix value given in (6.9). This is also equivalent to proving that, a) $f'(\mu) \leq 0$ for all $\mu > 0$, and that b) $lim_{\mu\to\infty} f(\mu) = 0$.

a) We have

$$f'(\mu) = \frac{\mu}{K^3 y_0^2} (e^{\frac{2Ky_0}{\mu}} - 1) - \frac{1}{K^2 y_0} (e^{\frac{2Ky_0}{\mu}} + 1).$$

Suppose that $f'(\mu) > 0$ for some $\mu > 0$. This implies that

$$e^{\frac{2Ky_0}{\mu}} (\mu - Ky_0) > (\mu + Ky_0).$$

Hence, if $(\mu - Ky_0) < 0$ then $e^{2Ky_0/\mu} < (\mu + Ky_0)/(\mu - Ky_0) < 0$, which is a contradiction since $e^{2Ky_0/\mu} > 0$ for $\mu > 0$. On the other hand, if $(\mu - Ky_0) > 0$,

then $e^{2Ky_0/\mu} > (\mu + Ky_0)/(\mu - Ky_0)$. Now suppose, $h(\mu) = e^{2Ky_0/\mu}$ and $j(\mu) = (\mu + Ky_0)/(\mu - Ky_0)$, then we have that $h(Ky_0) = e^2 < h(\mu)$ for all $\mu > Ky_0$. But $j(\mu) \to \infty$ as $\mu \to Ky_0$ implying that $h(Ky_0) < j(Ky_0)$. Since both, h and j are monotone decreasing functions such that $lim_{\mu\to\infty}h(\mu) = lim_{\mu\to\infty}j(\mu) = 1$, we can conclude $h(\mu) \leq j(\mu)$ for all $\mu > Ky_0$. Thus, $e^{2Ky_0/\mu} > (\mu + Ky_0)/(\mu - Ky_0)$ is also a contradiction. Therefore, $f'(\mu) \leq 0$ for all $\mu > 0$.

b) We have $e^{2Ky_0/\mu} = 1+2Ky_0/\mu+1/2(2Ky_0)^2+\psi(\mu)$ such that $\psi(\mu) = O(\mu^{-3})$. Thus,

$$\begin{aligned} f(\mu) &= \left[\frac{2Ky_0}{\mu} + \frac{1}{2}\left(\frac{2Ky_0}{\mu}\right)^2 + O(\mu^{-3})\right]\frac{\mu^2}{2K^3y_0^2} - \frac{\mu}{K^2y_0} - \frac{1}{K} \\ &= \frac{\mu}{K^2y_0} + \frac{1}{K} + 0(\mu^{-1}) - \frac{\mu}{K^2y_0} - \frac{1}{K} \\ &= 0(\mu^{-1}) \end{aligned}$$

Hence, $0(\mu^{-1}) \to 0$ as $\mu \to \infty$.

Biologically speaking, X_0^* represents a threshold value for the total follicle size that did not appear in the models of chapter 4 and 6. Hence, if at the beginning of the cycle the initial sum of follicle sizes does not exceed such a threshold, there is no hope for any follicle to ovulate, and all of them rather atrophy and die. This may imply that this model is in fact reflecting the cycle dynamics even before the follicular phase.

In contrast, for the case when $X(t)$ does not grow to infinity at a finite time, it is possible to compute a critical value for μ, which marks whether such a solution is either strictly decreasing or reaches a finite maximum and then decreases. For this case it is easier to explore the time derivative of X given in (6.7) than the one given in (6.11). In fact, if we substitute the value of X given in (6.8) into $dX/dt = G(t, X)$, where G is given in (6.7), we have that $G = F$. Thus, let us derive a value t_c such that $G(t_c, X) = 0$ for any $X > 0$, *i.e.*

$$t_c = -\frac{1}{\mu}\ln\left[\frac{\mu}{(1 + D\gamma X^2)Ky_0}\right].$$

Therefore, given any $X > 0$ the maximum of solution $X(t)$ exists as long as $t_c \geq 0$. Moreover, given γ as in (6.5) and $y_0 > 0$, if $\gamma > 0$ and $0 < X_0 < X_0^*$, there is a critical value $\mu^* = (1+\gamma X_0)y_0$, such that if $0 < \mu \leq \mu^*$ a maximum exists, *i.e.* $t_c \geq 0$, otherwise the solution is strictly decreasing. This means that although the follicle is doomed to die since its initial size is smaller than the minimum size required to

ovulate, if $\mu \leq \mu^*$ it will be able to grow at first, and then decrease. In contrast, if $\mu > \mu^*$, the follicle's atretic parameter is so large for its initial size that the follicle never grows but immediately regresses.

In the case of $\gamma < 0$, the follicle, no matter its initial size, will end up atrophying and dying, *i.e.* $X(t) \to 0$ as $t \to \infty$. However, whenever $\mu < Ky_0$ and $X_0 \leq X_0^\sharp$ such that,

$$X_0^\sharp = \sqrt{\frac{Ky_0 - \mu}{-\gamma DKy_0}} \tag{6.13}$$

a maximum exists since for those conditions, $0 < \mu \leq \mu^*$, *i.e.* $t_c \geq 0$. Otherwise, the solution is strictly decreasing. Such a maximum can also be obtained from equation (6.7) when $dX/dt = G(t, X) = 0$ and is given by,

$$X_{max} = \sqrt{\frac{Ky_0 e^{-\mu t_c} - \mu}{-\gamma DKy_0 e^{-\mu t_c}}} \tag{6.14}$$

Finally, we also have that for $\gamma < 0$, if $\mu > Ky_0$ and $\mu > \mu^*$, the solution is also monotone decreasing. Although we discuss this in greater detail below, it is worth saying that such a critical value μ^* is an ageing parameter threshold, which determines different types of behaviour. Except for the case when $X(t)$ tends to infinity at a finite time, *i.e.* ovulation, we can say that in general terms, once an initial oestradiol concentration is given, follicles manage to grow at the beginning of the cycle, as long as $0 < \mu \leq \mu^*$, *i.e.* as long as its decaying parameter is not too strong for it to die.

Some examples are shown for different types of behaviour for this solution when varying γ and μ and their corresponding biological interpretation are also described. As far as the parameter γ is concerned, we are basically interested in studying the behaviour for $\gamma > 0$ and $\gamma < 0$ since for the models of chapter 4 and 6, these two conditions respectively marked the ovulatory and anovulatory situations. Moreover, although units of follicular maturity or size are not specified, we work within a certain range of small values to be in agreement with previous models. Thus, we fix $X_0 = 1.0$ as a maximum initial condition, and analyse different kinds of behaviour when varying $\mu > 0$ and γ for $X_0 = 1.0$.

Given $y_0 = 1.0$ so that $\mu^* = 1+\gamma$ and $\mu = 1.1$ we have that if $\gamma < 0.1$ then $\mu > \mu^*$. Hence, the solution is a monotone decreasing function, see figure 6.2. This reflects the situation of a follicle with such a large ageing parameter that it just cannot grow

at all when the cycle begins, instead it starts degenerating and eventually dies.

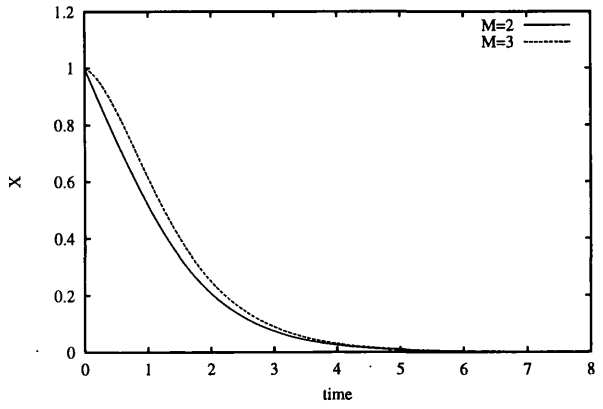

Figure 6.2: Solution (6.8) for $K = 1.0$, $\mu = 1.1$, $y_0 = 1.0$ and $X_0 = 1.0$. For $\gamma = 0.01 > 0$ and $\gamma = -0.4275 < 0$, $\mu > \mu^*$. Hence, for both parameter values the solution is monotone decreasing, meaning that in either case the follicle is not able to grow at all.

By decreasing the value of μ sufficiently enough, *e.g.* to $\mu = 0.4$, the solution has a maximum for $\gamma = 0.01$ or $\gamma < 0$, see figure 6.3. This means the follicle is able to grow in the first place, but eventually atrophies through atresia since its ageing parameter does not allow it to carry on growing.

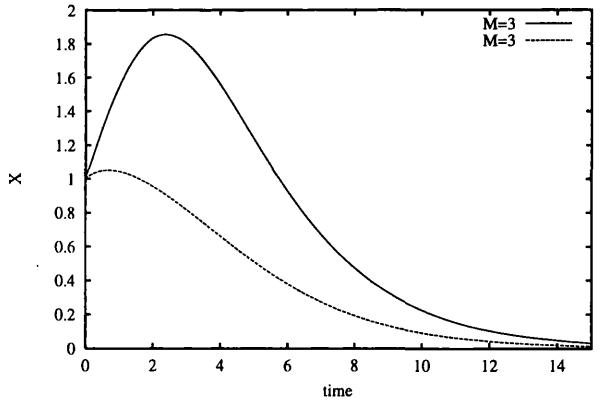

Figure 6.3: Solution (6.8) for $K = 1.0$, $\mu = 0.4$, $y_0 = 1.0$ and $X_0 = 1.0$. For $\gamma = 0.01 > 0$, $0 < \mu < \mu^*$; thus, the solution is unimodal. On the other hand, for $\gamma = -0.4275 < 0$, $X_0^\sharp = 1.185$, such that $X_0 < X_0^\sharp$; hence, the solution also has a maximum value.

So far, regardless of the sign of γ the follicle always atrophies. Whenever its ageing parameter is not too large, it may be able to grow at first, but it will eventually decrease and atrophy. Decreasing the ageing parameter to an even smaller value, $\mu = 0.2$, we get to the point where the sign of γ determines two different kinds of behaviour within the initial maturity interval $(0, 1]$ that we arbitrarily have fixed.

If $\gamma > 0$ there is a critical initial maturity value $0 < X_0^* < 1$ such that,

a) if $X_0 < X_0^*$ the follicle grows reaching a maximum from which it degenerates and ultimately atrophies, *i.e.* the follicle regresses by atresia (see figure 6.4).

b) if $X_0 > X_0^*$ the follicle grows to infinity at a finite time, which corresponds to the ovulatory case (see figure 6.4).

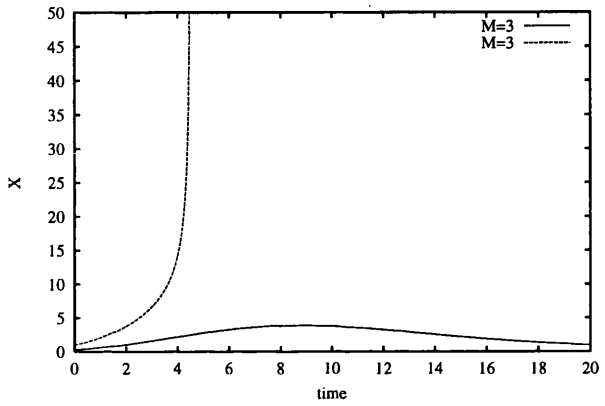

Figure 6.4: Solution of the non-autonomous equation (6.8) where $K = 1.0$, $y_0 = 1.0$, $\gamma > 0$ and $\mu = 0.2$. For this case, $X_0^* = 0.477106$. Thus, for $X_0 = 0.3$ the follicle reaches a maximum value and then atrophies, while for $X_0 = 1.0$ it ovulates.

In contrast, if $\gamma < 0$ the solution reaches a maximum

$$X_{max} = \sqrt{\frac{y - \mu}{-\gamma y}}$$

for a particular value of y. This X_{max} is exactly the same as in (6.14) when $y = y_0 e^{-\mu t}$. Comparing this situation with the case shown in figure 6.3, we observe $X(t)$ decreases slower (see figure 6.5).

Furthermore, if we decrease μ even more for this particular case of $\gamma < 0$, we see in figure 6.6 that the follicle appears to get stuck inside the ovary. This means that the follicle remains at almost the same size in the ovary as time goes by. It can also be noticed that whenever μ is very small, the maximum of the function approximates to the equilibrium point value for Lacker's simplified model, *i.e.*

$$X_{max} \to \sqrt{-\frac{1}{\gamma}} \; as \; \mu \to 0.$$

This does not surprise us because whenever $\mu \to 0$ we also approach Lacker's simplified growth equation given in (6.6).

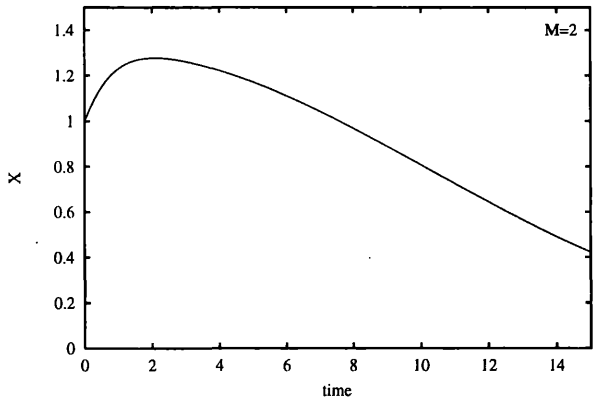

Figure 6.5: Solution (6.8) for $\mu = 0.2$, $\gamma = -0.4275 < 0$, $y_0 = 1.0$ and $X_0 = 1.0$. The follicle reaches a pre-ovulatory maturity and decreases slower than the equivalent solution in figure 6.3.

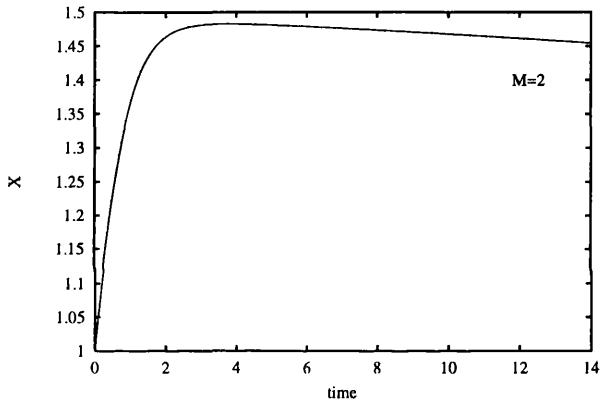

Figure 6.6: Anovulation for $\mu = 0.05$, $\gamma = -0.4275 < 0$, $y_0 = 1.0$ and $X_0 = 1.0$. The follicle appears to tend to the equilibrium value of the simplified Lacker's model, $X_{max} = 1.53$.

Therefore, features observed in figures 6.5 and 6.6, represent anovulation where the stuck follicle eventually disappears from the ovary. This is more realistic than the type of anovulation reflected in the models of previous chapters since the ovary does not hold the stuck pre-ovulatory follicle for ever. Instead, it disappears after some time despite the fact that its response to gonadotropins is adequate for initially maintaining a pre-ovulatory size.

We may deduce that ovulation occurs in the same fashion as ovulation in Lacker's model. However, we cannot conclude the same for the case of anovulation. For Lacker's anovulation case, the follicle reaches a non-trivial stable equilibrium point remaining there as time goes by. In contrast, for this revised model, the only equilibrium point is zero meaning that, due to its ageing factor the stuck follicle eventually dies rather than remaining indefinitely at a fixed large size.

6.4 Analysis for many interacting follicles

In this section we study and discuss the dynamics of many interacting follicles. Initially, we only consider them to be different in size, but having the same age. Later, we shall extend our analysis to the case where they differ in both, age and size.

6.4.1 Dynamics of follicles with different initial sizes but same age

We develop a theoretical and numerical analysis for the study of the dynamics for the situation where all follicles start with different initial maturities but they have the same initial age.

For this particular case, the follicle growth function is given by

$$g(x_i, X, y) = yg(x_i, X) - \mu$$

for all follicles, and it can also be separated into three different functions, so that we get the following system:

$$\begin{aligned} \frac{dx_i}{dt} &= x_i(y\delta(X)[\rho(X) + \xi(p_i)] - \mu) \\ \frac{dy}{dt} &= -\mu y, \end{aligned}$$

where the *separated functions* are the same as those that Lacker proposed and that were used in (4.14) of chapter 4. We also consider the same rescaling equation

$$\frac{d\tau}{dt} = \delta(X). \tag{6.15}$$

The resulting *interaction* and *intensity* dynamics are

$$\begin{aligned} \frac{dp_i}{d\tau} &= yp_i\left[\xi(p_i) - \bar{\xi}(\bar{p})\right] && (a) \\ \frac{dy}{d\tau} &= -\frac{\mu}{\delta(X)}y && (b) \\ \frac{dX}{d\tau} &= X\left[y\rho(X) + y\bar{\xi}(\bar{p}) - \frac{\mu}{\delta(X)}\right], && (c) \end{aligned} \tag{6.16}$$

where p_i is the ith follicle relative size and $\bar{p}$ and $\bar{\xi}(\bar{p})$ are just as in the *interaction* equation (4.8) of Lacker's symmetric model.

For the stability analysis of this system we start by analysing equation (6.16.a). We choose to re-scale it by defining τ' such that $d\tau'/d\tau = y$. Hence, we obtain the following *interaction dynamics*

$$\frac{dp_i}{d\tau'} = p_i \left[\xi(p_i) - \bar{\xi}(\bar{p})\right]. \tag{6.17}$$

Consequently, for equation (6.17) we have the same equilibrium condition as for the corresponding *interaction dynamics* for Lacker's model, which leads to the same $M - fold$ equilibrium point

$$\bar{p}_M = (\underbrace{\frac{1}{M}, \frac{1}{M}, \ldots, \frac{1}{M}}_{M}, \overbrace{0, \ldots, 0}^{N-M}). \tag{6.18}$$

Once again, it is possible to express equation (6.17) as a gradient system on the unit sphere, and then prove that its symmetric equilibrium point (6.18) is stable.

Therefore, as in the symmetric model of chapter 4, we observe that for the case of different interacting follicles with the same age, there is a stable equilibrium point towards which the M largest follicles tend to, while the remaining $N - M$ smaller follicles regress and die by atresia. What happens to the $M - fold$ equilibrium point (6.18) outside the unit sphere is determined by the corresponding *intensity dynamics* given by equations (6.16.b) and (6.16.c).

By substituting back the values of the *rescaled function*, $\delta(X)$ as well as expressing (6.16.b) and (6.16.c) in terms of t, we see that these two equations are equivalent to the ones describing the simplified system (6.4), for which a thorough stability analysis was already carried out in section 6.3.

Finally, to prove that the ovulation time is a finite value T, we study the dynamics of the *rescaled time* given in (6.15) for the case when X is large. First of all let us re-scale equations (6.16.b) and (6.16.c) by τ' such that $d\tau'/d\tau = y$. Hence, we obtain

$$\begin{aligned} \frac{dy}{d\tau'} &= -\frac{\mu}{\delta(X)} \\ \frac{dX}{d\tau'} &= X\left[\rho(X) + \bar{\xi}(\bar{p}) - \frac{\mu}{y\delta(X)}\right]. \end{aligned}$$

Thus, for X sufficiently large and $\bar{p} \approx \bar{p}_M$ we have that $dy/d\tau' \approx 0$, which implies that $y \approx y_c$, for y_c a constant value, and

$$\frac{dX}{d\tau'} > X\left[-D + \xi(\frac{1}{M})\right] > 0$$

since $\xi(1/M) > D$. Therefore, following the demonstration for the *rescaled time dynamics* of the non-symmetric model of chapter 6, we conclude that there exists a $0 < T < \infty$, such that $t \to T$ as $\tau' \to \infty$. And since $d\tau \approx 1/y_c d\tau'$, we have that $\tau \to \infty$ as $\tau' \to \infty$.

We present a number of numerical examples to show the kinds of behaviour obtained when we have follicles with different sizes but the same age. From the simplified model in (6.4), it was observed that the number of follicles ovulating is determined by the parameter values M_1 and M_2 just as in Lacker's model. Therefore, we start with a simple case where according to the initial size distribution, there would be either three ovulating, or two "stuck" follicles. Figure 6.7 shows that from a population of $N = 8$ follicles starting the cycle with different maturities chosen from a uniform distribution, follicles behave in the same way as in the original Lacker's symmetric model. This means that the three largest follicles ovulate and the remaining smaller ones die by atresia.

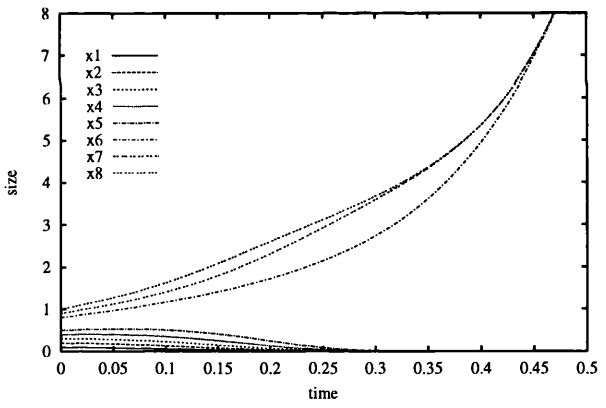

Figure 6.7: Numerical example similar to that of the symmetric model shown in figure 4.2 of chapter 4. The parameter values are $K = 5.0$, $D = 0.5$, $\mu = 0.2$, $M_1 = 2.9$, $M_2 = 3.9$, $y_{0_i} = 1.0\ \forall i = 1, \ldots, 8$. The three largest follicles x_6, x_7 and x_8 have relatively similar initial size, and are the ones ovulating. The rest, follicles x_1 to x_5, are the smaller ones which die by atresia.

Then, if we change the initial size distribution of the system, figure 6.8 indicates that the two largest follicles are selected and reach a pre-ovulatory size, yet they do not manage to ovulate but rather appear to remain at a fixed size. However, it is possible to observe that these pre-ovulatory follicles slowly decrease with time.

Moreover, we have also run the corresponding numerical simulations for the *interaction dynamics* given in system (6.16) for the two previous examples. Figure 6.9 shows the fact that for both situations, the three selected follicles for the ovulatory

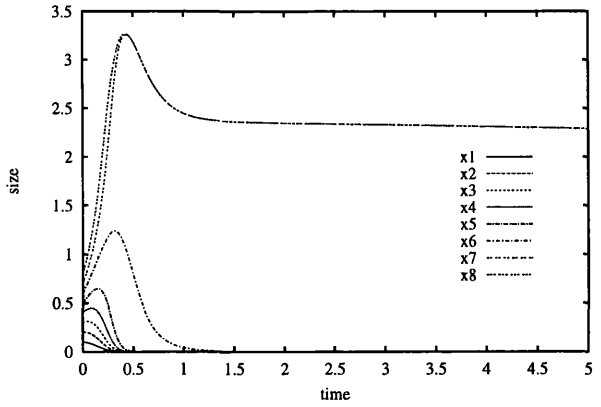

Figure 6.8: Numerical simulation equivalent to that shown in figure 4.1 of chapter 4. Parameters, K, D, μ, M_1, M_2, and initial conditions y_{0_i} $\forall i = 1, \ldots, 8$ are the same as in figure 6.7, but the initial maturity distribution changes. Follicles x_7 and x_8 reach the same pre-ovulatory maturity, but then decrease very slowly, while the reminding five follicles, $x_1, \cdots, x_5$, atrophy and die.

case and the two selected ones for the anovulatory case tend to the same fixed relative maturity value. Despite follicles x_7 and x_8 decreasing in size, figure 6.9.b shows that their corresponding relative maturity, p_7 and p_8, tends to a fixed value 1/2, as expected according to (6.18) and the stability Theorem (5.3.1).

Finally, we remark that although anovulation may occur in a biologically more realistic fashion in this ageing model, it is still possible to predict the number of follicles selected. This means that just by looking at the initial size distribution, we know how many and which follicles will be selected for either ovulation or anovulation. This is because the hierarchy of the largest follicles is still maintained.

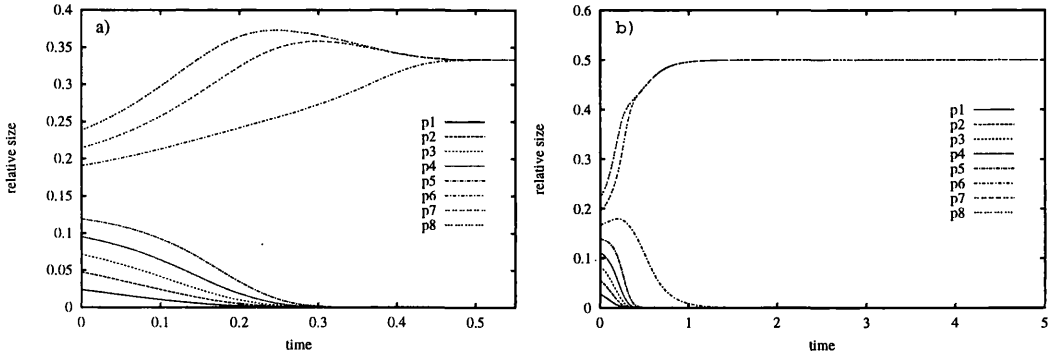

Figure 6.9: Solutions of follicles relative oestradiol secretion for $K = 5.0$, $D = 0.5$, $\mu = 0.2$, $M_1 = 2.9$, $M_2 = 3.9$, $y_{0_i} = 1.0$ $\forall i = 1, \ldots, 8$. a)Initial follicle sizes are the same as in figure 6.7; the relative maturity (oestradiol production) of p_6, p_7 and p_8 tend to the same value 1/3, the smaller ones, p_1 to p_5 regress and die. b)Initial follicle sizes similar to those of figure 6.8, follicles for which relative size are p_7 and p_8, reach the equilibrium value of 1/2, the rest smaller follicles $p_1, \cdots, p_6$ regress.

6.5 Dynamics of different follicles in size and age

Now we discuss the case when there are N follicles interacting with different initial maturities (sizes) and ages, with dynamics given by (6.3). However in this, the most general case of the three considered in this thesis, it is not possible to get a proper *separated dynamics* in order to obtain a gradient system on the unit sphere. Hence we started by investigating some numerical examples for the parameter values used in previous simulations.

Thus, for the same parameter values used in figures 6.7 and 6.8 of the previous section (6.4.1), we observe in figure 6.10 that for both situations, ovulation and anovulation, the selected follicles are amongst the largest, yet they are not necessarily the largest ones. Thus, although we can still predict the number of selected follicles, it is no longer true that they are always the largest ones.

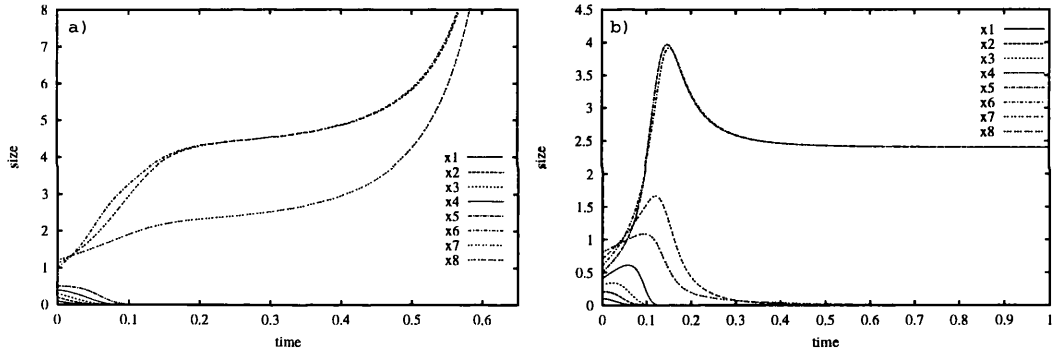

Figure 6.10: Simulation for the general situation where follicles interact with different initial size and age for the cases of either three or two follicles selected. The parameters, $K = 5.0$, $D = 0.5$, $\mu = 0.2$, $M_1 = 2.9$, $M_2 = 3.9$, and initial age distribution is uniformly decreasing from $y_{0_1} = 8.0$ to $y_{0_8} = 1.0$. a) The initial sizes are $x_{1_0} = 0.1, \cdots, x_{0_5} = 0.5, x_{06} = 1.0, x_{07} = 1.1, x_{0_8} = 1.2$. Ovulating follicles x_6 and x_7 grow faster than the initial largest one x_8. b) Initial sizes have the same value as in figure 6.8. Follicles x_5 and x_6 grow till a pre-ovulatory size, whereas the two largest follicles, x_7 and x_8, atrophy and die.

For the particular case shown in the previous figure 6.10, a numerical investigation was carried out to give some evidence that in fact, system (6.19) tends to the fixed point $\bar{p}_M$ in the space of the follicle relative size. An example of the results is shown in figure 6.11 where we see, for the ovulatory and anovulatory situations respectively, that the selected follicles tend to the same fixed equilibrium value in each case. This means that, although we are not able to determine which follicles reach pre-ovulatory maturity when starting with similar sizes and ages, the system appears to be stable in terms of the ovulation rate.

Therefore, since we are not able to prove that the interaction dynamics tends to

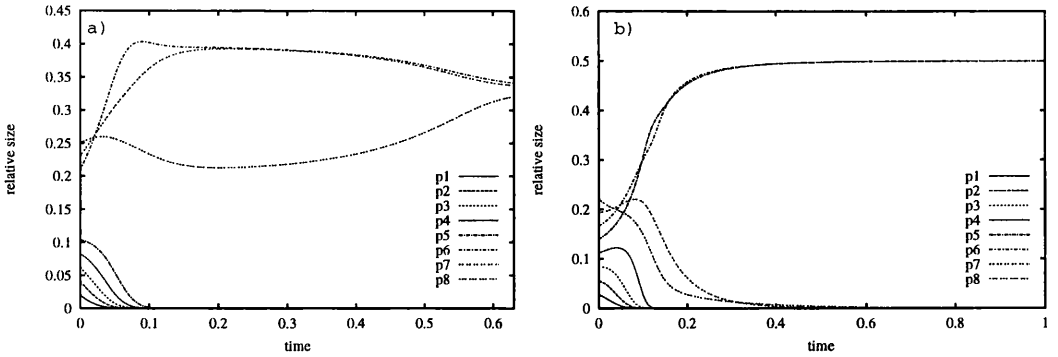

Figure 6.11: Simulation for the general situation where follicles interact with different initial size and age for the cases of either three or two follicles selected. The parameters, K, D, μ, M_1 and M_2, have the same value as figures 6.10. a) The three largest follicles tend to the same equilibrium point 1/3, and b) the follicles relative maturities p_5 and p_6 tend to a fixed value 1/2.

a stable equilibrium point by means of a gradient system, a linear stability analysis around a particular orbit is developed below.

In spite of the disadvantage of not obtaining a *separated dynamics* suitable for a gradient system analysis, we are able to derive an *interaction dynamics* and an *intensity dynamics* for system (6.3), where all follicles are different in size and age. Thus, considering $g(x_i, X) = \delta(X)[\rho(X) + \xi(p_i)]$ we get,

$$\begin{aligned}
\frac{dp_i}{d\tau} &= p_i \left[y_i\rho(X) + y_i\xi(p_i) - \rho(X)\sum_{j=1}^{N} y_j p_j - \sum_{j=1}^{N} y_j p_j \xi(p_j) \right] \qquad (a) \\
\frac{dy_i}{d\tau} &= -\frac{\mu}{\delta(X)} y_i \qquad (b) \qquad (6.19) \\
\frac{dX}{d\tau} &= X \left[y_i\rho(X) - \sum_{j=1}^{N} y_j p_j \xi(p_j) - \frac{\mu}{\delta(X)} \right]. \qquad (c)
\end{aligned}$$

Notice that equation (6.19.a) depends explicitly on X, which does not occur in any of the *interaction* equations obtained in previous models (refer to (4.8) and (5.2)). For the case of (6.16) of the previous section, we see X does not appear explicitly in equation (6.16.a), but rather indirectly through y. However, we can re-scale this equation in order to get rid of y, and therefore we can analyse the *interaction* equation independently of X.

Also note that if we simplify system (6.19) by supposing $y_i = y_j = y$, we also obtain the same *interaction dynamics* system as in (6.16). Hence, we see that (6.19.a) is a direct generalisation of (6.16.a). For the *interaction dynamics* of system (6.16), the equilibrium point $\bar{p}_M$ described in (6.18) is stable.

We can also say, that the solutions of system (6.16) lie along the lines of symmetry of the M-dimensional coordinate hyperplane in the N-dimensional space of follicle relative sizes, and along the lines of symmetry of the N-dimensional space of follicle ages. Therefore, we consider an orbit $\bar{y}_S = (y, \ldots, y)$ for any $y > 0$ such that

$$(\bar{p}_M, \bar{y}_S) \tag{6.20}$$

is the orbit around which we would like to develop a stability analysis of system (6.19). However, system (6.19) has an extra equation for X compared to system (6.3). Hence, system (6.19) is over-determined, which in fact complicates the analysis. This is because instead of computing a Jacobian of size $2N \times 2N$ for system (6.3), for which the dynamics of X is implicitly determined, we obtain a larger Jacobian of size $(2N+1) \times (2N+1)$. Its corresponding eigenvalues are more difficult to estimate. Therefore, we return to (6.3) and develop a linear stability analysis for the corresponding orbit in this system.

Let us establish then the corresponding orbit to (6.20) for system (6.3). Note that for $\bar{p}_M$ given in (6.18), $p_i = 1/M$ implies that $x_i/X = 1/M$. Therefore, $x_i = X/M$ for all $i = 1, \cdots, M$ and $x_i = 0$ for all $i = M+1, \cdots, N$ is the equivalent point for system (6.3) for any $X > 0$.

Hence,

$$p_e = (x_i, X, y) = \begin{cases} (X/M, X, y) & \forall\, i = 1, \cdots, M \\ (0, X, y) & \forall\, i = M+1, \cdots, N \end{cases} \tag{6.21}$$

for any $X > 0$ and any $y > 0$ is the orbit around which we develop a linear stability analysis below.

6.5.1 Linear stability analysis of the system of interacting follicles which are different in size and age.

Let us consider the original system

$$\begin{aligned} \frac{dx_i}{dt} &= y_i x_i [K - D(X - M_1 x_i)(X - M_2 x_i)] - \mu x_i = G_1(x_i, X, y_i) \\ \frac{dy_i}{dt} &= -\mu y_i = G_2(x_i, X, y_i), \end{aligned} \tag{6.22}$$

where X depends explicitly on x_i for all i as we see in (6.2).

Now we make a small perturbation $\tilde{x} = (\tilde{x}_1, \cdots, \tilde{x}_N)$ and $\tilde{y} = (\tilde{y}_1, \cdots, \tilde{y}_N)$ so that $\epsilon = (\tilde{x}, \tilde{y})$, around the solution for which all follicles have the same age y, *i.e.* around

p_e given in (6.21). Thus, let us consider the first order Taylor expansion,

$$F(\bar{x}+\tilde{x},\bar{y}+\tilde{y}) = F(\bar{x},\bar{y}) + D_{(x,y)}F\epsilon^T + o(\|\epsilon\|^2)$$

where, $\bar{x} = (x_1,\cdots,x_N)$, $\bar{y} = (y_1,\cdots,y_N)$ and $F = (\overbrace{G,\cdots,G}^{N})$, is the symmetric vector field of the system, for $G = (G_1, G_2)$ where G_1 and G_2 are given in (6.22).

To compute the Jacobian $J = D_{(\bar{x},\bar{y})}F$, we need

$$\begin{aligned}
\frac{dG_k}{dx_i} &= \frac{\partial G_k}{\partial x_i} + \frac{\partial G_k}{\partial X}\cdot\frac{\partial X}{\partial x_i} \\
\frac{dG_k}{dy_i} &= \frac{\partial G_k}{\partial y_i}
\end{aligned}$$

for every $k = 1, 2$ and $i = 1,\cdots,N$. Therefore, J is a $2N \times 2N$ matrix such that:

$$J = \begin{bmatrix} \left[\frac{\partial G_1}{\partial x} + \frac{\partial G_1}{\partial X}\right]_{ij} & \left[\frac{\partial G_1}{\partial y}\right]_{ij} \\ \left[\frac{\partial G_2}{\partial x} + \frac{\partial G_2}{\partial X}\right]_{ij} & \left[\frac{\partial G_2}{\partial y}\right]_{ij} \end{bmatrix}$$

for $i = 1,\cdots,N$ and $j = 1,\cdots,N$. Computing the various terms we have:

i) for $i = j$,

$$\begin{aligned}
\frac{\partial G_1}{\partial x_i} &= y_i[K - D(X - M_1x_i)(X - M_2x_i)] - \mu + x_iy_i[D(M_1+M_2)X - 2DM_1M_2x_i] \\
\frac{\partial G_1}{\partial X} &= x_iy_i[-2DX + D(M_1+M_2)x_i] \\
\frac{\partial G_1}{\partial y_i} &= x_i[K - DX^2 + D(M_1+M_2)Xx_i - DM_1M_2x_i^2] \\
\frac{\partial G_2}{\partial x_i} &= 0 \\
\frac{\partial G_2}{\partial X} &= 0 \\
\frac{\partial G_2}{\partial y_i} &= -\mu
\end{aligned}$$

ii) for $i \neq j$,

$$\begin{aligned}
\frac{\partial G_1}{\partial x_j} &= 0 \\
\frac{\partial G_1}{\partial X} &= x_i y_i[-2DX + D(M_1 + M_2)x_i] \\
\frac{\partial G_1}{\partial y_j} &= 0 \\
\frac{\partial G_2}{\partial x_j} &= 0 \\
\frac{\partial G_2}{\partial X} &= 0 \\
\frac{\partial G_2}{\partial y_j} &= 0.
\end{aligned}$$

We can now evaluate the Jacobian at p_e. Evaluating the non-zero terms for $i = j$, we have,

a) $i = 1, \ldots, M$

$$\begin{aligned}
\left.\frac{\partial G_1}{\partial x_i}\right|_{p_e} &= y\left[K - DX^2 + 2D(M_1 + M_2)\frac{X^2}{M} - 3DM_1M_2\frac{X^2}{M^2}\right] - \mu = a_1 \\
\left.\frac{\partial G_1}{\partial X}\right|_{p_e} &= y\left[D(M_1 + M_2)\frac{X^2}{M^2} - 2D\frac{X^2}{M}\right] = b_1 \\
\left.\frac{\partial G_1}{\partial y_i}\right|_{p_e} &= \frac{X}{M}\left[K - DX^2 + D(M_1 + M_2)\frac{X^2}{M} - DM_1M_2\frac{X^2}{M^2}\right] = c_1 \\
\left.\frac{\partial G_2}{\partial y_i}\right|_{p_e} &= -\mu
\end{aligned} \tag{6.23}$$

b) $i = M + 1, \ldots, N$:

$$\begin{aligned}
\left.\frac{\partial G_1}{\partial x_i}\right|_{p_e} &= y[K - DX^2] - \mu = a_2 \\
\left.\frac{\partial G_1}{\partial X}\right|_{p_e} &= 0 \\
\left.\frac{\partial G_1}{\partial y_i}\right|_{p_e} &= 0 \\
\left.\frac{\partial G_2}{\partial y_i}\right|_{p_e} &= -\mu
\end{aligned} \tag{6.24}$$

On the other hand, for $i \neq j$ we have,

a) $i = 1, \ldots, M$ and $j = 1, \ldots, M$:

$$\left.\frac{\partial G_1}{\partial X}\right|_{p_e} = b_1$$

b) $i = M+1, \ldots, N$ and $j = 1, \ldots, M$

$$\left.\frac{\partial G_1}{\partial X}\right|_{p_e} = 0$$

c) $i = 1, \ldots, M$ and $j = M+1, \ldots, N$

$$\left.\frac{\partial G_1}{\partial X}\right|_{p_e} = b_1$$

d) $i = M+1, \ldots, N$ and $j = M+1, \ldots, N$

$$\left.\frac{\partial G_1}{\partial X}\right|_{p_e} = 0.$$

Therefore, the resulting Jacobian evaluated at p_e is the block matrix,

$$J|_{p_e} = \left[\begin{array}{cc|cc} C & b_1 U & c_1 I & 0 \\ 0 & a_2 I & 0 & 0 \\ \hline 0 & & -\mu I & \end{array}\right]. \tag{6.25}$$

Here, C is the $(M \times M)$ circulant matrix

$$C = circ(\underbrace{a_1 + b_1, b_1, \cdots, b_1}_{M}).$$

This means that for all $i = 1, \cdots, M$, the ith row of C is obtained by shifting the $(i-1)$th row one entry to the right and the last element to the first, where the first row is given by the $1 \times M$ vector, $(a_1 + b_1, b_1, \cdots, b_1)$ (see 6.5.1).

Definition 6.5.1 *A circulant matrix is a $N \times N$ matrix*

$$C = \begin{pmatrix} c_0 & c_1 & \cdots & c_{N-1} \\ c_{N-1} & c_0 & \cdots & c_{N-2} \\ & & & \\ c_1 & c_2 & \cdots & c_0 \end{pmatrix},$$

such that each of its rows, apart from the first, can be obtained by shifting each element of the previous row one place to the right, and the last element to the first.

Matrix U is an $M \times (N-M)$ matrix such that all its entries are equal to one. Furthermore, $a_2 I$ is such that I is the identity matrix of size $(N-M) \times (N-M)$, and $c_1 I$ is such that I is the $(M \times M)$ identity matrix. Finally, $-\mu I$ is such that I is the identity matrix of size $(N \times N)$.

Since $J|_{p_e}$ is an upper triangular block matrix, it is possible to analytically compute its eigenvalues. The set of such eigenvalues is referred as the *spectrum* of $J|_{p_e}$, and it is given by

$$Spec(J|_{p_e}) = \bigcup [Spec(C), Spec(a_2 I), Spec(-\mu I)].$$

$Spec(C)$ is then given by,

$$\begin{aligned} \lambda_1 &= a_1 + M b_1 \quad \text{with multiplicity 1} \\ \lambda_2 &= a_1 \quad \text{with multiplicity M} - 1. \end{aligned}$$

The general formula for the jth eigenvalue of C is given by

$$\lambda_j = a_1 + b_1 + b_1 r_j + b_1 r_j^2 + \cdots + b_1 r_j^{M-1} = a_1 + b_1 + b_1 \sum_{k=1}^{M-1} r_j^k \tag{6.26}$$

(see (6.5.2)).

Proposition 6.5.2 *[Bellman, 1960] The eigenvalues λ_i of a circulant matrix C are*

$$\lambda_i = c_0 + c_1 r_i + \cdots + c_{N-1} r_i^{N-1},$$

where r_i is the ith root of 1. The associate eigenvector then is

$$(1, r_i, \cdots, r_i^{N-1}).$$

Here, $r_j^M = 1$ for all $j = 1, \cdots, M$, *i.e.* each r_j is one of the Mth roots of 1. Suppose that $r_1 = 1$, *i.e.* $\theta = 0$ (see figure 6.12). This implies that $r_1^k = 1$ for all $k = 1, \cdots, M-1$ such that

$$\sum_{k=1}^{M-1} r_1^k = \underbrace{1 + 1 + \cdots + 1}_{M-1} = M - 1.$$

Hence from (6.26) we get $\lambda_1 = a_1 + b_1 + b_1(M-1) = a_1 + M b_1$.

For $j = 2, \cdots, M$ we have that $\theta \neq 0$, such that r_j^k is equivalent to rotating r_j through an angle $k\theta$.. Then, we have that

$$\sum_{k=1}^{M} r_j^k = 0$$

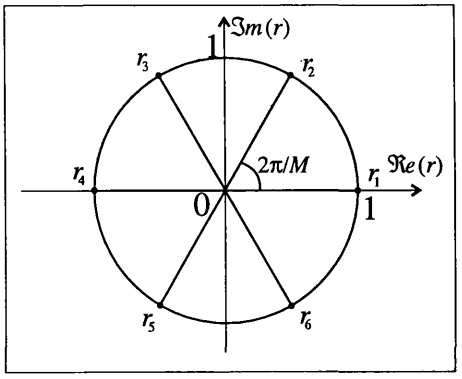

Figure 6.12: Diagram of $M = 6$ roots of 1, each of which can be associated with a vector on the complex plane. For the particular case of r_1, $\theta = 0$.

(see figure 6.13). This is also true since $r_j^M = 1$, we have that

$$0 = r_j^M - 1 = (r_j^{M-1} + r_j^{M-2} + \cdots + 1)(r_j - 1).$$

Hence, $\sum_{k=0}^{M-1} r_j^k = 0$ since $r_j \neq 1$. Then, $r_j \sum_{k=0}^{M-1} r_j^k = \sum_{k=1}^{M} r_j^k = 0$. Therefore, this implies

$$\sum_{k=1}^{M-1} r_j^k = \sum_{k=1}^{M} r_j^k - r_j^M = 0 - 1 = -1.$$

Thus, from (6.26) we obtain

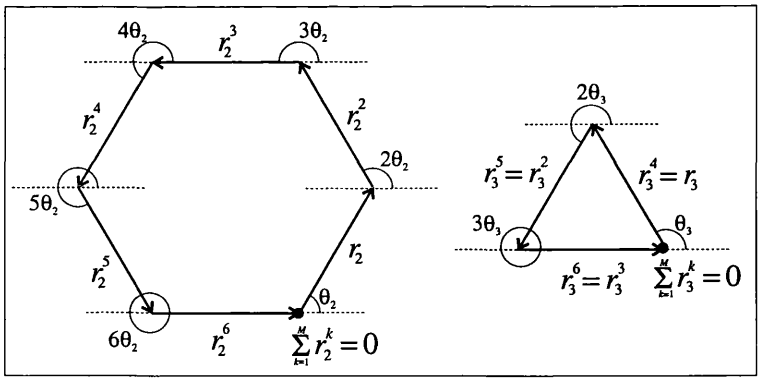

Figure 6.13: Two different examples of $\sum_{k=1}^{M} r_j^k = 0$, where r_j is the jth root of 1. Evaluating r_j^k is equivalent to rotating the vector associated to r_j with corresponding angle $\theta \neq 0$, an angle $k\theta$. In this diagram the particular cases of r_2 and r_3 of figure (6.12) are depicted.

$$\lambda_2 = a_1 + b_1 - b_1 = a_1.$$

Let λ_3 and λ_4 be the corresponding elements of $Spec(a_2 I)$ and $Spec(-\mu I)$ respectively, where

$$\lambda_3 = a_2 \quad \text{with multiplicity N} - \text{M}$$

$$\lambda_4 = -\mu \quad \text{with multiplicity N.}$$

Hence, substituting the values of a_1,b_1 and a_2 from (6.23) and (6.24), we get

$$\begin{aligned}
\lambda_1 &= y\left[K - 3DX^2\left(1 - \frac{(M_1+M_2)}{M} + \frac{M_1M_2}{M^2}\right)\right] - \mu \\
\lambda_2 &= y\left[K - DX^2\left(1 - \frac{2(M_1+M_2)}{M} + \frac{3M_1M_2}{M^2}\right)\right] - \mu \\
\lambda_3 &= y[K - DX^2] - \mu \\
\lambda_4 &= -\mu,
\end{aligned}$$

which are dependent on (X, y). Moreover, considering γ given in (6.5), we can rewrite the eigenvalues as,

$$\begin{aligned}
\lambda_1 &= y\left[K + 3D\gamma X^2\right] - \mu && (a) \\
\lambda_2 &= y\left[K + D\left(\gamma + \frac{(M_1+M_2)}{M} - \frac{2M_1M_2}{M^2}\right)X^2\right] - \mu && (b) \\
\lambda_3 &= y[K - DX^2] - \mu && (c) \\
\lambda_4 &= -\mu, && (d)
\end{aligned} \tag{6.27}$$

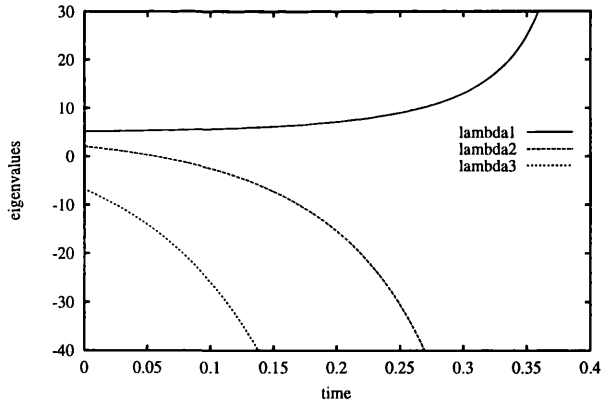

Figure 6.14: Eigenvalues evaluated for function $X(t)$ given in (6.8). Here $M = 3$, $y_0 = 1.0$ and the parameter values K, D, μ, M_1 and M_2 are the same as for the ovulating case of figure 6.10. The initial value $X_0 = 4.8$ is the sum of the initial follicles sizes given in figure 6.10. For this particular example, $\lambda_1(t) \to \infty$, and $\lambda_k(t) \to -\infty$ for $k = 2, 3$ as $t \to T$.

Thus we observe that λ_1, λ_2 and λ_3 are time dependent. If we evaluate each eigenvalue on $X(t)$ given in (6.8) as t increases, we see that whenever $\gamma > 0$, $\lambda_1(t) > 0$, and in fact $\lambda_1(t) \to \infty$ as $t \to T$ (see figure 6.14), where T is the fixed ovulation time, whereas $\lambda_k(t) \to -\infty$ for $k = 2, 3$. Since for $\gamma > 0$ we know that $X(t) \approx e^{\mu t}$

and $y(t) = y_0 e^{-\mu t}$, then $X^2 y \approx e^{\mu t}$. Therefore, $\lambda_k \to -\infty$ for both $k = 2, 3$ as $t \to T$ (see figure 6.14).

For the case when $\gamma < 0$, we observe that since $X(t) \to 0$ and $y(t) \to 0$, $\lambda_k(t) \to -\mu$ for all $k = 1, 2, 3$ as figure 6.15 shows.

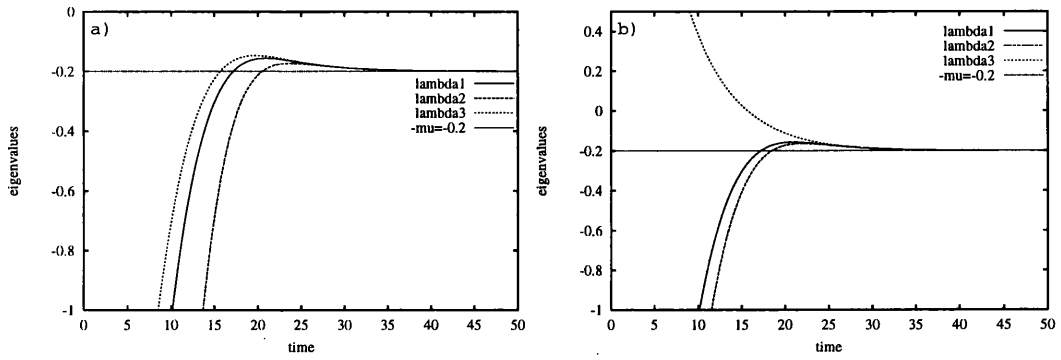

Figure 6.15: Eigenvalues evaluated for function $X(t)$ given in (6.8). Here $y_0 = 1.0$ and the parameter values K, D, μ, M_1 and M_2 are the same as for the ovulating case of figure 6.8, and $\gamma < 0$. In both examples $\lambda_k \to -\mu = -0.2$ as $t \to \infty$ for all $k = 1, 2, 3$. a) For this case the initial size distribution is such that $M = 2$, and all of the three eigenvalues are always negative. b) For this case the initial size distribution is such that $M = 1$, and $\lambda_3 > 0$ at the beginning of the cycle.

Notice that for the particular case shown in figure 6.15.b, the three eigenvalues are not all always negative. Here, the eigenvalues were evaluated for the anovulatory situation, where the parameter values are the same as in figures 6.7 and 6.8. However, by changing the initial size distribution so that we get one follicle relatively larger than the rest, we also obtain two anovulatory follicles as we see in figure 6.16. However, by the time the two pre-ovulatory follicles have been already selected, $\lambda_3(t) > 0$ (see figure 6.16 and 6.17). This may be intuitively contradictory, so let us compute the corresponding eigenvector for each eigenvalue to see in which directions the dynamic is either expanding or contracting.

Let us analyse the behaviour of the corresponding eigenvectors for each eigenvalue given in (6.27) along the orbit $X(t)$. Thus, let us solve system

$$\left[\begin{array}{cc|cc} C - \lambda I & b_1 U & c_1 I & 0 \\ \hline 0 & (a_2 - \lambda) I & 0 & 0 \\ \hline & & & \\ & 0 & (-\mu - 1) I & \\ & & & \end{array}\right] \bar{v} = \bar{0}$$

for the four different eigenvalues given in (6.27). Notice that $\bar{v} = (\bar{x}, \bar{y}) \in \mathbb{R}^{2N}$ and $\bar{0}$

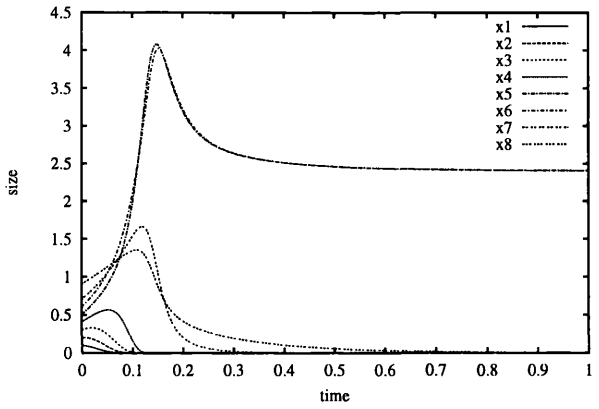

Figure 6.16: Numerical simulation of eight interacting follicles for parameters, $K = 5.0$, $D = 0.5$, $\mu = 0.2$, $M_1 = 2.9$, $M_2 = 3.9$, and initial conditions y_{0_i} $\forall i = 1, \ldots, 8$ are the same as in figure 6.10.b). The initial maturity distribution is such that follicle x_8 initial size is relatively larger than the rest seven follicles. Follicles x_5 and x_6 are the ones reaching the same pre-ovulatory maturity, while the reminding five follicles, $x_1, \cdots, x_4, x_7$ and x_8, atrophy and die.

is the null vector also in $\mathbb{R}^{2N}$. Thus, we obtain the following system,

$$\begin{aligned} [C - \lambda I]\bar{x}_M + b_1 U \bar{x}_{N-M} + c_1 I \bar{y}_M &= \bar{0}_M \qquad (a) \\ (a_2 - \lambda) I \bar{x}_{N-M} &= \bar{0}_{N-M} \quad (b) \\ (-\mu - \lambda) I \bar{y} &= \bar{0}_N \qquad (c) \end{aligned} \tag{6.28}$$

where, $\bar{x}_M$ and $\bar{x}_{N-M}$ are the vectors obtained from the first M and the remaining $N - M$ coordinates of $\bar{x}$ respectively, and $\bar{y}_M$ is the vector obtained from the first M entries of $\bar{y}$. The same notation is used for the vector $\bar{0}$.

Hence, for λ_1 we get $\bar{x}_{N-M} = \bar{0}_{N-M}$ and $\bar{y} = \bar{0}_N$ implying that $\bar{y}_M = \bar{0}_M$. From (6.5.2) we know that, $\bar{x}_M = \bar{u}_M$ where $\bar{u}_M$ is such that its all M coordinates are equal to one. This means that such a vector gives the direction of the M identical non-zero follicle sizes. Define $V_1 = \{\beta \bar{u}_M : \beta \in \mathbb{R}\} \subseteq \mathbb{R}^N$. For λ_2 we get $N - M$ eigenvectors $v = \bar{x}_M$ such that,

$$\sum_{k=1}^{M} v_k = 0$$

(see (6.5.2)). Observe that $v \perp \bar{u}_M$ for all v, so we define

$$V_1^{\perp} = \left\{ v : \sum_{k=1}^{M} v_k = 0 \right\}.$$

Finally, for λ_3, we see that from (6.28.c) $\bar{y} = \bar{0}_N$ and from (6.28.b) we get $\bar{x}_{N-M} \neq \bar{0}_{N-M}$. First suppose $\bar{x}_{N-M} = \bar{u}_{N-M}$, where $\bar{u}_{N-M}$ is the vector for which

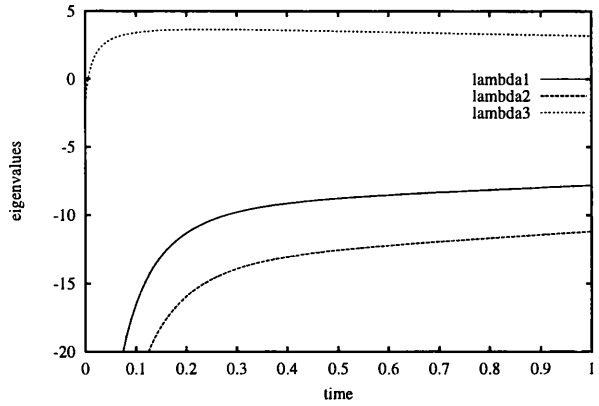

Figure 6.17: Eigenvalues obtained for the particular anovulation case shown in figure 6.16. We have evaluated function $X(t)$ given in (6.8) but in this case, $M = 1$, $y_0 = 1.0$ and $X_0 = 3.7$, which happens to be the sum of the initial follicles sizes given in figure 6.16. Then, $\lambda_k(t)$ is evaluated as t increases. For this particular case, $\lambda_1(t) < 0, \lambda_2(t) < 0$ and $\lambda_3(t) > 0$ as t increases.

all its $N - M$ entries are equal to one. Thus, from (6.28.a) we have to find $\bar{x}_M$ such that, $[C - \lambda_3 I]\bar{x}_M + b_1 U \bar{u}_{N-M} = \bar{0}_M$. If we take the i-th row, we get

$$(b_1, \cdots, b_1, \overbrace{a_1 + b_1 - \lambda_3}^{i-th}, b_1, \cdots, b_1)(x_1, \cdots, x_M)^T + (b_1, \cdots, b_1)(1, \cdots, 1)^T = 0$$

Thus, for the ith equation we obtain,

$$(a_1 - \lambda_3)x_i + b_1 \sum_{j=1}^{M} x_j + (N - M)b_1 = 0. \tag{6.29}$$

Since U is an $M \times (N - M)$ matrix and $\bar{u}_{N-M}$ is $(N - M) \times 1$, notice that $b_1 U \bar{u}_{N-M} = (N - M)b_1 \bar{u}_M \in V_1$, then $\bar{x}_M \in V_1$, *i.e.* $\bar{x}_M = \beta \bar{u}_M$ for a certain $\beta \in \mathbb{R}$. To compute such a β we get from equation (6.29),

$$(a_1 - \lambda_3)\beta + \beta M b_1 + (N - M)b_1 = 0$$

for all $i = 1, \cdots, M$. Thus,

$$\beta = -\frac{(N - M)b_1}{(\lambda_1 - \lambda_3)}.$$

Substituting the values of λ_1, λ_3, from (6.27), where we see that $\lambda_1 \neq \lambda_3$ for all X and y, and substituting the value of b_1 from (6.23), we get

$$\beta = -\frac{(N - M)\left[\frac{(M_1 + M_2)}{M^2} - \frac{2}{M}\right]}{3\gamma + 1}. \tag{6.30}$$

We thus see that β does not depend on t.

Now, let us suppose $\bar{x}_{N-M} = v$, such that $v \in V_{1b}^{\perp}$, where $V_{1b}^{\perp}$ is of dimension $N - M$, *i.e.* $\sum_{k=1}^{N-M} v_k = 0$, so that $\bar{u}_{N-M} \perp v$. Then, from system (6.28) we get $[C - \lambda_3 I]\bar{x}_M = \bar{0}_M$, which implies that $\bar{x}_M = \bar{0}_M$.

Since for the eigenvectors that we have computed for λ_1, λ_2 and λ_3, we have $\bar{y} = \bar{0}$, we analyse their behaviour only in the space of sizes $\bar{x} \in \mathbb{R}^N$. Hence, for the matrix

$$A = \left[\begin{array}{c|c} C & b_1 U \\ \hline 0 & a_2 I \end{array}\right]$$

the eigenvectors are,

$$\begin{aligned} \bar{v}_1^T &= (\bar{u}_M^T, \bar{0}_{N-M}^T) \\ \bar{v}_2^T &= (v^T, \bar{0}_{N-M}^T), \text{such that } v \in V_1^{\perp} \\ \bar{v}_{3a}^T &= (\beta \bar{u}_M^T, \bar{u}_{N-M}^T) \\ \bar{v}_{3b}^T &= (\bar{0}_M^T, v^T), \text{such that } v \in V_{1b}^{\perp}, \end{aligned} \tag{6.31}$$

where we notice that none of them depend on time. Note that all together, these eigenvectors give a basis for the whole space of follicular maturities. In particular, $\bar{v}_1$ gives the direction of the M identical non-zero follicle sizes. Moreover, changes in the direction of $\bar{v}_1$ correspond to changes in the follicles total size X. On the other hand, $\bar{v}_2$ corresponds to the direction of the $M - 1$ vectors perpendicular to $\bar{v}_1$, and any change in $\bar{v}_2$ does not affect the dynamics of X. Finally, $\bar{v}_{3a}$ and $\bar{v}_{3b}$ give two different directions for the remaining $N - M$ follicles. In particular, changes in $\bar{v}_{3a}$ give the dynamics of the total size of corresponding follicles, and any change in $\bar{v}_{3b}$ does not change X.

Therefore, the sign of λ_1 would determine whether we are in an ovulatory ($\lambda_1 > 0$) or anovulatory ($\lambda_1 < 0$) situation because its corresponding eigenvector, $\bar{v}_1$, points in the direction of the total oestradiol dynamics $X(t)$, which is equivalent to the dynamics of the M follicles having the same size or oestradiol production X/M. On the other hand, the sign of λ_2 determines whether the orbits approach or move away from the diagonal in the direction of $\bar{v}_1$. And finally, the sign of λ_3 indicates the behaviour in the remaining $N - M$ subspace of follicles with small initial size. Dynamics on the direction of $\bar{v}_{3a}$ gives the behaviour when all of the $N - M$ smallest follicles have the same initial size, whereas $\bar{v}_{3b}$ describes the dynamics in the direction perpendicular to $\bar{v}_{3a}$.

To study the local stability of the trajectory, let us apply the original linearised system to each of the eigenvectors, *i.e.* let us compute $d\bar{v}_k/dt = A\bar{v}_k$ for all $k = 1, 2, 3a, 3b$, and see how each $\bar{v}_k$ varies along $X(t)$.

From the eigenvectors given in (6.31) we obtain the following systems,

$$\begin{aligned}
\frac{d\bar{v}_1}{dt} &= A\bar{v}_1 = \lambda_1\bar{v}_1 && (a)\\
\frac{d\bar{v}_2}{dt} &= A\bar{v}_2 = \lambda_2\bar{v}_2 && (b)\\
\frac{d\bar{v}_{3a}}{dt} &= A\bar{v}_{3a} = \begin{pmatrix} \lambda_1\beta\bar{u}_M \\ \lambda_3\bar{u}_{N-M} \end{pmatrix} + (N-M)b_1(t)\begin{pmatrix} \bar{u}_M \\ \bar{0}_{N-M} \end{pmatrix} && (c)\\
\frac{d\bar{v}_{3b}}{dt} &= A\bar{v}_{3b} = \lambda_3\bar{v}_{3b}. && (d)
\end{aligned} \tag{6.32}$$

Then, for the non-zero coordinates of $\bar{v}_1$, $\bar{v}_2$, $\bar{v}_{3a}$ and $\bar{v}_{3b}$, we obtain the following system

$$\begin{aligned}
\dot{v}_{1j} &= \lambda_1 v_{1j} \quad \text{for all } j = 1, \cdots, M && (a)\\
\dot{v}_{2j} &= \lambda_2 v_{2j} \quad \text{for all } j = 1, \cdots, M && (b)\\
\dot{v}_{3bj} &= \lambda_3 v_{3bj} \quad \text{for all } j = M+1, \cdots, N && (c)
\end{aligned} \tag{6.33}$$

and,

$$\dot{v}_{3aj} = \begin{cases} \lambda_1 v_{3aj} + (N-M)b_1(t)v_{1j} & \text{for all } j = 1, \cdots, M \quad (a)\\ \lambda_3 v_{3aj} & \text{for all } j = M+1, \cdots, N. \quad (b) \end{cases} \tag{6.34}$$

However, the solution for the eigenvectors, $\bar{v}_1$ and $\bar{v}_2$ is given by,

$$\bar{v}_k(t) = \bar{v}_k(0)\exp\left(\int_0^t \lambda_k(s)ds\right)$$

for $k = 1, 2$. Similarly for $\bar{v}_{3b}$ we have

$$\bar{v}_{3b}(t) = \bar{v}_{3b}(0)\exp\left(\int_0^t \lambda_3(s)ds\right).$$

And for the $j = M+1, \cdots, N$ entries of $\bar{v}_{3a}$ we also have

$$v_{3aj}(t) = v_{3aj}(0)\exp\left(\int_0^t \lambda_3(s)ds\right).$$

Therefore, from (6.33.a) and (6.34.a) we observe that when $\gamma > 0$, since $\lambda_1(t) > 0$ the first M coordinates of $\bar{v}_1$ and $\bar{v}_{3a}$ grow to infinity. In contrast, the first M coordinates of $\bar{v}_2$ converge to zero since $\lambda_2(t) \to -\infty$. Moreover, from (6.33.c) and (6.34.b) we respectively notice that the $N - M$ coordinates of $\bar{v}_{3b}$ and $\bar{v}_{3a}$ tend to zero as $\lambda_3 \to -\infty$ (see figure 6.18).

On the one hand this means, that the corresponding vectors in V_1 formed by the M identical non-zero components of vectors $\bar{v}_1$ and $\bar{v}_{3a}$ point towards the same direction in which the orbit grows to infinity at a finite time, *i.e.* towards the direction given by $\bar{u}_M$. On the other hand, for the first M components of vector $\bar{v}_2$, the corresponding vector which points in a direction perpendicular to that given by the vectors in V_1 contracts with time. In other words, when M different but similar large follicles start the cycle, they will tend to the line along the direction given by $\bar{u}_M$, and then grow to infinity at a finite time.

The $N - M$ non-zero coordinates of $\bar{v}_{3a}$ and $\bar{v}_{3b}$ describe the dynamics of initial small follicles. Thus, when small different follicles start the cycle they will tend towards the line in the direction of $\bar{v}_{3a}$, and then tend to zero maturity.

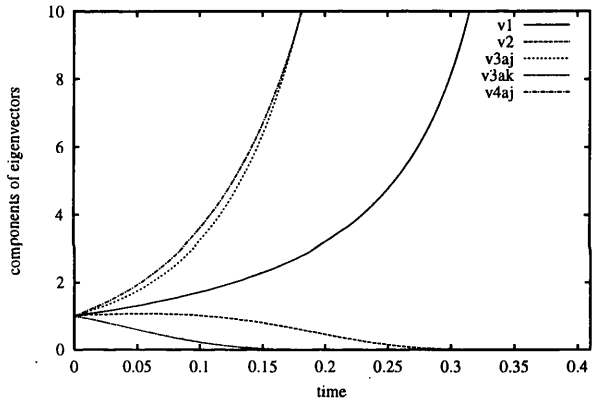

Figure 6.18: Dynamics of the different eigenvectors obtained from the eigenvalues computed for $\gamma > 0$ shown in figure 6.14. Dynamics of v_1, v_{3aj} and v_{4aj} represent the behaviour of $\bar{v}_1$, and the behaviour of the first M non-zero coordinates of $\bar{v}_{3a}$ and $\bar{v}_{4a}$ respectively. All of them grow to infinity at a finite time. In contrast, v_2 and v_{3ak} represents the dynamics of $\bar{v}_2$ and the $N - M$ non-zero coordinates of $\bar{v}_{3a}$, which tend to zero.

In the case of $\gamma < 0$, we have that since $\lambda_k \to -\mu$ for all $k = 1, 2, 3$, the M identical coordinates of the three different eigenvectors converge to zero as we see in figure 6.19.a. For the particular example given in figure 6.17, where $\lambda_3(t) > 0$ during the cycle, we observe in figure 6.19.b that also the first M coordinates of $\bar{v}_1$ and $\bar{v}_3$ tend to zero. This means that the dynamics along the line generated by $\bar{u}_M$ tends to zero. Furthermore, the M non-zero coordinates of $\bar{v}_2$ which generate a vector perpendicular to $\bar{u}_M$ also tend to zero. Thus, whenever the cycle starts with M different but similar large follicles, they will tend to the same size and then decrease and die.

For the dynamics of the $N - M$ coordinates of $\bar{v}_{3a}$ we have that since $\lambda_3(t) > 0$

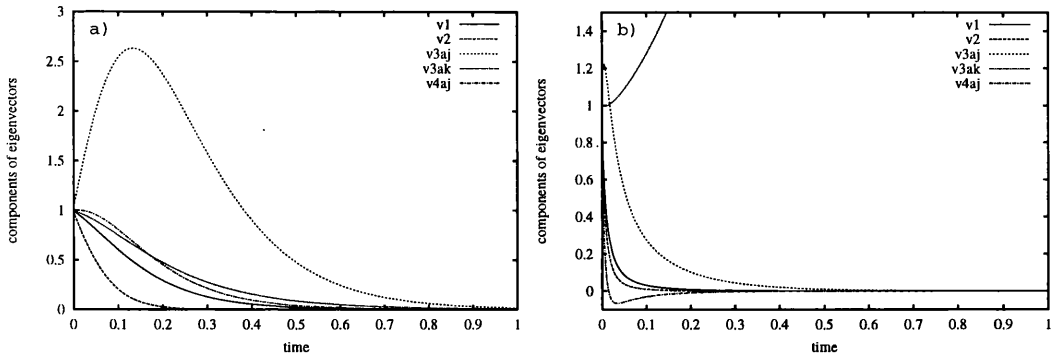

Figure 6.19: Dynamics of the different eigenvectors obtained from the eigenvalues computed for $\gamma < 0$ shown in figure 6.15. Dynamics of v_1, v_2, v_{3aj} and v_{4aj} represent the behaviour of $\bar{v}_1$, $\bar{v}_2$, and the first M non-zero coordinates of $\bar{v}_{3a}$ and $\bar{v}_{4a}$ respectively. All of them tend to zero in both figures a) and b). Moreover, v_{3ak} represents the dynamics of the $N - M$ coordinates of $\bar{v}_{3a}$, which also tends to zero in figure a), whilst grow in figure b).

during the cycle, as is seen in figure 6.17, the $N - M$ initially identical small follicles would grow to a large size. Nevertheless, although such coordinates grow to a very large value, they eventually tend to zero as expected since $\lambda_3(t) \to -\mu$ as $t \to \infty$ (see figure 6.20). At the same time, the $N - M$ follicles that initiate the cycle with different small sizes will tend to the line in the direction given by $\bar{v}_{3a}$, and then eventually tend to zero.

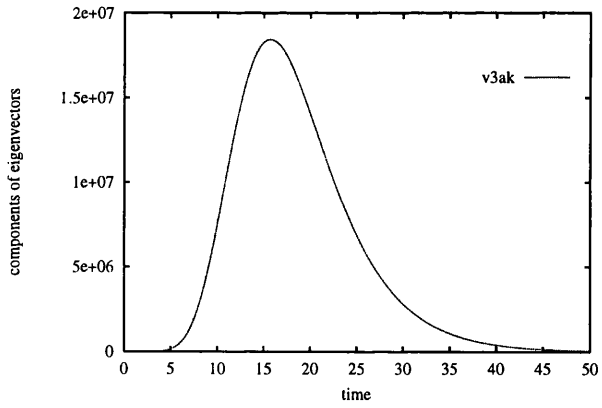

Figure 6.20: Dynamics of the $N - M$ coordinates of $\bar{v}_{3a}$obtained from λ_3 computed for $\gamma < 0$ shown in figure 6.15.b). Although such coordinates increase to a large value, they eventually tend to zero since $\lambda_3(t) \to -\mu$ as $t \to \infty$.

Finally, it remains to compute the eigenvectors for $\lambda_4 = -\mu$ corresponding to perturbations in $\bar{y}$. For that we consider the whole $2N$ dimensional space and solve system (6.28) for λ_4. Thus, from equation (6.28.c) we obtain that $\bar{y} \neq \bar{0}_N$, and from (6.28.b) we get $\bar{x}_{N-M} = \bar{0}_{N-M}$. To find the corresponding $\bar{x}_M$ we consider two

cases:

a) If $\bar{y} = \bar{u}_N$ (the vector for which its N coordinates are equal to one) corresponding to the same perturbation to all ages, then from (6.28.a) we obtain

$$[C - \lambda_4 I]\bar{x}_M + c_1 I\bar{u}_M = \bar{0}_M.$$

We find that for each $i = 1, \cdots, M$,

$$(a_1 - \lambda_4)x_i + bi\sum_{j=1}^{M} x_j + c_1 = 0.$$

Note that since $c_1 I\bar{u}_M = c_1\bar{u}_M \in V_1$, then $\bar{x}_M \in V_1$, so let $\bar{x}_M = \alpha\bar{u}_M$. Thus, for each i we obtain

$$(\lambda_1 - \lambda_4)\alpha + c_1 = 0$$

where,

$$\alpha = \frac{c_1}{\lambda_4 - \lambda_1},$$

such that $\lambda_4 \neq \lambda_1$ for all $X > 0$ and $y > 0$.

From the values of c_1 and γ given in (6.23) and (6.5) respectively, we get

$$c_1 = \frac{X}{M}[K + \gamma DX^2].$$

Therefore, from the eigenvalues given in (6.27), we finally obtain

$$\alpha = -\frac{X(t)[K + \gamma DX(t)^2]}{y(t)M\,[K + 3\gamma DX(t)^2]};$$

thus, $\alpha = \alpha(t)$. Therefore,

$$\bar{v}_{4a}^T = (\alpha(t)\bar{u}_M^T, \bar{0}_{N-M}^T, \bar{u}_N^T) \in \mathbb{R}^{2N},$$

which varies with time.

b) If $\bar{y} = v \in V_{1c}$, where $V_{1c}^{\perp} = \{v : \sum_{k=1}^{N} v_k = 0\}$ such that $\bar{u}_N \perp v$ for all $v \in V_{1c}^{\perp}$. Let $v^T = (\bar{v}_M^T, \bar{v}_{N-M}^T)$, where $\bar{v}_M$ is the first M entries of v, and $\bar{v}_{N-M}$ the remaining $N - M$ coordinates. Then, from (6.28.a) we get,

$$[C - \lambda_4 I]\bar{x}_M + c_1 I\bar{v}_M = \bar{0}_M,$$

from which we consider two sub-cases:

b.1) If $\bar{x}_M \in V_1$, then let $\bar{x}_M = \alpha'\bar{u}_M$ for a given $\alpha' \neq 0$. Thus for $i = 1, \cdots, M$ we get

$$(\lambda_1 - \lambda_4)\alpha' + c_1 v_i = 0.$$

From which,

$$v_i = \frac{(\lambda_4 - \lambda_1)\alpha'}{c_1} = \beta', \tag{6.35}$$

meaning that $\bar{v}_M = \beta'\bar{u}_M$, which implies $\bar{v}_M \in V_1$. Hence the eigenvector obtained is,

$$\bar{v}_{4b}^T = (\alpha'\bar{u}_M^T, \bar{0}_M^T, \beta'\bar{u}_M^T, \bar{v}_{N-M}^T).$$

b.2) If $\bar{x}_M \in V_1^\perp$, the ith equation in (6.28.a) is

$$(a_1 - \lambda_4)x_i + c_1 v_i = 0.$$

Hence,

$$v_i = \frac{(\lambda_4 - a_1)x_i}{c_1}, \tag{6.36}$$

which implies that $\bar{v}_M \in V_1^\perp$ since $\sum_{i=1}^M x_i = 0$, and

$$\sum_{i=1}^M v_i = \frac{\lambda_4 - a_1}{c_1}\sum_{i=1}^M x_i = 0.$$

Therefore, the eigenvector is

$$\bar{v}_{4c}^T = (\bar{x}_M^T, \bar{0}_{N-M}^T, \bar{v}_M^T, \bar{v}_{N-M}^T),$$

where $\bar{x}_M, \bar{v}_M \in V_1^\perp$.

Let us discuss the behaviour of $\bar{v}_k$ for the linearised dynamics $\dot{\bar{v}}_k = J|_{p_e}\bar{v}_k$, for $k = 4a, 4b, 4c$ and the matrix $J|_{p_e}$ given in (6.25). Just considering the non-zero terms of the resulting matrix, for $\bar{v}_{4a}$ we obtain,

$$\begin{bmatrix} \alpha(t)C\bar{u}_M + c_1 I\bar{u}_M \\ -\mu\bar{u}_N \end{bmatrix}.$$

Since $C\bar{u}_M = \lambda_1\bar{u}_M$, for the non-zero coordinates we get the following system,

$$\dot{v}_{4aj} = \begin{cases} \lambda_1 v_{4aj} + c_1(t)v_{1j} & \text{for all } j = 1, \cdots, M \\ \lambda_4 v_{4aj} & \text{for all } j = 1, \cdots, N. \end{cases} \tag{6.37}$$

For $\bar{v}_{4b}$ we get

$$\begin{bmatrix} \alpha' C\bar{u}_M + c_1 I\beta'\bar{u}_M \\ -\mu \begin{pmatrix} \beta'\bar{u}_M \\ \bar{v}_{N-M} \end{pmatrix} \end{bmatrix}.$$

Again, since $C\bar{u}_M = \lambda_1 \bar{u}_M$ and by substituting the value of β' given in (6.35) we get

$$\begin{bmatrix} \lambda_1 \alpha' \bar{u}_M + (\lambda_4 - \lambda_1)\alpha' \bar{u}_M \\ -\mu \begin{pmatrix} \beta' \bar{u}_M \\ \bar{v}_{N-M} \end{pmatrix} \end{bmatrix}.$$

Thus, for the non-zero coordinates we obtain the system,

$$\dot{v}_{4bj} = \begin{cases} \lambda_4 v_{4bj} & \text{for all } j = 1, \cdots, M \\ \lambda_4 v_{4bj} & \text{for all } j = 1, \cdots, N. \end{cases}$$

Finally, for $\bar{v}_{4c}$ when considering $\bar{v}_{N-M} = \bar{0}_{N-M}$ the non-zero terms of the resulting matrix are given by

$$\begin{bmatrix} C\bar{x}_M + c_1 I \bar{v}_M \\ -\mu \bar{v}_M \end{bmatrix}.$$

We have that $C\bar{x}_M = \lambda_2 \bar{x}_M$, and from (6.36) we see that $\bar{v}_M = (\lambda_4 - a_1)\bar{x}_M / c_1$, thus we get

$$\begin{bmatrix} \lambda_2 \bar{x}_M + (\lambda_4 - a_1)\bar{x}_M \\ -\mu \bar{v}_M \end{bmatrix}.$$

Hence, since $\lambda_4 - a_1 = \lambda_4 - \lambda_2$ as we can see from (6.23) and (6.27), we finally get the following system in coordinate form,

$$\dot{v}_{4cj} = \begin{cases} \lambda_4 v_{4cj} & \text{for all } j = 1, \cdots, M \\ \lambda_4 v_{4cj} & \text{for all } j = 1, \cdots, N. \end{cases}$$

for the non-zero terms.

The dynamics of vectors the $\bar{v}_{4b}$ and $\bar{v}_{4c}$, which were the ones obtained when considering $\bar{y} = v \in V_{1c}^{\perp}$ is given by,

$$\bar{v}_k(t) = \bar{v}_k(0) e^{-\mu t}$$

for $k = 4b, 4c$. This means that within both subspaces, the one of follicular sizes and the one of follicular ages, the dynamics along those two directions is contractive.

In more detail, the dynamics of coordinates v_{kj} for $j = 1, \cdots, N$ and $k = 4a, 4b, 4c$, within the space of follicular age is given by,

$$v_{kj}(t) = v_{kj}(0) e^{-\mu t}$$

Hence, it is clear that for the subspace of follicle ages, the dynamics of all of the eigenvectors $\bar{v}_k$ exponentially tends to zero at a rate given by $-\mu$. In particular for

the cases when $\bar{y} = v$ for $v \in V_{1c}^{\perp}$, this implies that when the cycle starts with follicles with different initial ages, their age values will tend to the diagonal given by $\bar{y} = \bar{u}_M$ within the age subspace, since the dynamics in the direction perpendicular to it is contractive. At the same time, the follicles' ages will tend to zero as the dynamics in the direction of $\bar{y} = \bar{u}_M$ also tends to zero as time goes by.

As for the dynamics of the follicle sizes, this analysis tells us that when $\gamma > 0$, the first M coordinates of $\bar{v}_{4a}$ tend to infinity at a finite time (see figure 6.18). For the first M coordinates of vectors $\bar{v}_{4b}$ and $\bar{v}_{4c}$ the dynamics tends to zero at the same rate $-\mu$. In contrast, when $\gamma < 0$, v_{4aj} for $j = 1, \cdots, M$ tend to zero as we see in both examples of figure 6.19. Furthermore, for $\gamma < 0$, the first M entries of $\bar{v}_{4b}$ and $\bar{v}_{4c}$ also tend to zero maturity. This means that the dynamics along the line generated by $\bar{u}_M$ is the same as the dynamics of the total amount of oestradiol X, and it would be either ovulatory, when $\gamma > 0$ or anovulatory, when $\gamma < 0$.

So far we have only considered linear stability. For the case of ovulation our analysis is about an unbounded trajectory. Hence, to decide stability of the nonlinear equations we require to prove that the second order term of the dynamics grows slower than the contracting eigenvalues. For the particular case of anovulation, this is pretty straight forward since $X(t) \to 0$ as $t \to \infty$. However, a better analysis needs to be developed for the ovulatory situation, where $X(t) \to \infty$ as $t \to T$. Nevertheless, for the purposes of this thesis we just consider the linear stability analysis as well as the numerical examples described to show that the system is locally stable at a linear and a non-linear level.

Therefore, we can just suggest that when the cycle starts with different follicles in size and age, the dynamics is at least locally stable. Hence, when the cycle begins with different follicles but similar in both age and size, the basic behaviour of the cycle is stable, and the number of follicles selected can still be predicted.

6.5.2 Further results

New results from this model can be observed when the initial conditions of the system are not similar. For example, in the cases where there are either three follicles ovulating or two stuck follicles, drastic alterations in the selection process may be obtained by sufficiently large perturbations of the initial conditions of the system. In this case the largest follicle's initial age was reduced to a value much smaller than the age of the remaining interacting follicles. Figure 6.21 shows for the particular

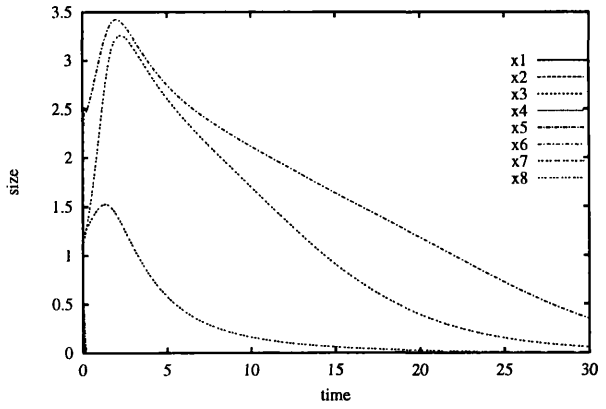

Figure 6.21: Simulation of the ageing model where $K = 5.0$, $D = 0.5$, $\mu = 0.2$, $M_1 = 2.9$ and $M_2 = 3.9$. Initial age values do not decrease uniformly as in previous examples, but $y_{0_1} = 8.0, \ldots y_{0_6} = 3.0$ while, $y_{0_7} = 0.2$ and $y_{0_8} = 0.1$. The three largest follicles, x_6,x_7 and x_8 reach pre-ovulatory maturity, yet they start to atrophy so slowly that it appears they remain stuck in the ovary. Rather than ovulatory, these three follicles get stuck inside the ovary.

situation where previously the largest three follicles would ovulate, now such follicles demonstrate anovulatory behaviour, and eventually tend to zero. Although these three follicles decrease in size, they are not atretic when we compare their decrease rate with smaller follicles x_1 to x_5. In fact, from the separatrix value given in (6.9) for the simplified model, we observe that X^* is inversely proportional to the initial age value y_0. Thus, for the case of follicles starting the cycle with different ages, the 'oldest' ones, may start growing with an initial size lower than the minimum threshold required to ovulate, which is given by X^*.

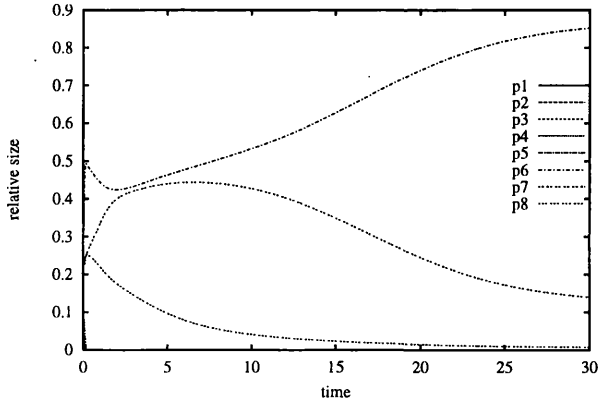

Figure 6.22: Numerical simulation of follicles relative oestradiol production corresponding to that of figure 6.21. Parameter values K, D, μ, M_1 and M_2 are the same and, the initial age distribution is also the same. Follicles with the largest relative maturity, do not tend to the equilibrium value of $1/3$, instead follicle p_8 tends to zero and follicles p_6 and p_7 tend to different equilibrium points.

Therefore, this means that it does not matter that the largest follicles have the opportunity to ovulate in terms of their hormonal sensitivity, if two of them are old enough at the beginning of the cycle, they would not ovulate and would also obstruct other follicles from ovulating. Hence, the symmetric ageing model gives the possibility of getting the same number of follicles ovulating or arresting only by a change in the initial conditions of the system. This is another feature that Lacker's model is unable to exhibit since, for that model, the number of ovulating follicles is always strictly larger than the number of stuck follicles. Therefore, incorporating the ageing factor into Lacker's original model suggests that such a decaying capacity may be the reason for anovulation when hormonal levels are at the correct levels for a normal selection process.

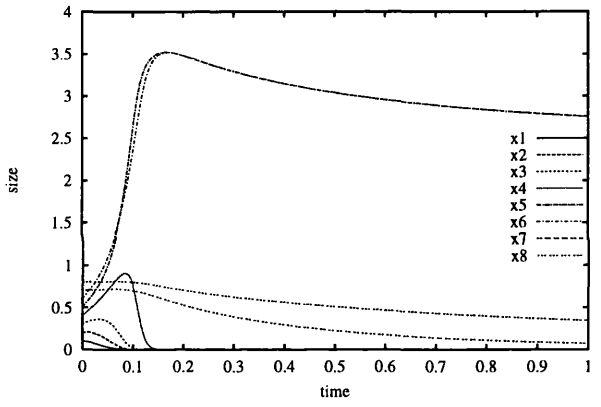

Figure 6.23: Anovulatory ovary for parameter values $K = 5.0$, $D = 0.5$, $\mu = 0.2$, $M_1 = 2.9$ and $M_2 = 3.9$, and initial age distribution like in previous figure 6.22. There is not a significant qualitative difference from that of figure 6.11, where the same follicles x_5 and x_6 are again selected. However, follicles x_7 and x_8 atrophy slower than follicles x_7 and x_8 of figure 6.11.

Furthermore, it is also observed in this example that the relative maturity of the selected follicles does not tend to the same fixed value as in figure 6.11. In contrast, we observe follicles p_7 and p_6 tending to a different equilibrium point, whereas the largest follicle relative maturity, p_8, tends to zero (see figure 6.22). This fact reflects that we can only guarantee local stability for the model of follicles with different size and age.

However, on the other hand, we would not get a significant alteration to the selection process if for the anovulatory case, the initial age of the two largest follicles is greatly reduced. For this situation figure 6.23 shows that follicle five and six are again selected and remain stuck, but the two largest follicles decrease much more

slowly than in the case shown in figure 6.11.b. However, we would not consider follicles seven and eight as being anovulatory since they still decrease much faster than follicles five and six. Furthermore, figure 6.24 shows follicles five and six are still the selected ones. This agrees with the fact that for the anovulatory case, there is no minimum threshold required for follicles to be able to reach a pre-ovulatory size.

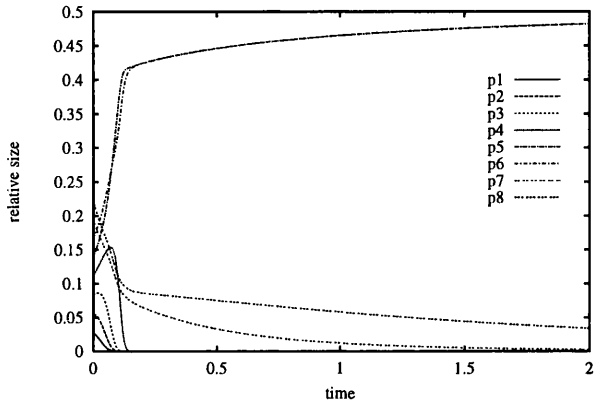

Figure 6.24: Corresponding numerical simulation of follicles relative oestradiol secretion to that of the previous figure. The two selected follicles tend to the same relative maturity value 1/2.

6.6 Discussion

The implementation of the *ageing* variable complicates the mathematical expression of the system, but it is still possible to develop a relevant theoretical analysis. The theoretical and numerical analysis that this chapter gives of Mariana's *et al.* model is able to give new tentative conclusions about the control of ovulation cycle in mammals.

The analysis begins with the most simplified case of many growing follicles with initially the same size and age, or which would be the same, only one growing follicle. The resulting equation is analytically integrable, and three possible behaviours are detected when the ageing parameter is not too large with respect to the initial size of the follicle. Thus, whenever the ageing parameter is small enough so that it does not beat the selection process, the dynamics of a single follicle may present ovulatory, anovulatory and atretic behaviour for different values of the relevant parameters.

However, a modified feature for the particular case of anovulation is reflected by this model. Instead of getting an indefinitely stuck follicle with a fixed size, it

eventually regresses due to its deteriorating capacity. Nevertheless, this regression occurs in a much slower manner so that there is a visible difference between this follicle and an atretic one. This suggests that the pre-ovulatory follicle that did not manage to ovulate does eventually disappear, so that it does not remain inside the ovary for the next cycle. However, since the model does not specify any time units, it is not possible to actually determine when the stuck follicle finally dies.

When complicating the system further by supposing that many follicles grow with different initial sizes, but still retaining the same initial age, the model can still be studied analytically. The growth rate function can be separated into three different functions, leading to three different dynamics. A gradient system for the relative maturity of the follicles can be found, for which there exists a stable M-fold equilibrium point. However, for this particular case, the pre-destination of having the largest follicles selected is still maintained.

Finally, for the most general case of many interacting follicles with different size and age, it is not possible to get a non-linear stability analysis. For this case the dynamics cannot be separated and therefore, it is not possible to find a gradient system for the *interaction dynamics*. However, a linear stability analysis is developed to show that, at least locally, the system for different follicles in age and size can still control the number of selected follicles.

The pre-destination of the system from the initial size of the follicles no longer holds. This means that when the cycle begins with different follicles, but with similar size and age, the selected follicles are amongst the largest, but they are not necessarily the largest ones. Therefore, some crossing between the follicles' growth curves can result from this model. This is in better agreement with biological data since it has been shown that size is not the only factor determining selection.

Some numerical examples produced in this thesis show that the symmetric model with an ageing decaying factor is not globally stable. Therefore, when the system begins with, for instance, one "very old" follicle compared to the remaining follicles, the number of expected ovulatory follicles is not maintained. Nonetheless, this could present new insight into the selection of the control dynamics. This example in particular breaks the hierarchy of the number of ovulating follicles being strictly larger than the number of pre-ovulatory stuck follicles. For this case, from a certain number of ovulating follicles, there could be exactly the same number of stuck follicles. This could therefore suggest, that there are other local factors that affect follicular

sensitivity to gonadotropins, and produce a polycystic ovary.

Nevertheless, the biological interpretation of such an ageing factor is not really specified. Although many biological entities decay at an exponential rate, the particular mechanisms through which the follicles deteriorate are not defined through the ageing variable of this modified version of the symmetric model. Therefore, it can only be concluded that this model supposes an atretic potential for all growing follicles. This atresia dynamics, also present in pre-ovulatory follicles, may interfere with the ovulation rate dynamics. Thus, whenever some of the largest follicles entering the follicular phase of the cycle are old enough, they will not be selected and, furthermore, they may affect the response of the remaining large follicles to hormone levels. Therefore, no other pre-ovulatory follicle may ovulate, but will rather remain within the ovary for a period of time. This is another way, the models suggests, of obtaining PCO in the human ovary.

It would be of great interest to be able to discern the origins of such an ageing factor in order to provide a better biological understanding of the regulation of the ovulation number in terms of this model. However, the most important hypothesis this model actually suggests is that follicle sensitivity to gonadotropins can be strongly affected by this deteriorating capacity. As a consequence, the system may no longer control the ovulation rate of pre-ovulatory follicles. Therefore, a PCOS can be due to the ageing factor of the follicle, which overcomes follicle sensitivity to gonadotropins.

Chapter 7

FOLLICLE GROWTH AND GONADOTROPIC RECEPTORS OF GRANULOSA CELLS

7.1 Introduction

Although the models analysed in the previous two chapters are biologically motivated and reflect the overall feedback loop via the pituitary, the specific response functions used in these models are somewhat arbitrary. This makes it impossible to give a reliable biological interpretation to the parameters in these models. Effects resulting from the manipulation of such parameters on the behaviour of the model may suggest a biological interpretation, but nothing beyond that can be asserted. Therefore, these models cannot be tested against real biological data. This is basically due to the fact that the way follicles react to gonadotropin stimulation is not expressed explicitly within the follicle growth function.

In the present chapter we develop a new model based on the same framework as the symmetric, non-symmetric and symmetric ageing models, but using a more biologically motivated follicle growth function. It is well known that follicular cells have protein-like receptors on their plasma membranes which bind to gonadotropins. This binding process signals the follicle cells to initiate a series of internal transduction pathways, which culminate in follicle growth and steroid production [Mason, 1994]. We base our follicle growth function on this process.

Despite the different kinds of follicular cells involved in the process of gonadotropin

stimulated development, we start by describing a simple interaction between the granulosa cells (GCs) and FSH. In fact, it has been shown that once the follicle has reached its hormonal dependent maturity, it is able to reach pre-ovulatory status by mainly reacting to FSH through the GCs [Zelinski-Wooten *et al.*, 1995]. In chapter 2, we have briefly described the LH influence on follicle growth. However, in spite of the LH contribution through the theca interna cells (TICs), estrogen production is basically due to the FSH influence just before the LH surge. Moreover, it is also known that the follicle grows due to continuing GC proliferation strongly promoted by a FSH signalling process [Monniaux *et al.*, 1994]. Therefore, there is a direct relationship between the FSH binding process and GC steroidogenesis and proliferation.

In order to develop a mathematical model, we describe how the process of FSH binding leads to the production of estrogens within the GCs. The FSH coming from the blood stream gets to the GCs through the basement membrane. Such FSH binds to FSH receptors on the GCs until an equilibrium of FSH density is established. This equilibrium assumption is valid since the time taken for the binding reaction is much shorter than that of changes of FSH levels. At equilibrium there exists both bound and unbound receptors as well as bound and unbound FSH molecules. Since equilibrium has been reached, the unbound concentration of FSH molecules is the same inside and outside the follicle.

7.2 The kinetics of the binding process

The binding process can be described by

$$H + R \rightleftharpoons HR \tag{7.1}$$

where H denotes an FSH molecule, R a GC free receptor and HR the FSH-GC bound complex. Consider h to be the concentration of FSH unbound molecules, r as the concentration of free GCs receptor molecules and c as the FSH-GC bound complex concentration. We assume that FSH binds to its GC receptor by the Law

of Mass Action [Becker *et al.*, 1996]. Therefore the corresponding equations are

$$\begin{aligned} \frac{dh}{dt} &= -k_1 r h + k_{-1} c \quad (a) \\ \frac{dr}{dt} &= -k_1 r h + k_{-1} c \quad (b) \\ \frac{dc}{dt} &= k_1 r h - k_{-1} c \quad (c) \end{aligned} \tag{7.2}$$

where k_1 and k_{-1} are the binding and disassociation rate constants respectively. The dynamics for the FSH and receptor concentrations are exactly the same. Moreover, since $dr/dt + dc/dt = 0$ and $dh/dt + dc/dt = 0$, the total concentration of both bound and unbound FSH molecules is conserved, and the same happens for the receptors. This can also be written as

$$r(t) = r(0) - c(t) \text{ and } h(t) = h(0) - c(t) \tag{7.3}$$

for all t, and for some initial free receptor concentration, $r(0) = r_0 \neq 0$, and initial free FSH concentration, $h(0) = h_0 \neq 0$. Substituting (7.3) in (7.2.c) we get

$$\frac{dc}{dt} = k_1 r_0 h_0 - k_1 h_0 c - k_1 h_0 c + k_1 c^2 - k_{-1} c. \tag{7.4}$$

Now, considering the following change of variables:

$$\tau = k_1 r_0 t, \; w(\tau) = c/h_0 \text{ and } v(\tau) = c/r_0;$$

we obtain the non-dimensional equation

$$\epsilon \frac{dv}{d\tau} = 1 - w - (1 - w + K)v, \tag{7.5}$$

where $\epsilon = r_0/h_0$ and $K = k_{-1}/(k_1 h_0)$. The latter is known as the intrinsic disassociation constant, or Michaelis-Menten constant [Segel, 1980; Segel, 1984; Murray, 1993]. Consequently, the equilibrium value for the bound receptor dynamics is

$$v = \frac{(1 - w)}{(1 - w) + K}.$$

Let u be the proportion of free FSH molecules, *i.e.* $u = 1 - w$, then the equilibrium is also given by

$$v = \frac{u}{u + K}. \tag{7.6}$$

In the following section, we describe how such a term is incorporated into the follicle growth equation.

7.3 Mathematical model for the follicle growth in terms of the granulosa cell FSH receptors

From the simple reaction described in (7.2), it is clear that the concentration of FSH molecules bound to a GC receptor is equal to the GC bound receptor density. Therefore, the average number of FSH molecules associated with each GC is

$$v \equiv \frac{\text{total number of FSH molecules bound to GC receptors}}{\text{total number of GCs.}} \tag{7.7}$$

On the other hand, if we define b to be the equilibrium density of GC bound sites, and x_i the total density of GCs of the ith follicle, then according to definition (7.7) the mean association function is

$$v = \frac{b}{x_i}. \tag{7.8}$$

As in previous models we assume that the dynamics of the FSH serum levels is much faster than that of follicular growth, so we may use the same rescaled variable u for the circulating and follicular FSH levels. Furthermore, let us define X as the total concentration of oestradiol as in Lacker's model. Thus, the rescaled FSH concentration is such that

$$u = f(X) \tag{7.9}$$

for some particular function f that will be defined below.

Then, the follicle growth rate equation proposed is

$$\frac{dx_i}{dt} = \gamma_1 x_i b - \gamma_2 x_i,$$

for all $i = 1, 2, \ldots, N$. Thus, from (7.6) and (7.8) we find the GC bound receptor density is

$$b = x_i v = \frac{x_i u}{u + K}. \tag{7.10}$$

If K is given by $K = k_{-1}/k_1$, from (7.9) and (7.10), we get the follicle growth rate

$$\frac{dx_i}{dt} = \gamma_1 \frac{x_i^2 f(X)}{f(X) + K} - \gamma_2 x_i, \tag{7.11}$$

where again

$$X = \sum_{i=1}^{N} x_i$$

for all $i = 1, 2, \ldots, N$. The constant values of γ_1 and γ_2 respectively correspond to the proportionality parameters for follicular exponential growth and linear decay terms.

This expression corresponds to the simplest growth equation we are able to formulate in terms of the bound receptors. A linear decay term is first considered for simplicity. The positive growth term is the only one being regulated by the pituitary hormone, explicitly introduced by $f(X)$. This function should be decreasing in order to reflect the negative feedback of the total oestradiol serum concentration X upon the pituitary FSH secretion.

7.3.1 Stability analysis

Let us apply Lacker's stability analysis to the general equation,

$$\frac{dx_i}{dt} = \gamma_1 x_i^2 v(X) - \gamma_2 x_i$$

for all $i = 1, 2, \ldots, N$. This is clearly a system of standard Lacker type, *i.e.*

$$\frac{dx_i}{dt} = x_i g(x_i, X).$$

Separating g as in previous cases we get,

$$g(x_i, X) = \delta(X)[\xi(p_i) - \rho(X)] \tag{7.12}$$

where p_i is the relative oestradiol production of the ith follicle, and

$$\begin{aligned} \xi(p_i) &= \tfrac{\gamma_1}{K} p_i \\ \rho(X) &= \frac{\gamma_2}{X v(X)} \\ \delta(X) &= X v(X) \end{aligned}$$

Hence, as in chapter 4 from (7.12) we obtain the same *interaction dynamics*, (4.8), and the same *rescaled time dynamics*, (4.10). For the *intensity dynamics*, we get the equation

$$\frac{dX}{d\tau} = X[\bar{\xi}(p) - \rho(X)]. \tag{7.13}$$

As far as the *interaction dynamics* is concerned, we observe that $\xi(0) = 0$ and obtain the same equilibrium condition as in (4.11). Thus, the only possible stable M-fold equilibrium point $\bar{p}_M$ is

$$\bar{p}_1 = (1, 0, \ldots, 0).$$

This is because

$$\xi(p_1) = \frac{\gamma_1}{K} = \sum_{i=1}^{N} p_i \xi(p_i) = \bar{\xi}(\bar{p}),$$

and furthermore, $\xi'(p_i) = \gamma_1/K > 0$ for at most one $p_i \neq 0$, as well as

$$\sum_{i=1}^{N} \frac{1}{\xi'(p_1)} = \frac{K}{\gamma_1} > 0.$$

Therefore, for $\bar{p}_1$ the equilibrium point for the *interaction dynamics*, $\bar{\xi}(\bar{p}_1) = \lambda$, and if any point $\bar{p}$ tends to $\bar{p}_1$ then, $\bar{\xi}(\bar{p}) \to \lambda$ as $\tau \to \infty$.

This is saying that the only behaviour that this model is able to produce is that of a monovulatory ovary. Although, this is the case for primates, as we have stressed throughout the thesis, we also wish to model some kind of anovulation or PCO. Furthermore, there is no evidence that the selection mechanism in other mammalian species is significantly different, and hence any reasonable model should be capable of multiple ovulation. Nevertheless, we shall complete the stability analysis for the whole dynamics of this model, and see what other kind of information we can obtain.

Since very little is known about a specific quantitative relationship between FSH levels and the total amount of oestradiol during the early follicular phase and the mid follicular phase period, we assume a simple rational decreasing function such as, $f(X) = 1/(X+1)$.

Hence, we have that

$$\begin{aligned} \rho(X) &= \gamma_2 \frac{1 + K(1+X)}{X} \\ \delta(X) &= \frac{X}{1 + K(X+1)}. \end{aligned} \tag{7.14}$$

Therefore, in this case, ρ is monotone decreasing for all $X > 0$ so that $\rho(X) \to \gamma_2$ for some $\gamma_2 > 0$ as $X \to \infty$ and $\rho(X) \to \infty$ as $X \to 0$. We also notice that $\delta(0) = 0$ and $\delta(X) \to \gamma_2$ as $X \to \infty$; in fact $\rho(X) = \gamma_2 \delta^{-1}(X)$. In the case of Lacker's model, these two functions satisfy the same characteristics, except for $\lim_{X\to\infty} \rho(X) = -D < 0$ and $\delta(X) \to \infty$ as $X \to \infty$.

For the analysis of the total oestradiol concentration dynamics, it is easier to re-write equation (7.13) as

$$\frac{dX}{dt} = \gamma_1 \frac{X^2}{[1 + K(X+1)]} - \gamma_2 X = G(X). \tag{7.15}$$

The two possible equilibria are

$$\begin{aligned} X_1^* &= 0 \\ X_2^* &= \frac{\gamma_2(1+K)}{\gamma_1 - K\gamma_2}, \end{aligned}$$

so that the non-trivial equilibrium, X_2^* exists as long as $K < \gamma_1/\gamma_2$.

Now, given

$$G'(X) = \frac{2\gamma_1 X[1 + K(X+1)] - \gamma_1 X^2}{[1 + K(X+1)]} - \gamma_2,$$

we observe that $G'(X_1^*) = -\gamma_2$ and $G'(X_2^*) > 0$. Therefore, this implies X_1^* is always a stable equilibrium point, while $X_2^* > 0$ is unstable as long as $K < \gamma_1/\gamma_2$, which is equivalent to the condition, $\lambda > \gamma_2$ for the rescaled *intensity dynamics* (7.13), where

$$\frac{dX}{d\tau} \approx X(\lambda - \gamma_2)$$

for X sufficiently large.

Figure 7.1.a shows the phase portrait for the intensity dynamics, where $X_2^* > 0$ represents a minimum oestradiol concentration required for the follicles to start growing. Whenever $0 < X_0 < X_2^*$ the solution decreases to zero as we see in figure 7.1.b. On the other hand, if $X_0 > X_2^*$ the total oestradiol concentration exponentially increases to infinity as figure 7.1.b also shows.

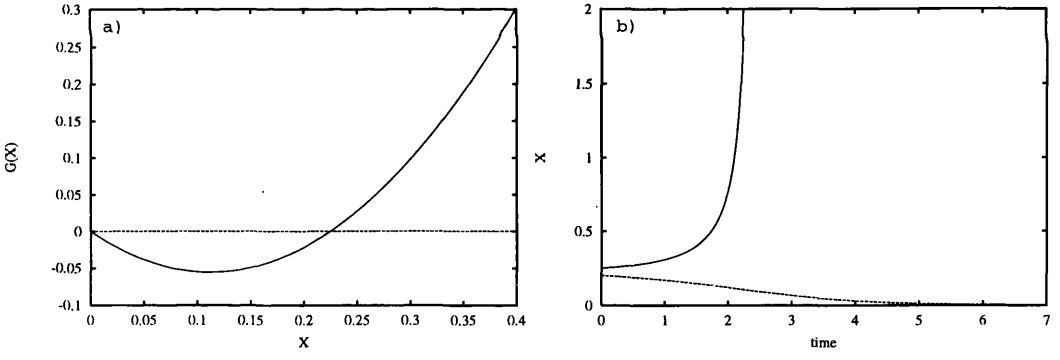

Figure 7.1: a) Phase space of the simplified dynamics of the model in terms of the GCs bound receptors for $f(X) = 1/(X+1)$. Parameter values are such that $\gamma_1 = 5.0$, $\gamma_2 = 1.0$ and $K = 0.1$. b) Solutions corresponding to the growth rate function depicted in figure a). Whenever the initial condition is smaller then $X_2^* \neq 0$ such that $G(X_2^*) = 0$, $X(t) \to 0$, otherwise $X(t) \to \infty$.

On the other hand, if $K > \gamma_1/\gamma_2$ there is no positive equilibrium point and $G(X) < 0$ for all $X > 0$ as we see in figure 7.2. Hence, no follicle is able to grow what ever the value of its initial size.

To finish the stability analysis, we see that for this particular rescaled function $\delta(X)$ we have that for $\lambda < \gamma_2$ there exists $X_e > 0$ such that $\rho(X_e) = \gamma_2\delta(X_e) = \lambda$; thus, $dt/d\tau \approx 1/\delta(X_e)$, which implies,

$$t(\tau) \approx \frac{\gamma_2}{\lambda}\tau + c;$$

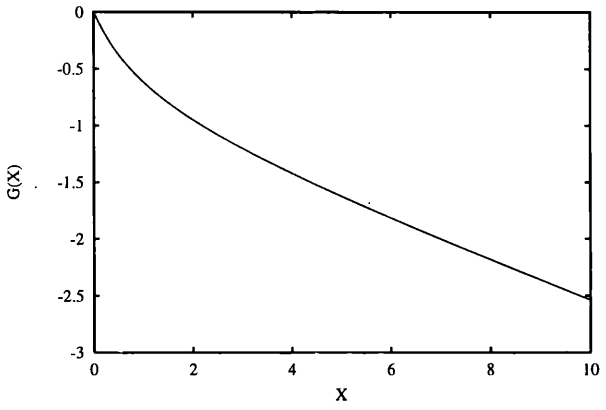

Figure 7.2: Phase space of the simplified dynamics of the model in terms of the GCs bound receptors for $f(X) = 1/(X+1)$. Parameter values are such that $K > \gamma_1/\gamma_2$, in particular γ_1 and γ_2 are just like in figure 7.1, but $K = 6.0$. Hence, $G(X) < 0$ for all $X > 0$.

hence, t tends to infinity as τ grows. On the other hand, if $\lambda > \gamma_2$ we have,

$$\frac{dX}{d\tau} < X(\lambda - \gamma_2) \tag{7.16}$$

for every $X > 0$. Furthermore,

$$\frac{dt}{d\tau} = \frac{1}{\delta(X)} \Rightarrow \lim_{\tau\to\infty} t(\tau) = \int_0^\infty \frac{d\tau}{\delta(X(\tau))},$$

and from (7.16) we have,

$$\frac{1}{\lambda - \gamma_2}\int_{X(0)}^{X(\infty)} \frac{dX}{X\delta(X)} < \int_{X(0)}^{X(\infty)} \frac{dX}{\delta(X)}\frac{d\tau}{dX},$$

which implies,

$$0 < \frac{1}{\lambda - \gamma_2}\int_{X(0)}^{X(\infty)} \frac{dX}{X\delta(X)}.$$

However, $\delta(X)$ does not grow faster than X^ε for some $\varepsilon > 0$. Thus,

$$\int_{X(0)}^{X(\infty)} \frac{dX}{X\delta(X)}$$

does not converge implying that,

$$\lim_{\tau\to\infty} t(\tau) = \infty.$$

Consequently, for the ovulation case the selected follicle grows to infinity as time grows to infinity. Therefore, the *intensity function* is in fact different to that of Lacker since the ovulatory follicle does not grow to infinity in finite time.

From the stability analysis we may assert that whenever the system starts with enough initial oestradiol concentration to allow the *interaction dynamics* to reach

its equilibrium point $\bar{p}_1$, the total amount of oestradiol monopolised by the single selected follicle grows to infinity at an exponential rate. To observe a numerical example of such a behaviour we fix a maximal follicular size in order to allow the remaining smaller follicles to complete their atretic regression (see figure 7.3). Therefore, we integrate the system for eight growing follicles and once the ovulating follicle reaches or exceeds a size of $x_{max} = 10^3$, we fix its size to that maximum until the remaining follicles finish their atretic regression. In this way, we are in fact altering the dynamics of the system in an artificial manner.

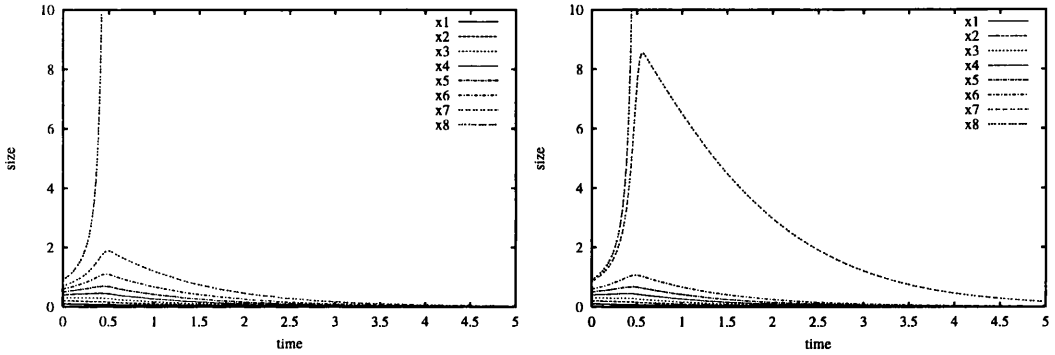

Figure 7.3: Dynamics described in system (7.11) for eight growing follicles with relatively similar initial sizes, where $f(X) = 1/(X+1)$. Parameter values are such that $K < \gamma_1/\gamma_2$, in particular $\gamma_1 = 5.0$, $\gamma_2 = 1.0$ and $K = 0.1$. a) Initial conditions are $x_1 = 0.1, \cdots, x_7 = 0.7$, and $x_8 = 0.9$. Only the largest follicle, x_8, is selected for ovulation, *i.e.* it reaches a maximum size of $x_{max} = 10^3$, whilst the remaining smaller ones, $x_1, \cdots, x_7$, degenerate through atresia. b) Initial conditions are $x_1 = 0.1, \cdots, x_6 = 0.6$, and $x_7 = 0.85$, $x_8 = 0.9$. Again, only one follicle, x_8, is the one ovulating.

However, some interesting features can be observed, *e.g.* if the maximum size of the pre-ovulatory follicle is lowered a little, we observe that if the two largest follicles start growing with very similar sizes, both of them can reach a pre-ovulatory maturity, *i.e.* both of them are selected as figure 7.4 reflects. This of course contradicts the theoretical analysis, but we shall explain below to what conclusions this artificial alteration to the model has led us to.

In Lacker's original model each of the selected follicle's rates is auto regulated since the positive growth rate of follicle x_i has a maximum for any X, as we can see in figure 7.5. This allows a follicle just below the minimum size to escape atresia to have a positive growth rate when the total oestradiol concentration rises even more. This is so since the monopolised oestradiol produced by the first selected follicle does not grow at an infinite rate.

For the case of the model we have developed so far, however, the situation is very different. For this model, once the largest follicle passes the minimum size

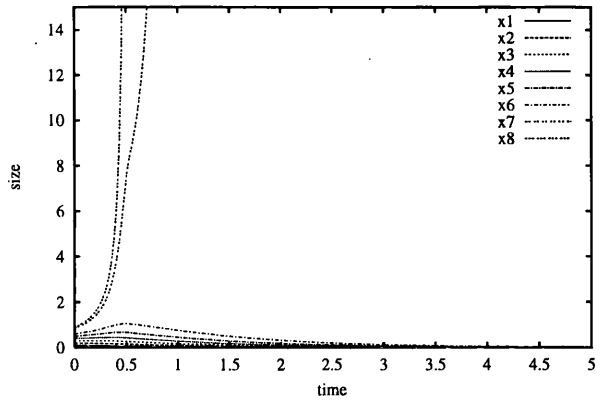

Figure 7.4: Dynamics for eight growing follicles as in figure 7.3. However, in this case the maximum size fixed for the numerical simulation is smaller than in figure 7.3, here it corresponds to $x_{max} = 10^2$. In this way, the two largest follicles x_7 and x_8 are selected for ovulation, whilst the remaining smaller ones, $x_1, \cdots, x_6$, degenerate through atresia.

x_i^* required for a positive growth rate, it grows exponentially and nothing stops it. Furthermore, it does not allow any other follicle to pass the minimum size. Therefore an artificial way was chosen to diminish such a rapid growth, and once the follicle reached a pre-ovulatory size its velocity was made zero. In this way, a second largest follicle which is not much smaller than the largest one has time to escape beyond the minimum value x_i^* and grow exponentially. In this way it is possible to have more than one follicle to be selected. So far, we do not have any biological evidence to support this artificial method.

Furthermore, it is possible to change the model growth equation so the follicle selected to a pre-ovulatory maturity does not grow to infinity, and the model naturally fixes its pre-ovulatory maturity. This is achieved by changing the function f to $f(X) = 1/(1 + X^3)$. For this particular case, when the initial follicle size is larger than the minimum to escape immediate atresia, the follicle grows to a fixed equilibrium value (see figure 7.6).

It is important to notice that by changing the function f, the interaction function is not affected meaning that there is still only one follicle that is theoretically selected. However, we would expect that since the pre-ovulatory follicle does not grow to infinity we would obtain more than one chosen follicle. Figure 7.7 shows the two different growth rate functions for the two particular models considered in this chapter. Observe that the minimum follicle maturity x_i^* required to escape atresia increases much faster for the second model (see figure 7.7.b) as X increases than

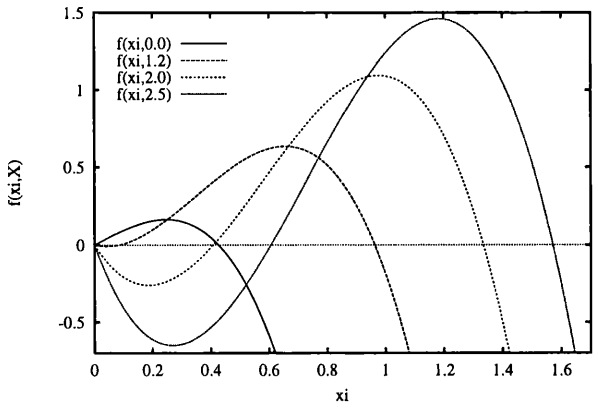

Figure 7.5: Follicular growth rate space for Lacker's original model. Different curves $\dot{x_i} = f(x_i, X)$ *vs* x_i for different oestradiol concentration values X. For each curve, there is a minimum and maximum follicle sizes in order to have a positive growth rate. As X increases, each minimum and maximum also increase.

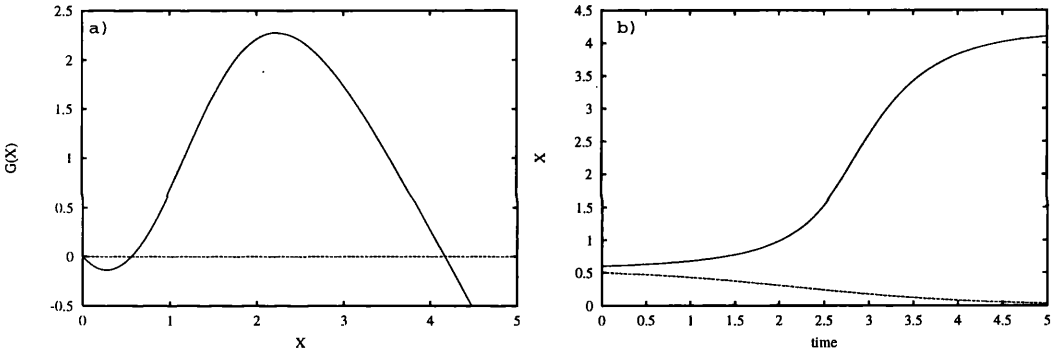

Figure 7.6: a) Growth rate function of the total oestradiol concentration for the simplified dynamics of the model in terms of the GCs bound receptors. Here, $f(X) = 1/(X^3 + 1)$. b) Solutions corresponding to the growth rate function depicted in figure a). Whenever the initial condition is smaller that $X_2^* \neq 0$ such that $G(X_2^*) = 0$, $X(t) \to 0$. Otherwise, $X(t) \to X_{max}$, such that $G(X_{max}) = 0$, which is a stable finite equilibrium point.

for the first model (see figure 7.7.a). The fact that for the second model the largest follicle monopolises the total oestradiol concentration up to a certain fixed value does not help other follicles reach a pre-ovulatory size. Two numerical examples are shown in figure 7.8 to illustrate that no matter how close the two largest follicles start the cycle, only one is selected.

From the results obtained for these two models we believe that such a follicle growth equation is still not good enough to describe the dynamics of follicular selection by itself. It is true that a selection process takes place, but only one follicle is chosen. Therefore, as long as $K < \gamma_1/\gamma_2$, only one follicle is selected and the rest atrophy. The alternative behaviour given by $K > \gamma_1/\gamma_2$ is that all of the interacting

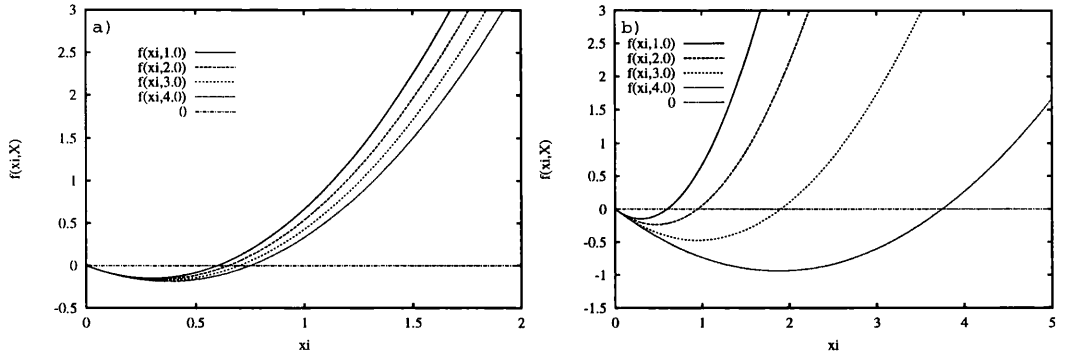

Figure 7.7: Follicular growth rate space for two different models in terms of GCs bound receptors. Different curves $\dot{x}_i = f(x_i, X)$ *vs* x_i for different oestradiol concentration values X are plotted in both cases. a) This corresponds to the model for which $f(X) = 1/(X+1)$. The minimum size required for a follicle to have positive growth rate increases linearly as X increases. b) This corresponds to the model for which $f(X) = 1/(X^3+1)$. The minimum size required for a follicle to have positive growth rate increases as X^3.

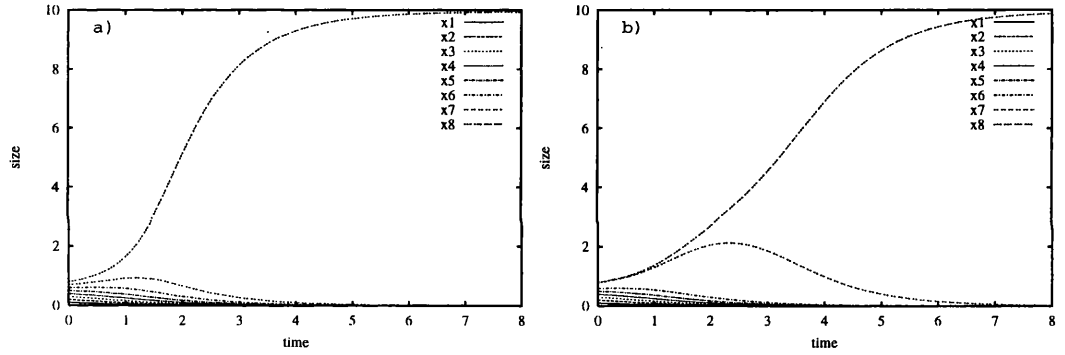

Figure 7.8: Numerical example of eight growing follicles for the model in terms of GCs bound receptors, where $f(X) = 1/(X^3+1)$. The parameter values are such that $K < \gamma_1/\gamma_2$, where $\gamma_1 = 10.0$, $\gamma_2 = 1.0$, and $K = 0.1$. In both figures only the largest follicle reaches ovulatory size, the rest smaller ones atrophy and die.

follicles atrophy and die.

Therefore, there is no other way of either manipulating the parameters of the equation or the initial conditions of the system, in order to obtain any other type of behaviour. In particular we are interested in being able to reflect the possibility of having more than one follicle selected. We believe that just to consider the number of bound FSH receptors of GCs is insufficient.

As we have mentioned in chapter 2, LH effects have an important role during the follicular phase of the cycle. In the particular case of pre-ovulatory follicles, LH stimulates their granulosa to the aromatisation of oestradiol. We believe that a failure of GCs of pre-ovulatory follicles in responding to LH signalling input may prevent those follicles from ovulating. This failure can be due to irregular secretion

of LH associated with PCO [Watson *et al.*, 1993]. Therefore, we think it is important to consider FSH and LH effects separately.

7.4 Development and effects of LH receptors of granulosa cells during terminal folliclegenesis

In order to improve the follicle growth function we have decided to also consider the concentration of LH bound receptors of GCs. By the time the follicle has reached the *Graaphian* state, it is thought that its GCs start developing LH receptors on their plasma membranes [Baird, 1983]. Since the follicle will soon be lacking FSH signalling stimulation, LH receptors are believed to take over. Therefore, during the last stage of the follicular phase the selected follicles oestradiol production within their granulosa is stimulated by LH. As we have described in chapter 2, the follicle oestradiol production has a positive feedback effect upon pituitary LH secretion. Therefore, at the same time FSH decreases, LH is still available from the blood stream.

It is also thought, however, that the LH serum concentration basically remains constant during the follicular phase of the menstrual cycle. By the end of the follicular phase, the LH surge takes place as a sudden and rapid pituitary discharge. It is difficult to relate these two LH dynamics since the pituitary control of tonic levels of LH and the pituitary control of the LH surge are thought to be due to different mechanisms. Moreover, progesterone has an important role in the latter. By the time of the LH surge, pre-ovulatory follicles have developed enough LH receptors on their GCs, which help them to ovulate a few hours later.

Nevertheless, since we are basically interested in modelling the selection procedure, we thus propose a follicle growth rate function in terms of a constant LH contribution, and an increasing concentration of LH bound receptors of GCs in the follicle.

7.4.1 Mathematical models of follicle growth in terms of FSH and LH receptors of granulosa cells.

As in the previous model, we consider the GCs to be the only follicular cells interacting within the cycle. Let us suppose LH bound receptors of granulosa cells increase with the number of GCs in a hyperbolic manner, *i.e.* if v_2 denotes the concentration

of LH bound receptors we have

$$v_2(x_i) = \frac{x_i}{x_i + K}.$$

Although we know that the disassociation parameter K would in reality be different for each of the GCs type of receptors, for simplicity we consider both of these types as having the same disassociation constant.

Let $v_1(X) = v(X)$, where $v(X)$ is the same function for the FSH bound receptors described in the previous section. Let γ_0 be the constant LH contribution, and α the constant atretic parameter. Therefore, the model proposed is

$$\frac{dx_i}{dt} = (v_1(X) + \gamma_0 v_2(x_i) - \alpha)x_i. \tag{7.17}$$

For this model we are not considering the follicle exponential growth rate ($\gamma_1 x_i$) times the concentration of FSH bound receptors as in the models of previous section. Hence, the positive terms of the follicle growth rate function only depend on the concentration of the two kinds of GC receptors.

7.4.2 Simplified model analysis

We also propose to use $f(X) = 1/(1 + X)$ for the function of FSH in terms of the total oestradiol concentration. Thus, we proceed by analysing the model for a single follicle. This means that if $x_i = X$ for all $i = 1, \cdots, N$ we get,

$$\frac{dX}{dt} = \frac{X}{1 + K(X + 1)} + \gamma_0 \frac{X^2}{X + K} - \alpha X = G(X).$$

Therefore, the equilibrium points obtained are,

$$X_1^* = 0$$

$$X_{2,3}^* = \frac{-1+\alpha(1+K+K^2)-\gamma_0(1+K) \pm [4K^2(-1+\alpha(K+1)(-\alpha+\gamma_0)+(1-\alpha(1+K+K^2)+\gamma_0(1+K))^2]^{\frac{1}{2}}}{2K(\gamma_0-\alpha)},$$

for $\gamma_0 \neq \alpha$. Let us analyse the behaviour for the different possibilities considered for the relative value of the parameters.

a) If $\gamma_0 > \alpha$ and $K + 1 < 1/\alpha$, we have that $X_{2,3}^*$ are complex. However as we see in figure 7.9.a. $G(X) > 0$ for all $X > 0$. This represents an ovulatory feature, where X grows at an exponential rate.

b) If $\gamma_0 > \alpha$ but $K + 1 > 1/\alpha$, then $X_2^* > 0$, whilst $X_3^* < 0$. Hence, as figure 7.9.b reflects, for this case there is a minimum non-zero follicle size, or total oestradiol concentration required to grow just like in the models of section (7.3) This means

that, if $0 < X < X_2^*$ there is no chance of surviving atresia since the total oestradiol concentration drops to zero. On the other hand, if $X > X_2^*$ we also have an ovulatory situation, where the total oestradiol concentration of the selected follicle grows at an exponential rate (see figure 7.9.b).

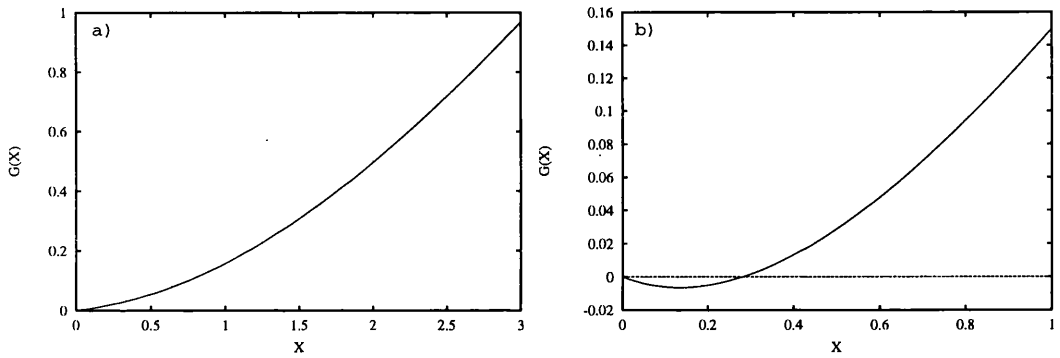

Figure 7.9: Growth rate function of a single follicle or of the total oestradiol concentration for the model in terms of FSH and LH bound receptors of GCs. Both cases correspond to an ovulatory condition. a) Parameter values satisfying condition (a) with $\gamma_0 = 1.0$, $K = 5.0$, and $\alpha = 0.1$. There are no non-trivial equilibria and $G(X) > 0$ for all $X > 0$. b) Parameter values satisfying condition (b) with $\gamma_0 = 1.0$, $K = 1.5$, and $\alpha = 0.5$. There is only one positive equilibrium point, $X_2^* = 0.28$, such that $G(X) < 0$ for $X < X_2^*$, and $G(X) > 0$ for $X > X_2^*$. Therefore, there exists a non-zero minimum size or total oestradiol concentration initially required to escape atresia.

c) If $\gamma_0 < \alpha$ and $K + 1 > 1/\alpha$, then $X_2^* > 0$ and $X_3^* > 0$. Figure 7.10.a shows that X_2^* is unstable, whilst X_3^* is a stable equilibrium point. This represents the anovulation situation, where once the follicle starts with a size larger than X_2^*, it grows until a maximum pre-ovulatory fixed size given by X_3^* (see figure 7.10.a). However, when $\gamma_0 = 1.0$, $\alpha = 1.5$ and $K = 1.0$, although they satisfy this condition, there are no positive equilibria and $G(X) < 0$ for all $X > 0$ (see figure 7.10.b). For these particular parameter values the negative influence on follicular growth overcomes any positive term. Therefore, the cycle is atretic for any initial size or any initial oestradiol serum concentration.

d) If $\gamma_0 < \alpha$ and $K + 1 < 1/\alpha$ we have only one positive equilibrium point X_2^*, which happens to be stable as we see in figure 7.11. Hence, whatever the initial size of the follicle or the total oestradiol concentration at the beginning of the cycle, it grows till a fixed pre-ovulatory size or concentration given by X_2^*.

Therefore, by changing the relevant parameter values, this model is able to reflect the basic features of the menstrual cycle.

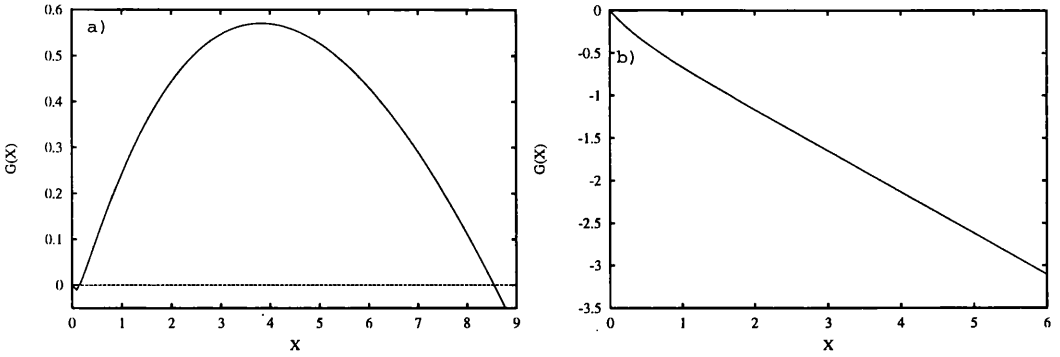

Figure 7.10: Growth rate function of a single follicle or of the total oestradiol concentration for the model in terms of FSH and LH bound receptors of GCs. a) Parameter values satisfying condition (c) with $\gamma_0 = 1.0$, $K = 0.1$, and $\alpha = 1.5$. There are two positive equilibria $X_3^* = 0.152$ and $X_2^* = 8.55$, such that $G(X) < 0$ for all $0 < X < X_2^*$, whilst $G(X) > 0$ for all $X_2^* < X < X_3^*$. This corresponds to the anovulatory condition. If the follicle starts growing with a size larger than X_2^*, it will reach a pre-ovulatory fixed size given by X_3^*. b) Parameter values also satisfying condition (c) with $\gamma_0 = 1.0$, $K = 1.0$, and $\alpha = 1.5$. There is no positive equilibrium and, $G(X) < 0$ for all $X > 0$. The follicle atrophies and dies for any positive initial size.

7.4.3 Numerical analysis for different follicles

If we express equation (7.17) as $\dot{x}_i = x_i g(x_i, X)$, it is possible to observe that we cannot separate the function g as in Lacker's model or model (7.11). Therefore, it is not possible to obtain separated functions that would lead us to a separated dynamics of the system. Thus, there is no obvious way to theoretically analyse the ovulation rate dynamics for the case of many growing follicles. Hence, we restrict ourselves to a numerical exploration of a number of examples that reflect different types of behaviour in this model.

As before, a maximum pre-ovulatory size is fixed for the numerical experiments. Once again, when the first pre-ovulatory follicle is selected it grows so fast that it is not possible to numerically observe the terminal fate of the remaining follicles.

For the parameter values of condition (a) of the simplified model analysis, when the cycle begins with a relatively large follicle, that particular follicle is the only one ovulating, and the reminder die by atresia (see figure 7.12.a). However, figure 7.12.b shows that if the cycle starts with a uniform size distribution, two follicles are able to ovulate.

Let us now increase the value of parameter γ_0, but still keep the relative values of the parameters as in figures 7.12. This means that since the cycle starts with a higher LH concentration than in the case of figure 7.12, more follicles ovulate (see figure 7.13.a). In order to obtain only one ovulatory follicle for the same parameter

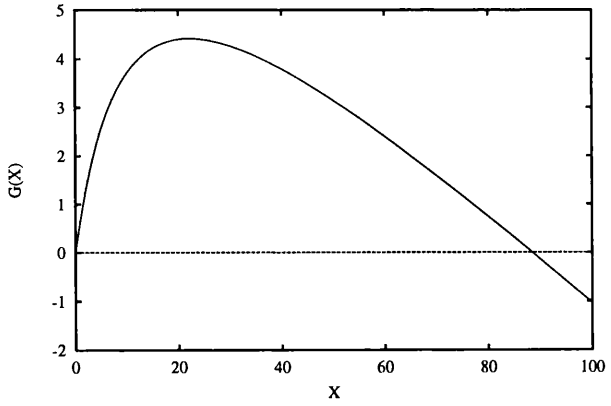

Figure 7.11: Growth rate function of a single follicle or of the total oestradiol concentration for the model in terms of FSH and LH bound receptors of GCs. Parameter values satisfy condition (d), in particular $\gamma_0 = 0.5$, $\alpha = 0.6$, and $K = 0.1$. There is only one positive stable equilibrium point $X_2^* = 88.43$.

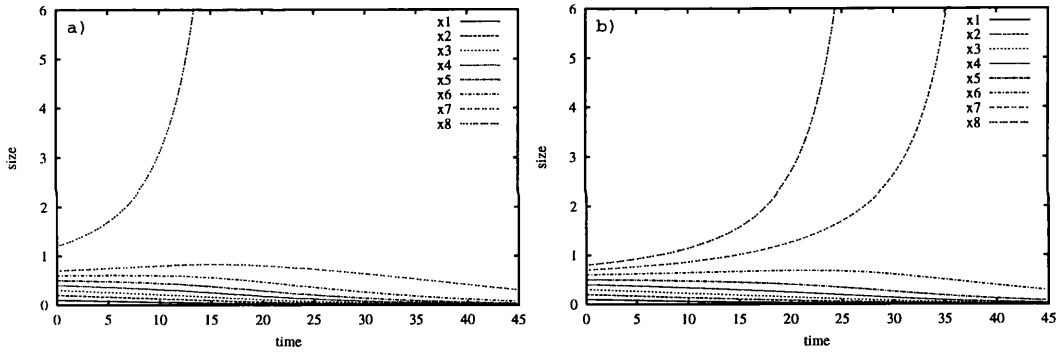

Figure 7.12: Numerical example of eight growing follicles for the model in terms of FSH and LH bound receptors of GCs. For this example the parameter values keep condition (a) of the previous subsection, *i.e.* $\gamma_0 > \alpha$ and $K + 1 < 1/\alpha$. In particular $\gamma_0 = 0.6$, $K = 5.0$, and $\alpha = 0.1$. a) The initially largest follicle x_8 ovulates, the remaining seven smaller follicles atrophy. b) The cycle starts with a uniform size distribution and two follicles ovulate.

values, the initial largest follicle has to be even larger than the case of the ovulatory follicle shown in figure 7.12.b (see figure 7.13.b).

When the parameter values of the model satisfy condition (b) given in the simplified model analysis, we observe that ovulation takes place. For this situation, the model is also sensitive to the initial size distribution and the ovulation rate varies as we see in figure 7.14.

For the particular case of anovulation we fix the parameter values so that they satisfy condition (c) of the simplified model analysis, and integrate the system for eight growing follicles. For the particular case of $\gamma_0 = 1.0$, $K = 0.1$ and $\alpha = 1.5$ figure 7.15.a shows that only one follicle is able to reach pre-ovulatory size, and

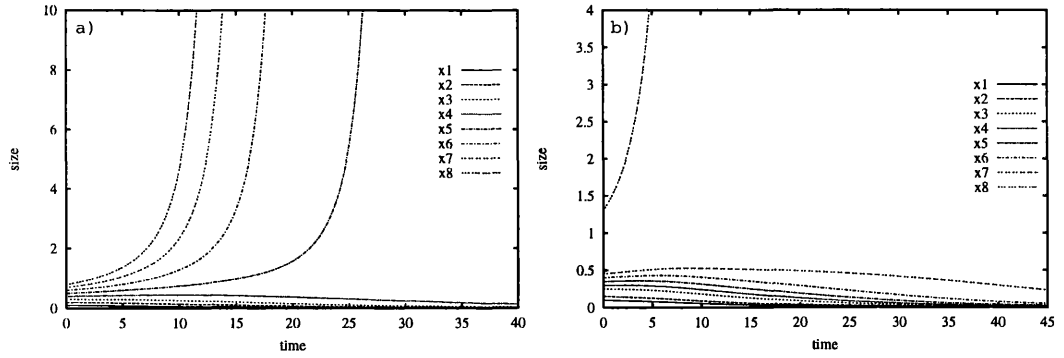

Figure 7.13: Numerical example of eight growing follicles for the model in terms of FSH and LH bound receptors of GCs. For this example the parameter values keep condition (a) of the previous subsection, *i.e.* $\gamma_0 > \alpha$ and $K+1 < 1/\alpha$. In particular $\gamma_0 = 1.0$, $K = 5.0$, and $\alpha = 0.1$. a) The cycle starts with a uniform size distribution and four follicles ovulate, whilst the remaining three smaller follicles atrophy. b) The initial significantly largest follicle x_8 ovulates, the remaining smaller ones die.

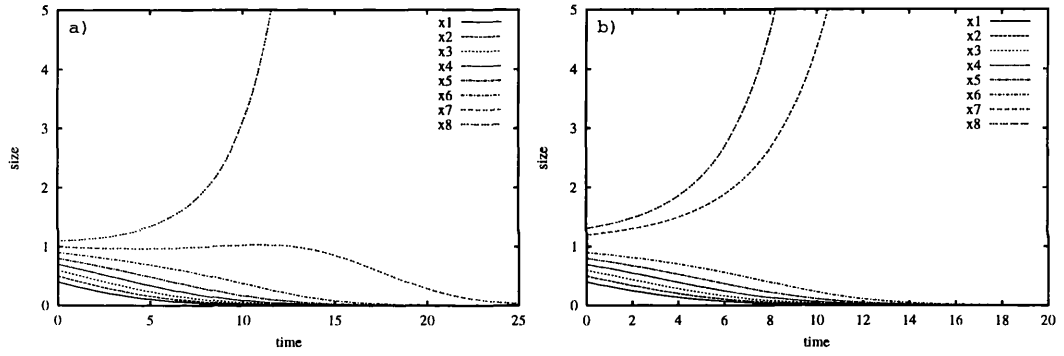

Figure 7.14: Numerical example of eight growing follicles for the model in terms of FSH and LH bound receptors of GCs. For this example the parameter values keep condition (b) of the previous subsection, *i.e.* $\gamma_0 > \alpha$ and $K+1 > 1/\alpha$. In particular $\gamma_0 = 1.0$, $K = 1.5$, and $\alpha = 0.5$. a) The cycle starts with a uniform size distribution and only one follicle ovulates, whilst the remaining seven smaller ones atrophy. b) The cycle begins with two relatively large follicles, x_7 and x_8, which ovulate with a difference of approximately one unit of time, whilst the remaining smaller follicles die.

the remaining seven smaller ones atrophy and die. If we change the initial size distribution so the cycle begins with three relatively largest follicles, in figure 7.15.b we observe that still only one follicle is the selected one.

In analogy to the models of section 7.3, we would expect that since the selected follicle does not grow to infinity at an exponential rate, some other follicles would manage to reach pre-ovulatory maturity when starting the cycle with a similar size to that of the largest follicle. However, this appears not to be the situation. From figure 7.16 we observe that the minimum size value required to escape atresia, increases much faster in the case of anovulation than in the case of ovulation as X increases.

Since for parameter values satisfying condition (d) of the simplified model analysis

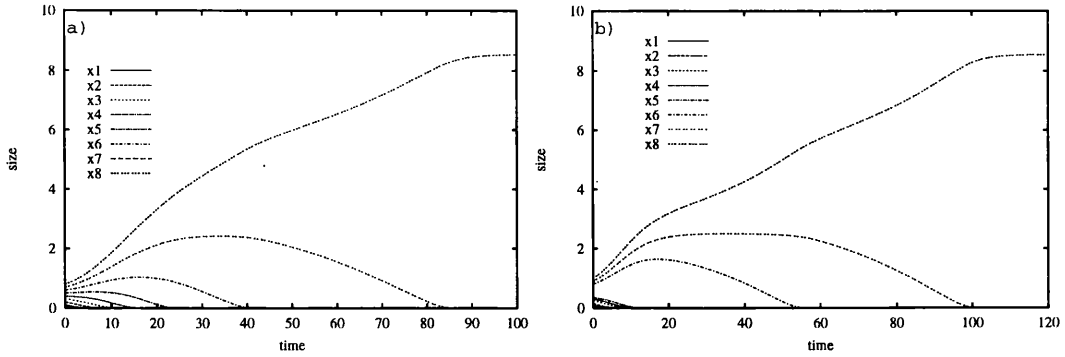

Figure 7.15: Numerical example of eight growing follicles for the model in terms of FSH and LH bound receptors of GCs. For this example the parameter values satisfy condition (c) of the previous subsection, *i.e.* $\gamma_0 > \alpha$ and $K + 1 > 1/\alpha$, which correspond to the anovulatory condition. In particular $\gamma_0 = 1.0$, $K = 1.5$, and $\alpha = 0.1$. a) The cycle starts with a uniform size distribution and only one follicle reaches a pre-ovulatory size with out ovulating, whilst the remaining seven smaller follicles atrophy. b) The cycle begins with three relatively largest follicles, x_6 and x_7 and x_8, however only one of them, x_8, is selected, and the other two die some time after the smallest five follicles.

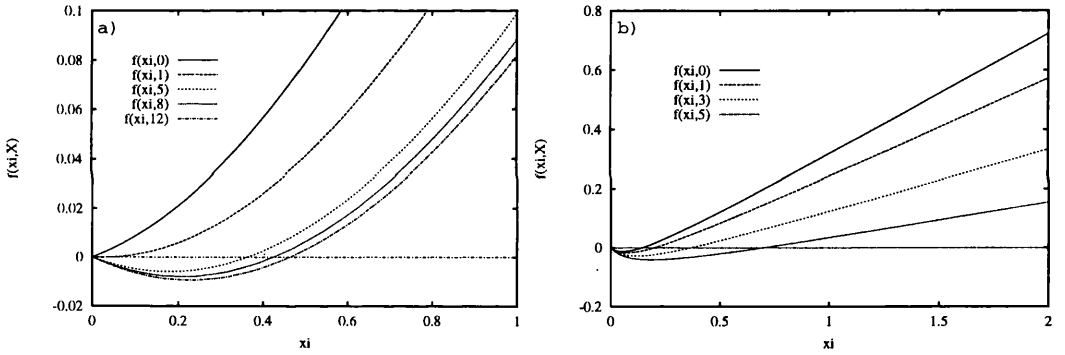

Figure 7.16: Examples of the follicular growth rate function $\dot{x}_i = f(x_i, X)$ given in (7.17), with respect to the follicle size x_i for different values of X. a) Parameter values for the ovulatory condition given in figure 7.13. b) Parameter values for the anovulatory condition given in figure 7.15. The minimum size required to escape atresia increase faster in the anovulatory situation than in the ovulatory one.

the dynamics is basically the same as that of the previous case, we do not present any numerical examples for many interacting follicles.

Although model (7.17) reflects a more diverse dynamics than model (7.11) above, it still presents some limitations. In the first place, we need to fix a maximum pre-ovulatory size for the ovulatory condition, which artificially interferes with the dynamics. Secondly, we observe that the number of anovulatory follicles is usually less than the number of ovulatory ones, contrary of what it is often observed in a PCOS.

However, for the case of anovulation we notice that the time it takes for follicles, x_6 and x_7 to atrophy (especially in the example of figure 7.15.b) is relatively longer

than the time it takes for the smallest follicles $x_1, \cdots, x_5$. Therefore, we could argue that at least for a considerable period of the cycle, there are three relatively large follicles within the ovary, although the only one presenting an actual pre-ovulatory condition is the largest follicle x_8.

In view of these observations we continue to try to improve such a model.

7.5 Hormonal control of atresia

The study of atresia in follicles is in itself a subject of extensive research. Atretic follicles emerge at different stages of the ovarian cycle reaching a proportional peak during the last days of the follicular phase. As we have mentioned before, almost all of the *Graafian* follicles entering this last phase of the cycle end up as atretic follicles. Therefore, atresia is considered as the normal fate of the follicular maturation process [Hsueh *et al.*, 1994].

Strictly speaking, atresia is an antral follicle degenerative process, which closes the natural opening or antrum of the follicle. However, it is now known that apoptosis of follicular cells marks the earliest stages of atresia [Jolly *et al.*, 1997b; Jolly *et al.*, 1997a]. Moreover, apoptosis of GCs has been widely studied, and is thought to have a more significant role in atresia than apoptosis of TICs. Since proliferating, differentiating and apoptotic GCs are found within the same follicle, it has been proposed that atresia should be determined by a dynamic equilibrium between cell division, differentiation and apoptosis [Jolly *et al.*, 1997b; Clément *et al.*, 1997].

However, it is as difficult to specify the way in which atresia is controlled within the ovarian dynamics as to specify the whole selection process of pre-ovulatory follicles. Nevertheless, many studies have detected that, gonadotropins are survival factors that suppress apoptosis of GCs [Hsueh *et al.*, 1994; Sites *et al.*, 1994; Jablonka-Shariff *et al.*, 1996]. At the same time, androgens have been shown to be atretogenic factors for follicles [Brailly *et al.*, 1981; Hillier and Tetsuka, 1997].

As we have mentioned in chapter 2, androgens are produced from progestins in response to LH signalling in TICs. Since GCs of atretic follicles are thought to have lower aromatisation activity than GCs of healthy follicles [Tsonis *et al.*, 1984], they are not able to convert such androgens into oestradiol. As a result, the levels of androgens increase within GCs of atretic follicles [Brailly *et al.*, 1981]. Moreover, an increase in androgen receptors within GCs has been detected in atretic follicles,

whilst a decrease of these receptors is found in GCs of pre-ovulatory follicles [Garrett and Guthrie, 1996; Hillier and Tetsuka, 1997].

It is the aim of this section to consider a follicular atresia rate, which is incorporated within the feedback mechanism of the menstrual cycle.

7.5.1 Mathematical model including a steroid controlled atresia rate

From the above introduction we have seen that atresia is actually a steroid controlled mechanism, basically through the local action of androgens. More specifically, androgens are thought to induce apoptosis in GCs, a process which in different proportions is present in both healthy and atretic follicles.

In the following model we suggest a function for the androgen bound receptor concentration of GCs to depend on the total oestradiol concentration. In such a way, atresia is a hormonally controlled regression process.

Therefore, as in the previous section, let us consider the functions $v_1(X)$ and $v_2(x_i)$ for the concentration of FSH and LH bound receptors of GCs respectively. Let us propose

$$v_3(X) = \frac{X}{X+K}$$

to describe the concentration of androgen bound receptors. Then the resulting model is

$$\frac{dx_i}{dt} = (x_i v_1(X) + \gamma_0 v_2(x_i) - v_3(X))x_i. \tag{7.18}$$

It is worth observing that here again, the follicle growth rate is considered to be proportional to the GCs concentration times the concentration of the FSH bound receptors, just as in model (7.11).

When simplifying the system for a single follicle we obtain the following equation

$$\frac{dX}{dt} = \left(\frac{X^2}{1+K(X+1)} + (\gamma_0 - 1)\frac{X}{X+K} \right) X.$$

Hence, the equilibrium points are

$$\begin{aligned} X_1^* &= 0 \\ X_2^* &= \frac{1-\gamma_0(1+K)}{1-K(1-\gamma_0)}. \end{aligned}$$

Where, $X_2^* > 0$ if and only if

$$K < \frac{1-\gamma_0}{\gamma_0} \text{ and } \frac{1}{K} > 1-\gamma_0 \tag{7.19}$$

or

$$K > \frac{1-\gamma_0}{\gamma_0} \text{ and } \frac{1}{K} < 1-\gamma_0. \tag{7.20}$$

If K and γ_0 do not satisfy any of the conditions above we may have that $X_2^* < 0$, so $X_1^* = 0$ is the only possible equilibrium point, which is unstable (see figure 7.17). On the other hand, if K and γ_0 satisfy either condition (7.19) or (7.20), it can be proved that $X_1^* = 0$ is a stable equilibrium point, whereas $X_2^* > 0$ is unstable (see figure 7.17).

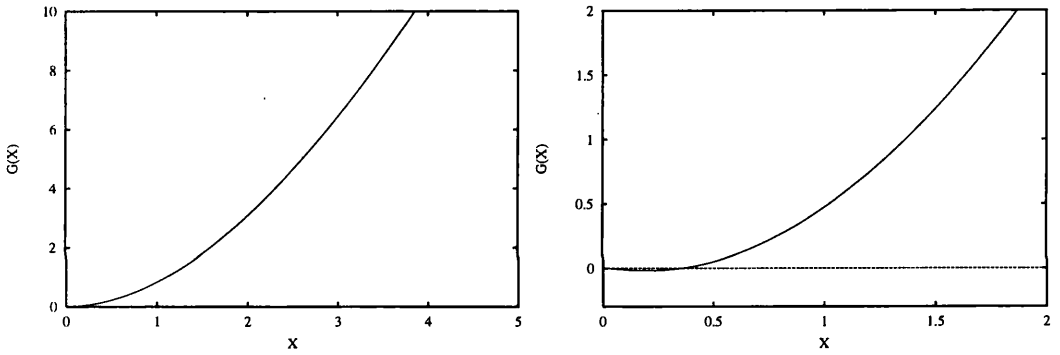

Figure 7.17: Growth rate function of a single follicle or of the total oestradiol concentration for the model including the gonadotropic dependent atretic decay. a) Parameter values are $\gamma_0 = 1.0$, $K = 0.1$, such that they do not satisfy condition (7.19) nor condition (7.20). Hence, zero is the only equilibrium point, which is unstable. b) Parameter values are $\gamma_0 = 0.6$ and $K = 0.1$ such that they satisfy condition (7.19). In this case, $X_0^* = 0$ is stable and $X_2^* = 0.35$ is an unstable equilibrium point.

So far, this model does not show great difference from the previous ones, thus let us analyse the case for several growing follicles. However, before this, let us inspect the follicle growth rate space for different total oestradiol concentrations. For that, see figure 7.18.

Therefore, we do not expect any improvement for this particular model. When studying Lacker's growth equation given in (4.12), we have observed that the cube of the follicle maturity variable is the one that makes the curves in the space of follicular growth rate reach a finite maximum for different total oestradiol concentrations. Therefore, we have decided to incorporate such a factor in the equation given in (7.18) and observe the dynamics.

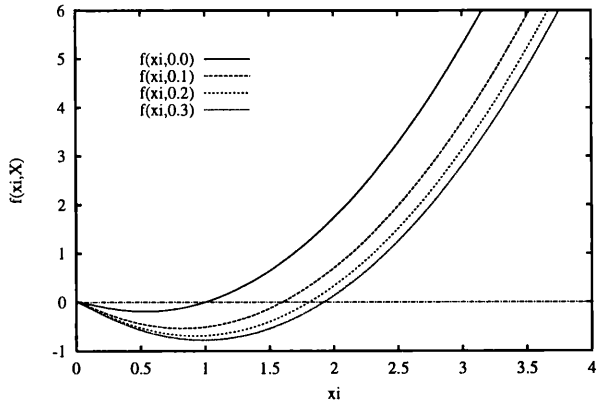

Figure 7.18: Follicular growth rate space for model (7.18). Different curves $\dot{x_i} = f(x_i, X)$ *vs* x_i are plotted for different oestradiol concentration values X. As in previous cases each curve grows to infinity for every value of X.

7.5.2 Mathematical model including a steroid controlled atresia rate and a cubic decay factor

Let us consider the new equation to analyse

$$\frac{dx_i}{dt} = (x_i v_1(X) + \gamma_0 v_2(x_i) - v_3(X))x_i - \alpha x_i^3, \tag{7.21}$$

which happens to be the same as equation (7.18) with a cubic decay factor. Although, we cannot derive any kind of biological interpretation for this term, once this cubic decay has been added, the space of follicles' growth rate looks similar to that of Lacker's shown in figure 7.5 (see figure 7.19).

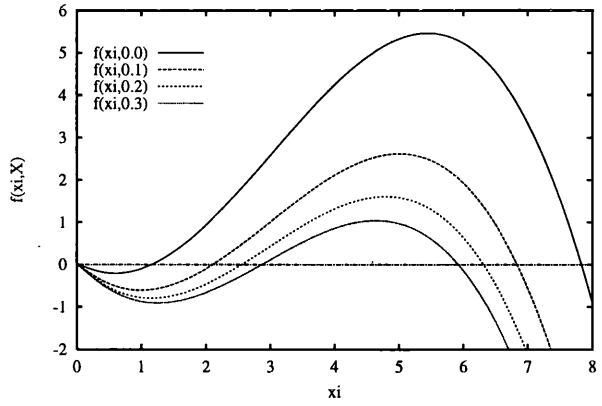

Figure 7.19: Follicular growth rate space for model (7.21). Different curves $\dot{x_i} = f(x_i, X)$ *vs* x_i are plotted for different oestradiol concentration values X. For each curve, there is a minimum and maximum follicle sizes in order to have a positive growth rate. As X increases, the minimum size increases, whilst the maximum size decreases.

Nevertheless, for this case, the positive growth rate window shrinks as X in-

creases. In other words, as X increases, the minimum size required for the follicle to escape atresia increases, whilst the maximum size needed in order not to start decreasing is smaller every time.

If we simplify the system for a single follicle, the equation we get is

$$\frac{dX}{dt} = \left(\frac{X^2}{1+K(X+1)} + (\gamma_0 - 1)\frac{X}{X+K} \right) X - \alpha X^3.$$

Although it is possible to analytically compute the non-zero equilibria of this equation, the expressions are complex. Therefore, we only give two examples of the main type of orbits this simplified model is able to produce (see figure 7.20).

In the first place, we set the parameter values such that $\gamma_0 > \alpha$ and $\gamma_0 - 1 \geq 0$. There is only one positive stable equilibrium point as we observe in figure 7.20.

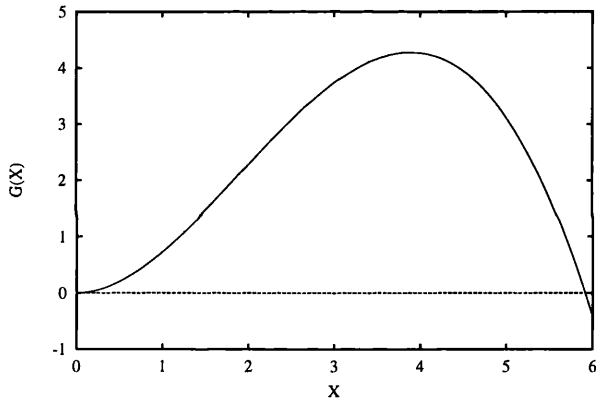

Figure 7.20: Growth rate function of a single follicle or of the total oestradiol concentration for the model including the gonadotropic dependent atretic decay. The parameter values are $\gamma_0 = 1.0$, $K = 0.1$, and $\alpha = 0.1$, such that they satisfy condition $\gamma_0 - 1 \geq 0$. There is one positive stable equilibrium point, hence a growing follicle tends to a fixed pre-ovulatory size given by $X_1^* = 5.913$.

Secondly, let us propose a smaller value for γ_0 so that $\gamma_0 - 1 \leq 0$, but still $\gamma_0 > \alpha$. In such a case, there are two positive equilibria $0 < X_1^* < X_2^*$, such that X_1^* is unstable and X_2^* is stable. This means that a minimum non-zero size or total oestradiol concentration is required in order to escape atresia (see figure 7.21).

It appears that this model does not simulate the same type of ovulation as the previous models. It could be argued that indeed this model is only reflecting the selection dynamics, *i.e.* from the early follicular till the mid-follicular phase of the cycle. This is mainly due to the fact that once the follicles are selected, their corresponding cubic terms do not let them grow to infinity. And moreover, the only possible dynamics for the total oestradiol concentration is that of reaching a stable

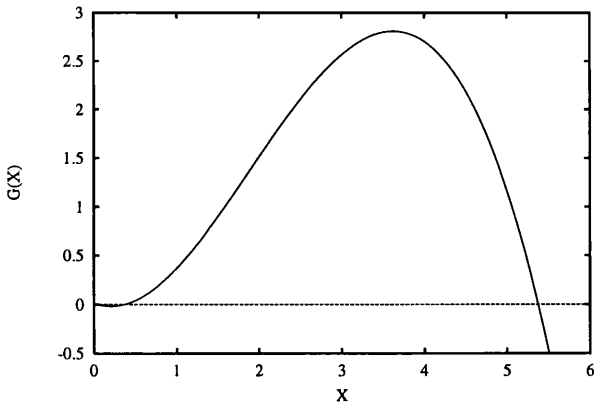

Figure 7.21: Growth rate function of a single follicle or of the total oestradiol concentration for the model including the gonadotropic dependent atretic decay. The parameter values are $\gamma_0 = 0.6$, $K = 0.1$, and $\alpha = 0.1$, such that they satisfy condition $\gamma_0 - 1 \leq 0$. There are two positive equilibria, $X_1^* = 0.375$ and $X_2^* = 5.376$. When $X > X_1^*$ the follicle is able to grow in the first place and tend to a fixed pre-ovulatory size given by X_2^*, whereas if $0 < X < X_2^*$ the follicle atrophies and dies.

equilibrium value as we see in figures 7.20 and 7.21. Therefore, the positive feedback effect of the monopolised oestradiol production of the selected follicles upon the pituitary LH secretion is not included in this particular model.

Let us study the dynamics of the ovulation rate when many follicles interact in the cycle.

7.5.3 Numerical analysis for different follicles

Since $\dot{x}_i = f(x_i, X)$ is even more complex than in the previous models (7.11) and (7.17), it is not possible to even separate it in different types of functions. Therefore, we only discuss some numerical examples we consider important to somehow reflect the way this model controls the number of selected follicles.

In figure 7.22 we observe how, when the cycle starts with a size uniform distribution of eight growing follicles, five of them reached the same pre-ovulatory maturity. On the other hand, when such initial distribution changes, and the cycle begins with four relatively large follicles, only those four are the ones selected.

When decreasing the initial LH concentration parameter to smaller values, it is also possible to obtain different numbers of pre-ovulating follicles without changing the initial distribution of follicle sizes (see figure 7.23).

Therefore, this model is able to select more than one pre-ovulatory follicle, either by changes in the parameter values or the initial conditions of the system. As we first suggested, this model is basically modelling the menstrual cycle from the early follic-

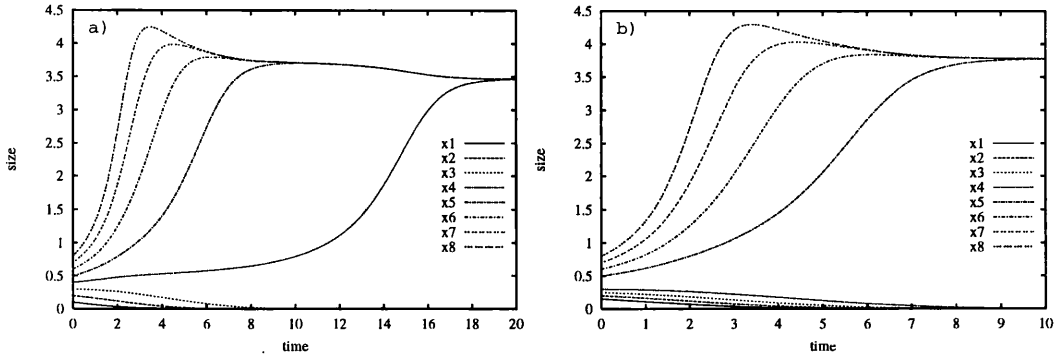

Figure 7.22: Numerical example of eight growing follicles for the model which includes a gonadotropic dependent atretic factor. For this example the parameter values are $\gamma_0 = 1.0$, $K = 0.1$ and $\alpha = 0.1$. a) The cycle starts with a uniform size distribution and the five largest follicles reach the same pre-ovulatory size, whilst the remaining three smaller follicles atrophy. b) The cycle begins with four relatively large follicles, which are the ones selected and reach the same pre-ovulatory size.

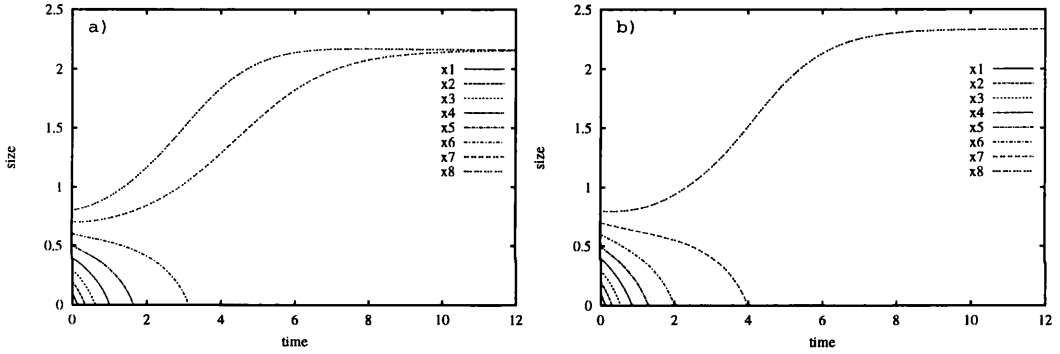

Figure 7.23: Numerical example of eight growing follicles for the model which includes a gonadotropic dependent atretic factor. In both cases the cycle starts with a uniform size distribution of follicle sizes. a) Parameter values are $\gamma_0 = 0.6$, $K = 0.1$ and $\alpha = 0.1$, the two largest follicles reach the same pre-ovulatory size, whilst the six smaller ones atrophy. b) Parameter values are $\gamma_0 = 0.5$, $K = 0.1$ and $\alpha = 0.1$. Only one follicle reaches pre-ovulatory size, whilst the remaining seven atrophy and die.

ular till the mid-follicular phase, before the LH concentration levels start increasing to trigger the mid-cycle LH surge. Although the particular cubic term of the follicle GC concentration lacks a clear biological interpretation, it allows regulation of follicular growth without any need of artificial alterations to the dynamics.

7.6 Discussion

As a result of the symmetric, non-symmetric and symmetric ageing models, it is possible to suggest that follicle sensitivity to gonadotropins is a basic feature determining the ovulation rate of the cycle. Moreover, such follicle sensitivity also distinguishes an ovulatory cycle from a PCO cycle in terms of these models. Nevertheless, the explicit way of expressing follicular sensitivity to gonadotropins is not

given in the growth function first proposed by Lacker. Therefore, this chapter provides four basic suggestions of how follicles react to hormone stimulation keeping the basic framework of the models previously analysed.

The first model considers the follicle growth rate proportional to the granulosa cell (GC) concentration times the equilibrium concentration of FSH bound receptors of GCs. A negative linear decay in terms of GC concentration is first considered for the atretic demise of the follicles. Two basic behaviours are obtained when analysing the system for a single follicle, which are either ovulation or atresia. As in the ageing symmetric model, a minimum oestradiol concentration (or follicle size) is required for any follicle to be able to grow in the first place. However, when analysing the system for several interacting follicles, the 1-fold equilibrium point of the *interaction dynamics* is the only stable equilibrium point found for this model.

Therefore, this model only reflects the ovulation cycle in primates, where there is usually only one follicle ovulating. Also, there is no possibility for this model to reflect any kind of PCOS, either by changing the relevant parameter values, or by manipulating the initial conditions of the system. An artificial method, however, is imposed when carrying out some of the numerical experiments for this model. In such a way, it is able to produce a cycle where more than one follicle may ovulate.

To avoid the use of this rather arbitrary method, a different response function of FSH to oestradiol concentration levels is proposed for the follicle growth function. A sigmoid rather than an hyperbolic decreasing function is now considered for the FSH vs. total oestradiol concentration function. However, such an alteration does not give a different M-fold equilibrium point for the *interaction dynamics* from that of the previous model. This means, that such an alteration to the follicle growth equation is not enough to allow more than one follicle to be selected.

Furthermore, for this model the selected follicle does not grow to infinity, but rather reaches a fixed size, which can be considered as an ovulatory size. Hence, there is no need for an artificial way of fixing the maximum size of the selected follicle when numerically integrating this system. Nevertheless, it does not matter how similar the two largest follicles may be at the beginning of the cycle, only one is selected and the second largest one ends up atrophying. This is due to the fact that the minimum size required to escape atresia increases three times faster than the in previous model.

Therefore, this model in terms of the concentration of FSH bound receptors of

GCs is not sufficient to exhibit more interesting dynamics. As a second step, a model also incorporating the effects of LH bound receptors is proposed. It is well known that just after follicles enter the gonadotropin dependent growth state, they start developing LH receptors on their GCs membranes. Thus, when the pre-ovulatory follicle is lacking of FSH signalling stimulation to aromatise oestradiol, LH takes over and the follicle is still able to secrete oestradiol into the blood stream.

However, for this particular model the follicle growth function is only considered in terms of the concentration of bound GC receptors. This means that the positive growth term being proportional to the GCs concentration *per-se* is now neglected. Moreover, since the LH concentration levels remain basically constant prior to selection, the particular concentration of LH bound receptors function depend on the size of the follicle in an hyperbolic manner, times a constant LH concentration parameter. Finally, the atretic factor of the follicle is again considered as a linear decay.

As in the previous model, the dynamics of a single growing follicle is analysed for different parameter values. Four main features are obtained when the parameter value of the LH constant concentration is manipulated with respect to the GCs receptor disassociation constant, and the atretic parameter. Therefore, atresia as the follicle size decreasing to zero, ovulation as the follicle size growing to infinity, and anovulation as the follicle size reaching a pre-ovulatory stable equilibrium point are results of this model.

Even though this model presents richer dynamics in terms of the different types of behaviour than the model that only considers FSH receptors, it does not seem to improve the selection dynamics itself. Since the mathematical expression of this new model is quite complicated, it is not even possible to separate the growth rate function to obtain an *interaction dynamics* equation. Therefore, numerical experiments are the only possible way of analysing the system.

Although a fixed maximum size of the ovulatory follicles is again artificially fixed, this model seems to allow more than one ovulatory follicle. On the other hand, when parameter values are set for an anovulatory condition, only one follicle appears to be able to reach pre-ovulatory maturity, independently of the follicles initial size distribution.

A comparison of the space of the i-th follicle growth rate with respect to the i-th follicle size between the ovulatory and the anovulatory situations is provided. It is observed that the rate at which the minimum size required for the follicle to escape

atresia, increases much faster in the anovulatory situation than in the ovulatory one. Therefore, this model is in principle able to switch from a single stuck follicle to one or more ovulatory follicles by varying the pertinent parameter values. This model is qualitatively more interesting that the previous one, however, it is still not able to select more than one follicle.

Therefore, a final attempt developed in this chapter is a model where a variable atretic parameter is considered. Some biological experiments suggest that androgens are the steroid that enhances atretic regression [Hsueh *et al.*, 1994; Garrett and Guthrie, 1996; Hillier and Tetsuka, 1997]. Therefore, not only follicular cell proliferation and differentiation are hormonally controlled, but also apoptotic cell death, which triggers follicular atresia. A model in which the atretic parameter is proportional to the concentration of androgen bound receptors is proposed. However, this atretic demise seems not to be enough, and as in Lacker's model, an extra decaying term proportional to the cubic GCs concentration is added to the negative terms of the growth function.

In such a way, the only possible behaviour for a single growing follicle is that of growing to a pre-ovulatory fixed size. As in the previous model, it is not possible to separate the dynamics to produce a non-linear stability analysis. From the numerical experiments shown in this chapter, it is possible to see that the number of selected follicles changes according to the initial size distribution, and according to the initial LH concentration parameter. More importantly, it is possible to obtain more than one follicle selected.

It is puzzling that the arbitrary Lacker function works so well, whilst the biologically motivated models work so poorly. The particular case of the model with the hormonally controlled atresia with the "extra" cubic decay seems to work much better. However, we were not able to derive any biological interpretation in accordance to the variables proposed. It could be argued, that if x_i representing the GC concentration, is proportional to the radius of the follicle, then the follicle's growth is limited by its volume. However, the way we have associated the concentration of bound receptors would not concur since receptors would at least be proportional to the surface of the follicle, not the radius.

Nevertheless, we could at least speculate that this particular function says some thing about how apoptosis and GC proliferation regulate follicle growth and take part into the selection of pre-ovulatory follicles. However, it would be very helpful

if a biologist could find any basis for the function proposed here.

Chapter 8

GENERAL CONCLUSIONS

This thesis presents some mathematical models of the ovarian dynamics that controls follicle growth, steroid production, atresia and selection of pre-ovulatory follicles during each estrous/menstrual cycle in mammals. The fact that from the large follicle population present at menarche, only 0.2% of all follicles are selected to ovulate; together with PCOS often occurring in humans, is a strong motivation for investigating the mechanisms involved in the control of the ovulation number.

Since the control mechanism of the ovarian cycle is dynamically rich and extremely complex, a number of different mathematical models previously developed by other authors are described in this thesis. These models focus on different parts of the control system, and the extent to which they deal with the selection mechanism is therefore discussed.

Although descriptive models in terms of follicle populations or follicle cell numbers measured at different stages of the cycle accurately describe folliclegenesis, they give little insight to the selection process itself. Hence, functional models are required, which reflect the feedback dynamics of the most important hormones involved. However, it is observed that an explicit equation for follicle growth is necessary to adequately model the cyclic behaviour of estrogens, and to accurately produce instant ovulation after each LH surge.

Nevertheless, such functional models say very little about the actual control of ovulation number, and how the mechanism can fail leading to PCO or any kind of anovulation. The first models which reproduce the cycle for many growing follicles interacting within the endocrine feedback mechanism first developed in the early eighties. Although, the model of Thalabard and collaborators gives a good stochastic approximation of the selection dynamics, Lacker's model serves as the main basis for

a deterministic analysis.

Lacker's model of the control of ovulation is based on simple assumptions about the properties of the primary feedback loop involving the ovary and the pituitary. Because of its simplicity, it is amenable to a complete mathematical analysis, and yet, despite this, it is able to exhibit many of the qualitative features of the mammalian ovulatory cycle and follicle selection process.

However, in its current form it makes the unrealistic assumption that all follicles behave identically, and in particular respond to gonadotropins in precisely the same way. One consequence of this is that Lacker's model cannot correctly reproduce the spectrum of behaviour associated with human PCOS. Another important aspect of Lacker's symmetric model which lead to further modification is the fact that the largest follicles are always those selected to reach pre-ovulatory maturity. This has been observed not to be always the case, or at least not to be the situation for all mammals.

We have dealt with these two particular issues in the non-symmetric generalisation and the symmetric model with an age decaying factor. In the former, a much better representation of PCO has been achieved since it is possible to jump from a monovulatory to a PCO cycle or vice-versa just by changing the initial follicle distribution. As mentioned before, this is the case for a significant proportion of women of reproductive age. Furthermore, the pre-destination of the largest follicles always being the selected ones no longer occurs and follicle growth curves may intersect. All of these results are due to the fact that the follicle growth equation is no longer the same for each follicle, which is something more biologically realistic.

On the other hand, the symmetric ageing model first proposed by Mariana *et al.* also breaks the hierarchy of the largest follicles being chosen to reach pre-ovulatory maturity. This was previously mentioned when this model was first published. However, due to the stability and numerical analysis developed in this thesis, this model has more to say about the selection dynamics. For the case when follicles interact with similar initial age and size the model still regulates the selection process and ovulation rate of the cycle. However, if the cycle begins with a considerable perturbation in the age of one of the largest follicles, this may disrupt the cycle to an extent that no potentially ovulatory follicles will actually ovulate, but rather become stuck in the ovary. Moreover, the number of ovulatory and anovulatory follicles can be the same, whilst in Lacker's model the number of ovulatory follicles is always larger

than the anovulatory ones.

Up to this point, the symmetric, non-symmetric generalisation and the symmetric ageing model are able to provide some insight in the control of ovulation rate, and some possible causes underlying PCOS. Particularly, the non-symmetric model suggests PCOS is a local problem regulated by the effects of abnormal responsive follicles interacting with healthy follicles. Whilst for the symmetric ageing model, old follicles interacting with healthy ones can affect follicle response to gonadotropins.

Although we may interpret the relevant parameters as being related to follicle sensitivity to gonadotropins, these parameters cannot be measured experimentally. This is because the growth function used in the models is arbitrary. Thus, the next main objective of this thesis was to give a biologically based growth function that could specify the parameters determining follicle sensitivity more precisely.

We have therefore considered follicle cell surface receptors binding to gonadotropins in terms of the Law of Mass Action. As a first step, we have only considered GC receptors for FSH. However, this appears insufficient to model the cycle for different kinds of mammals since only one follicle is always selected. The model is still sufficiently simple for the stability of the corresponding interaction dynamics to be analysed in terms of a gradient system. This analysis actually proves the fact that only one follicle is selected.

This suggests that only considering FSH receptors in modelling the selection dynamics is insufficient. Hence, we have to incorporate LH receptors of GCs, which the follicle starts acquiring by the time it enters the follicular phase of the cycle. In this case, the model is too complicated to permit a theoretical analysis. Hence, based on the parameter values used for the simpler case of one growing follicle, numerical examples were used to show that this model can produce ovulation of one or many follicles, but anovulation of a single one. Thus, this still does not reflect the kind of control observed in the cycle.

The previous models in terms of GC receptors considered an atretic linear decay for the follicle. Hence, the next step was to study if hormonal control of atresia could intervene in the selection dynamics. Androgens are believed to trigger follicular atresia, thus the atretic parameter of the model is now considered to be proportional to the concentration of androgen bound receptors. This bound receptor concentration, in turn depends on the total oestradiol concentration. In such a way, the atresia rate is no longer constant and interacts in the feedback loop. However, not much

improvement was achieved. Hence, the final step was to add an extra decaying factor proportional to the cubic GC concentration to the negative terms of the growth function of this model. In such a way, selected follicles could only reach a pre-ovulatory fixed size, but by changing the initial distribution of follicle sizes, different numbers of selected follicles were obtained.

For the symmetric model selection occurs once the initial total size of follicular population is greater than zero. In contrast, for the symmetric ageing model and for the general case of the models in terms of GCs receptors, a minimum positive total size is required, otherwise no follicle will ever reach pre-ovulatory maturity, but rather atrophy. It would be interesting to verify whether such "atretic" cycles are another kind of anovulatory infertility.

Moreover, since Lacker's model is not biologically specified, we can only say that it reflects the follicular phase of the cycle up to ovulation. As mentioned before, it is believed that selection takes place some time during this phase, but the exact moment has not been yet accurately determined. However, it is suggested that selection occurs at the mid follicular phase. Whether selected follicles are ovulatory or remain stuck inside the ovary may be determined from the mid-follicular phase till the LH surge.

Rapid changes on pre-ovulatory follicles occur up to the time of ovulation. Therefore, oestradiol serum levels increase rapidly from the mid follicular phase till the LH surge. Hence, LH levels are regarded as constant up to selection, but after that things change dramatically. In particular, the model with LH receptors considered LH serum levels as constant, thus we could say it is describing the first part of the follicular phase up to selection. However, it appears that the cubic term is necessary to slow down the selected follicles' growth in order to have more than one follicle selected.

This cubic term implies that the controlled atresia rate proposed in this last model is still insufficient to control the selection number. It would be very useful if experimental biologists could provide better evidence to the way in which atresia is regulated, and to what extent it intervenes in the regulation of ovulation dynamics. Up to now, we believe this particular aspect of the cycle remains too obscure to develop appropriate mathematical models.

Finally, we conclude by saying that the models in terms of bound GC receptors are just a first approximation to model follicle sensitivity to hormone stimu-

lation. The complex signal transduction pathway triggered by this binding process is modulated by many other factors, such as the effects of steroids, growth factors and cytokines. For the particular case of understanding PCOS, it would be useful to incorporate the effects of insulin growth factors on the follicle sensitivity to gonadotropins.

Furthermore, although these models are our first attempt to incorporate the different roles of FSH, LH and atresia in the control of ovulation rate, they still ignore the modulation of pituitary gonadotropin secretion by the hypothalamus, as well as the pulsatile LH secretion by the pituitary. Further study in how these elements affect the cycle and the ways to incorporate them into a mathematical model are subject of extensive future research.

References

- Adashi, E.Y. and Hsueh, A.J.W. (1982). Estrogens augment the stimulation of ovarian aromatase activity by Follicle-Stimulating Hormone in cultured rat Granulosa cells. *Journal of Biological Chemestry*, **257** (11) pp. 6077–83.
- Akin, E. and Lacker, H.M. (1984). Ovulation control: The right number or nothing. *Journal of Mathematical Biology*, **20** pp. 113–32.
- Alouf, C.A., Reichert, L.E., Kellom, T.A. and Lee, D.W. (1997). Cultured human granulosa cells secrete a follicle stimulating hormone receptor-binding inhibitor. *Human Reproduction*, **12** (12) pp. 2735–2740.
- Armstrong, D.T., Xia, P., De Gannes, G., Tekpetey, F.R. and Khamsi, F. (1996). Differential Effects of Insulin-Like Growth Factor-I and Follicle-Stimulating Hormone on Proliferation and Differentiation of Bovine Cumulus Cells and Granulosa Cells. *Biology of Reproduction*, **54** pp. 331–38.
- Austin, C.R. and Short, R.V. (1982). *Reproduction in mammals: 1, Germs cells and fertilization.* Cambridge Univ. Press.
- Austin, C.R. and Short, R.V. (1984). *Reproduction in mammals: 3, Hormonal Control of reproduction.* Cambridge Univ. Press.
- Avez, A. (1986). *Differential Calculus.* John Wiley & Sons.
- Baird, D.T. (1983). Factors regulating the group of the preovulatory follicle in the sheep and human. *Journal of Reproduction and Fertilization*, **69** pp. 343–352.
- Baker, G.L. and Gollub, J.P. (1990). *Chaotic dynamics, an introduction.* Cambridge Univ. Press.
- Bao, B., Thomas, M.G., Griffith, M.K., Burghardt, R.C. and Williams, G.L. (1995). Steroidogenic Activity, Insulin-Like Growth Factor-I Production, and

Proliferation of Granulosa and Theca Cells Obtained from Dominant Preovulatory and Nonovulatory Follicles during the Bovine Estrous Cycle: Effects of Low-Density and High-Density Lipoproteins. *Biology of Reproduction*, **53** pp. 1271–1279.

- Becker, W.M., Reece, J.B. and Poenie, M.F. (1996). *The world of the cell.* Benjamin/Cummings.

- Bellman, R. (1960). *Introduction to matrix analysis.* Mc Graw-Hill.

- Bogumil, R.J., Ferin, M., Rootenberg, J., Speroff, L. and Vande-Wiele, R.L. (1972a). Mathematical Studies of the Human Menstrual Cycle. I. Formulation of a Mathematical Model. *Journal Clinical Endocrinology and Metabolism*, **35** pp. 126–143.

- Bogumil, R.J., Ferin, M. and Vande-Wiele, R.L. (1972b). Mathematical Studies of the Human Menstrual Cycle. II. Simulation Performance of a Model of the Human Menstrual Cycle. *Journal Clinical Endocrinology and Metabolism*, **35** pp. 144–156.

- Brailly, S., Gougeon, A., Milgrom, E., Bomsel-Helmreich, O. and Papiernik, E. (1981). Androgens and Progestins in the Human Ovarian Follicle: Differences in the Evolution of Preovulatory, Healthy Nonovulatory and Atretic Follicles. *Journal Clinical Endocrinology and Metabolism*, **53** (1) pp. 128–134.

- Cargille, C.M., Ross, G.T. and Yoshimi, T. (1969). Daily variation in plasma follicle stimulating hormone, luteinizing hormone, and progesterone in the normal menstrual cycle. *Journal Clinical Endocrinology and Metabolism*, **29** (12).

- Chang, R.J. (1996). *Polycystic Ovary Syndrome.* Springer-Verlag, Berlin.

- Chávez-Ross, A., Franks, S., Mason, H.D., Hardy, K. and Stark, J. (1997). Modelling the Control of Ovulation and Polycystic Ovary Syndrome. *Journal of Mathematical Biology*, **36** pp. 95–118.

- Clément, F. (1997). *Modelisation mathematique de la cinetique cellulaire au sein de la granulosa des follicules ovariens au cour de leur developpement terminal.* Thèse por l'obtention du Diplôme de Docteur de l'Université Paris 7, Spécialité: Biomathématiques.

- Clément, F., Gruet, M.A., Monget, P., Terqui, M., Jolivet, E. and Monniaux, D. (1997). Growth kinetics of the granulosa cell population in ovarian follicles: an approach by mathematical modelling. *Cell Proliferation*, **30** pp. 255–270.

- Dewailly, D. (1997). Definition and significance of polycystic ovaries. *Bailliere's Clinical Obstetrics and Gynaecology International Practice and Research*, **11** (2) pp. 349–368.

- Eppig, J.J. (1991). Intercommunication Between Mammalian Oocytes and Companion Somatic Cells. *BioEssays*, **13** (11) pp. 569–574.

- Erickson, G.F., Hsueh, M.E., Quigley, M.E., Rebar, M.R.W. and Yen, S.S.C. (1979). Functional Studies of Aromatase Activity in Human Granulosa Cells from Normal and Polycystic Ovaries. *Journal Clinical Endocrinology and Metabolism*, **49** (4) pp. 514–519.

- Faddy, M.J. (1976). A Note on the General Time-Dependent Stochastic Compartmental Model. *Biometrics*, **32** pp. 443–448.

- Faddy, M.J. and Gosden, R.G. (1995). A mathematical model of follicule dynamics in the human ovary. *Human Reproduction*, **10** (4) pp. 770–775.

- Faddy, M.J., Jones, E.C. and Edwards, R.G. (1976). An Analytical Model for Ovarian Follicle Dynamics. *Journal Experimental Zoology*, **197** pp. 173–186.

- Faddy, M.J. and Jones, M.C. (1988). Fitting Time-Dependent Multicompartment Models: A Case Study. *Biometrics*, **44** pp. 587–593.

- Feng, L., Rodbard, D., Rebar, R. and Ross, G.T. (1977). Computer Simulation of the Human Pituitary-Ovarian Cycle: Studies of Follicular Phase Estradiol Infusions and the Midcycle Peak. *Journal Clinical Endocrinology and Metabolism*, **45** pp. 775–787.

- Fletcher, R. (1981). *Practical Methods of Optimization: Constrained Optimization*, volume 2. John Wiley & Sons.

- Fortune, J.E. (1994). Ovarian Follicular Growth and Development in Mammals. *Biology of Reproduction*, **50** pp. 225–232.

- Franks, S., Robinson, S. and Willis, D.S. (1996). Nutrition, Insulin, and Polycystic Ovary Syndrome. *Reviews of Reproduction*, **1** pp. 47–53.
- Garrett, W.M. and Guthrie, H.D. (1996). Expression of Androgen Receptors and Steroidogenic Enzymes in Relation to Follicular Growth and Atresia Following Ovulation in Pigs. *Biology of Reproduction*, **55** pp. 949–955.
- Glendinning, P. (1994). *Stability, instability and chaos: an introduction to the theory of nonlinear differential equations.* Cambridge Univ. Press.
- Gougeon, A. (1984). Le follicule ovulatoire humain. A quel moment du cycle est'il selectionne et par quels mecanismes? Une tentative de reponse. *Contraception-fertilite-sexualite*, **12** (12) pp. 1397–1405.
- Gougeon, A. (1986). Dynamics of follicular growth in the human: a model from preliminary results. *Human Reproduction*, **1** (2) pp. 81–87.
- Gougeon, A. (1996a). Dynamics of Follicle Development in the Human Ovary. *Sereno Symposia*, pp. 21–36.
- Gougeon, A. (1996b). Regulation of Ovarian Follicular Development in Primates: Facts and Hypotheses. *The Endocrine Society*, **17** (2) pp. 121–155.
- Gougeon, A., Ecochard, R. and Thalabard, J.C. (1994). Age-Related Changes of the Population of Human Ovarian Follicles: Increase in the Disappearance Rate of Non-Growing and Early-Growing Follicles in Aging Women. *Biology of Reproduction*, **50** pp. 653–663.
- Gougeon, A. and Lefèvre, B. (1983). Evolution of the diameters of the largest healthy and atretic follicles during the human menstrual cycle. *Journal of Reproduction and Fertilization*, **69** pp. 497–502.
- Hartshorne, G.M., Sargent, I.L. and Barlow, D.H. (1994). Growth rate and antrum formation of mouse ovarian follicles in vitro in response to follicle-stimulating hormone, relaxin, cyclic amp and hypoxanthine. *Human Reproduction*, **9** (6) pp. 1003–1012.
- Hillier, S.G. (1994). Current concepts of the roles of follicle stimulating hormone and luteinizing hormone in folliculogenesis. *Human Reproduction*, **9** (2) pp. 188–191.

- Hillier, S.G. and Tetsuka, M. (1997). Role of androgens in follicle matiration and atresia. *Bailliere's Clinical Obstetrics and Gynaecology International Practice and Research*, **11** (2) pp. 249–260.

- Hodgen, G.D. (1982). The dominant ovarian follicle. *Fertilty and Sterility*, **38** (3) pp. 281–300.

- Hofbauer, J. and Sigmund, K. (1988). *The Theory of Evolution and Dynamical Systems*. Cambridge Univ. Press.

- Hsueh, A.J.W., Billig, H. and Tsafriri (1994). Ovarian Follicle Atresia: A Hormonally Controlled Apoptotic Process. *Endocrinology*, **15** pp. 707–724.

- Jablonka-Shariff, A., Reynolds, L.P. and Redmer, D.A. (1996). Effects of Gonadotropin Treatment and Withdrawal on Follicular Growth, Cell Proliferation, and Atresia in Ewes. *Biology of Reproduction*, **55** pp. 693–702.

- Jolly, P.D., Smith, P.R., Heath, D.A., Hudson, N.L., Lun, S., Still, L.A., Watts, C.H. and McNatty, K.P. (1997a). Morphological Evidence of Apoptosis and the Prevalence of Apoptotic versus Mitotic Cells in the Membrana Granulosa of Ovarian Follicles during Spontaneous and Induced Atresia in Ewes. *Biology of Reproduction*, **56** pp. 837–846.

- Jolly, P.D., Tisdall, D.J., De'ath, G., Heath, D.A., Lun, S., Hudson, N.L. and McNatty, K.P. (1997b). Granulosa Cell Apoptosis, Aromatase Activity, Cyclic Adenosine 3',5'-Monophosphate Response to Gonadotropins, and Follicular Fluid Steroid Levels during Spontaneous and Induced Follicular atresia in Ewes. *Biology of Reproduction*, **56** pp. 830–836.

- Lacker, H.M. (1981). Regulation of ovulation number in mammals. A Follicle Interaction Law that Controls Maturation. *Biophysical Journal*, **35** pp. 433–454.

- Lacker, H.M. and Akin, E. (1988). How do ovaries count? *Mathematical Biosciences*, **90** pp. 305–332.

- Lacker, H.M., Beers, W., Mueli, L.E. and Akin, E. (1987). A theory of follicle selection: I and II. *Biology of Reproduction*, **37** pp. 570–580.

- Lacker, H.M. and Percus, A. (1991). How do ovarian follicles interact? A many-body problem with unusual symmetry and symmetry-breaking properties. *J. Stat. Phys.*, **63** pp. 1133–1161.

- Lamport, H. (1940). Periodic changes in blood estrogen. *Endocrinology*, **27** pp. 673–680.

- Lang, S. (1987). *Calculus of Several Variables.* Springer-Verlag, Berlin.

- Ledger, W.L. and Baird, D.T. (1995). Ovulation 3: Endocrinology of ovulation. In Gvudzinskas, J.G and Yovich, J.L., editors, *From Gametes - The Oocyte*, pages 193–209. Cambridge Univ. Press.

- Mariana, J.C., Corpet, F. and Chevalet, C. (1994). Lacker's model: Control of follicular growth and ovulation in domestic species. *Acta Biotheorica*, **42** pp. 245–262.

- Mason, H.D. (1994). *Investigation of the Mechanism of Anovulation in Polycystic Ovary Syndrome.* PhD Thesis, University of London.

- Mason, H. and Franks, S. (1997). Local control of ovarian steroidogenesis. *Bailliere's Clinical Obstetrics and Gynaecology International Practice and Research*, **11** (2) pp. 261–279.

- Mason, H.D., Willis, D.S., Beard, R.W., Winston, R.M.L., Magara, R. and Franks, S. (1994). Estradiol Production by Granulosa Cells of Normal and Polycystic Ovaries: Relationship to Menstrual Cycle History, and Concentrations of Gonadotrophins and Sex Steroids in Follicular Fluid. *Journal Clinical Endocrinology and Metabolism*, **79** pp. 1355–1360.

- McGee, E.A., Rainey, W.E., Sawetawan, C., Carr, B.R. and Bird, I. (1996). The effect of insulin and insulin-like growth factors on the expression of steroidogenic enzymes in a human ovarian thecal-like tumor cell model. *Fertilty and Sterility*, **65** (1) pp. 87–93.

- McLachlan, R.I., Cohen, N.L., Dahl, K.D., Bremner, W.J. and Soules, M.R. (1990). Serum inhibin levels during the periovulatory interval in normal women: Relationships with sex steroid and gonadotrophin levels. *Clinical Endocrinology*, **32** pp. 39–48.

- Mesarovic, M.D. (1968). *Systems Theory and Biology.* Springer-Verlag, Berlin.

- Meuli, L.E., Lacker, H.M. and Thau, R.B. (1987). Experimental Evidence Supporting a Mathematical Theory of the Physiological Mechanism Regulating Follicle Development and Ovulation Number. *Biology of Reproduction*, **37** pp. 589–594.

- Misrahi, M., Beau, I., Ghinea, N., Vannier, B., Loosfelt, H., Meduri, G., Vu Hai, M.T. and Milgrom, E. (1996). The LH/CG and FSH receptors: different molecular forms and intracellular traffic. *Molecular and Cellular Endocrinology*, **125** pp. 161–167.

- Monniaux, D., Huet, C., Besnard, N., Clément, F., Bosc, M., Pisselet, C., Monget, P. and Mariana, J.C. (1997). Follicular growth and ovarian dynamics in mammals. *Journal of Reproduction and Fertilization*, **51** pp. 3–23.

- Monniaux, D., Pisselet, C. and Fontaine, J. (1994). Uncoupling between proliferation and differentiation of ovine granulosa cells in vitro. *Journal of Endocrinology*, **142** pp. 497–510.

- Murray, J.D. (1993). *Mathematical Biology.* Springer-Verlag, Berlin.

- Perko, L. (1991). *Differential Equations and Dynamical Systems.* Springer-Verlag, Berlin.

- Polson, D.W., Wadsworth, J., Adams, J. and Franks, S. (1988). Polycystic ovaries: a common finding in normal women. *Lancet*, pp. 870–872.

- Rainey, W.E., Sawetawan, C., McCarthy, J.L., McGee, E.A., Bird, I.M., Word, R.A. and Carr, B.R. (1996). Human Ovarian Tumor Cells: A Potential Model for Thecal Cell Steroidogenesis. *Journal Clinical Endocrinology and Metabolism*, **81** (1) pp. 257–263.

- Richards, J. (1975). Estradiol Receptor Content in Rat Granulosa Cells During Follicular Development: Modification by Estradiol and Gonadotropins. *Endocrinology*, **97** (5) pp. 1174–1184.

- Rosenfield, R.L. (1997). Current concepts of polycystic ovary syndrome. *Bailliere's Clinical Obstetrics and Gynaecology International Practice and Research*, **11** (2) pp. 307–333.

- Scaramuzzi, R.J., Adams, N.R., Baird, D.T., Campbell, B.K., J.A., Downing, Findlay, J.K., K.M., Henderson, Martin, G.B., McNatty, K.P., McNeilly, A.S. and Tsonis, C.G. (1993). A model for follicle selection and the determination of ovulation rate in the ewe. *Reprod. Fertl. Dev.*, **5** pp. 459–78.

- Schlosser, P.M. and Selgrade, J.F. (1997). A model of gonadotropin regulation during the menstrual cycle in women: Qualitative features. Preprint.

- Schwartz, N.B. and Waltz, P. (1970). Role of ovulation in the regulation of the estrous cycle. *Federation Proceedings*, **29** (6) pp. 1907–1912.

- Segel, L.A. (1980). *Mathematical models in molecular and cellular Biology.* Cambridge Univ. Press.

- Segel, L.A. (1984). *Modelling dynamic phenomena in molecular and cellular Biology.* Cambridge Univ. Press.

- Selgrade, J.F. and Schlosser, P.M. (1999). A Model for the Production of Ovarian Hormones during the Menstrual Cycle. *Fields Institute Communications*, **21** pp. 429–446.

- Shack, W.J., Tam, P.Y. and Lardner, T.J. (1971). A mathematical model of the human menstrual cycle. *Biophysical Journal*, **11** pp. 835–848.

- Sites, C.K., Patterson, K., Jamison, C.S., Degen, S.J.F. and Labarbera, A.R. (1994). Follicle-Stimulating-Hormone (FSH) increases FSH Receptor Messenger Ribonucleic Acid while decreasing FSH binding in cultured porcine Granulosa cells. *Endocrinology*, **134** (1) pp. 411–417.

- Spears, N., Bruni, J.P. and Gosden, G. (1996). The establishment of follicular dominance in co-cultured mouse ovarian follicles. *Journal of Reproduction and Fertilization*, **106** pp. 1–6.

- Taymor, M.L. (1996). The regulation of follicle growth: some clinical implications in reproductive endocrinology. *Fertility and Sterility*, **65** (2) pp. 235–247.

- Thalabard, J.C., Thomas, G. and Metivier, M. (1989). The emergence of the dominant ovarian follicle In primates: A random driven event? *Cell to Cell Signalling: From Experiments to Theoretical Models*, **8** pp. 387–393.

- Thompson, H.E., Horgan, J.D. and Delfs, E. (1969). A simplified mathematical model and simulations of the hypophysis-ovarian endocrine control system. *Biophysical Journal*, **9** pp. 278–291.

- Tsonis, C.G., Carson, R.S. and Findlay, J.K. (1984). Relationship between aromatase activity, follicular fluid oestradiol-17β and testosterone concentrations, and diameter and atresia of individual ovine follicles. *Journal of Reproduction and Fertilization*, **72** pp. 153–163.

- Vande-Wiele, R.L., Bogumil, J., Dyrenfurth, I., Ferin, M., Jewelewicz, R., Warren, M., Rizkallah, T. and Mikhail, G. (1970). Mechanisms Regulating the Menstrual Cycle in Women. *Recent Prog. Horm. Res.*, **26** pp. 63–103.

- Watson, H., Kiddy, D.S., Hamilton-Fairley, D., Scanlon, M.J., Barnard, C., Collins, W.P., Bonney, R.C. and Franks, S. (1993). Hypersecretion of Luteinizing Hormone and Ovarian Steroids in Women with Recurrent Early Miscarriage. *Human Reproduction*, **8** (6) pp. 829–833.

- Yen, S.S.C. (1980). The Polycystic Ovary Syndrome. *Clinical Endocrinology*, **12** pp. 177–208.

- Zelinski-Wooten, M.B., Hutchison, J.S., Hess, D.L., Wolf, D.P. and Stouffer, R.L. (1995). Follicle stimulating hormone alone supports follicle growth and oocyte development in gonadotrophin-releasing hormone antagonist-treated monkeys. *Human Reproduction*, **10** (7) pp. 1658–1666.